SOME NEWTONIAN AND NON-NEWTONIAN ASPECTS OF RADIAL FACE SEALS

by

TARA SHANKAR NAILWAL

DEPARTMENT OF MATHEMATICS

INDIAN INSTITUTE OF TECHNOLOGY, KANPUR

JUNE, 1983

SOME NEWTONIAN AND NON-NEWTONIAN ASPECTS OF RADIAL FACE SEALS

A Thesis Submitted
In Partial Fulfilment of the Requirements
for the Degree of
DOCTOR OF PHILOSOPHY

by
TARA SHANKAR NAILWAL

to the

DEPARTMENT OF MATHEMATICS
INDIAN INSTITUTE OF TECHNOLOGY, KANPUR

JUNE, 1983

DEDICATION

TO MY

FATHER - SHRI CHINTA MANI

MOTHER - SMT. LAXMI DEVI

AND

ELDER BROTHER

SHRI KAILASH CHANDRA NAILWAL

CERTIFICATE

This is to certify that the matter embodied in the thesis entitled ''Some Newtonian And Non-Newtonian Aspects of Radial Face Seals'' by Mr. Tara Shankar Nailwal for the award of the degree of Doctor of Philosophy of the Indian Institute of Technology, Kanpur, is a record of bonafide research work carried out by him under my supervision and guidance. The thesis, in my opinion, has reached the standard fulfilling the requirements of the Ph.D. degree. The results embodied in this thesis have not been submitted to any other University or Institute for the award of any degree or diploma.

[Prawal Sinha]
Thesis Supervisor
Department of Mathematics
Indian Institute of Technology
KANPUR-208016, U.P.
INDIA.

June - 1983.

ACKNOWLEDGEMENTS

At the very outset, I take the opportunity to express my profound indebtedness and extreme gratitudes to my thesis supervisor Dr. Prawal Sinha, Department of Mathematics, I.I.T.Kanpur, for his untiring guidance during the progress of this dessertation. His constructive criticisms, invaluable suggestions and persistent surviellance had been a source of inspiration and encouragement throughout this work.

I wish to express my indebtedness to Prof.J.B.Shukla, Head of the Department of Mathematics, I.I.T.Kanpur and Prof. P. Singh for their constant inspirations and encouragements from time to time.

I take this opportunity to thank to Dr. Chandan Singh for his invaluable help, both academic and non-academic, during his stay at I.I.T. Kanpur. Thanks are also due to Dr.D.P.Shukla, Mr. Arun Kumar, Mr. Vishnu Kant, Mr. Rajiv Sharma, Mr. A. Raj, Mr. Chandan Singh Bisht, Dr. Atul Nautiyal, Dr. Axay Mishra and all other friends for their cooperation as and when required.

My power of expression fails when I think of the affectionate and loving care, cooperation and inspirations given by Miss. Kamala Joshi.

The very idea of dedicating this piece of work to my parents, Shri Chinta Mani and Smt. Laxami Devi, and to my elder brother Shri Kailash Chandra Nailwal puts me into extreme emotional state. They have worked so unfailingly and so hard all these years to support me both morally, emotionally and materially with tender care and unfathomable affection without which the opportunity for higher education would not have born for me.

Thanks are also due to I.I.T. Kanpur for providing financial assistance and other facilities during this period.

Finally, I wish to express my thanks to Mr. Ashok Kumar Bhatia for his unfailing patience in type-cutting stencils, to Mr. A.N. Upadhyay for neat cyclostyling and to Mr. B.N.Srivastava for drawing the figures.

June, 1983. T.S.Nailwal

ABSTRACT

In its simplest form, a radial face mechanical seal consists of two annular rings, one of them is mounted on a flexible support and is called the primary seal ring and the other is set on the rotating shaft and is termed as the secondary seal ring. For smooth operation of face seal over a long period of time, the faces of the seal have to remain properly separated. Thus an adequate amount of separating axial force is required to be maintained for this purpose. But too big a separation leads to massive leakage of the lubricant whereas too small a separation results in the rapid wear of the faces. Thus short seal life and sudden seal failure, because of uncontrolled leakage or wear or both are common problems.

Recently it was held that restoring moment (the moment about x axis) and transverse moment (the moment about y axis) have direct bearing on the stability of face seals. Both hydrodynamic and hydrostatic effects were shown to have enormous influence on various seal characteristics namely, axial force, radial force, leakage, frictional force, transverse moment and restoring moment. Misalignment and coning of the faces is shown to be inevitable phenomenon and they influence these characteristics

considerably. Also, squeeze effects are shown to have significant effects on various seal characteristics.

The non-Newtonian character of the lubricant was shown to have insignificant influence on the performance of a radial face seal. But these findings were made without taking into account the inevitable misalignment of the faces and the flexibility of the face material. However, it is likely that the study of radial face seals when coupled with the concepts of misalignment and flexibility may lead to significant non-Newtonian effects. Further, it is likely that the study of these non-Newtonian effects through the power law model may yield additional information which will help in the designing of seals.

The present thesis is designed to study some of these aspects of a radial face seal. The seal faces are assumed to be narrow in that it renders Reynolds equation worth yielding analytical solution for some cases, as a consequence of elimination of the circumferential pressure gradient from the original Reynolds equation. In fact, for narrow seals, the circumferential pressure gradient is neglegible as compared to the radial pressure gradient. The present thesis is devided into two parts — Newtonian effects and non-Newtonian effects. The chapterwise brief discussion of the work presented is as follows.

Chapter I is indroductory type. Starting from the basic definition of seals, this chapter deals with the various aspects of designing of seals, their applications and their classifications. Besides, the chronological developments in the field have also been touched upon. Some of the important investigations have been described in detail.

Chapter II deals with the effects of centrifugal inertia on the performance of a parallel face seal. It is found that both axial force and side leakage increase with an increase in inertia parameter whereas transverse moment decreases.

In Chapter III, squeeze effects on face seals are studied. The faces of seal are considered to be misaligned and one of them carries coning on it. It is concluded that squeeze with coning may be desirable where the large values of separating forces produce massive leakage, because coning causes reduction in these forces.

In Chapter IV, hydrodynamic effects in misaligned radial face seals, with porous faces, are analysed. It is concluded that when there is a case of excessive leakage, due to large values of separating forces, rendering the faces porous reduces the leakage thus saving the face seal from early failure.

In Chapter V, the problem of misaligned radial face seal is dealt with where one of the faces is onsidered to be flexible which may be due to coating of a soft material on the face seal. It is found that the axial force increases with the elastic parameter whereas the radial force decreases. The conclusion is that the flexibility of faces improves the stability of face seal.

In Chapter VI, the problem of misaligned radial face seal is considered, where the non-Newtonian behaviour of the lubricant is accounted for through the power law lubricant . It is seen that the axial force and the tilt moment are increased by the use of pseudoplastic fluids as lubricant. However, they are decreased by the use of dilatants.

In Chapter VII, the effects of misalignment on radial and frictional forces are studied. It is assumed that the lubricant obeys the power law. The curvature effects neglected by earlier workers are also given due attention. It is seen that the pseudoplastic fluid increases the radial and frictional force whereas the dilatant fluid decreases them. Furthermore, higher the radii ratio higher the radial and frictional forces.

In Chapter VIII, elastohydrostatic lubrication, with power law lubricants, of circular plate thrust bearing of the type used in face seals is studied. It is found that an elastic layer on the surface improves amply the bearing performance. When extended to face seals, it amounts to saying that axial separating forces are increased by an elastic layer on the faces of a face seal.

A part of the work embodied in the thesis has been published in the form of the following research papers.

1. ''Squeeze Effects in a Misaligned Radial Face Seal With Coning'', Wear, Volume 85, 1983, page 143. (Chapter III).
2. ''Radial and Frictional Forces in Misaligned Radial Face Seal With Non-Newtonian Fluid'', Presented at The Winter Annual Meeting of the American Society of Mechanical Engineers, Phoenix, Arizona, November, 1982, (To be published in Jour. Fluids. Engng., Trans. ASME). (Chapter VII).
3. ''Elastohydrostatic Lubrication of Circular Plate Thrust Bearing With Power Law Lubricants'', Journal of Lubrication Technology, Transaction of American Society of Mechanical Engineers, Volume 104, 1982, page 243. (Chapter VIII).

CONTENTS

NOMENCLATURE

c	seal clearance
C_L	load coefficient
E	modulus of elasticity
E'	elastic constant, i.e. $E' = \frac{1}{E}\left[1 - \frac{2\nu^2}{1-\nu}\right]$
F_r	radial force
F_R	frictional force
F_v	translational damping coefficient
F_z	axial separating force
$F_{\dot{\gamma}}$	cross-coupled dampling coefficient
H	thickness of the porous shell
h	film thickness for rigid seals
h'	film thickness for flexible seals, i.e. $h'=h+sp$
h_1	film thickness corresponding to the inner periphery of seal, i.e. $h_1 = c + \gamma\, r_1 \cos\theta$
h_2	film thickness corresponding to the outer periphery of seal, i.e. $h_2 = c + \gamma\, r_2 \cos\theta$
M_v	cross-coupled damping coefficient
M_x	restoring moment
M_y	transverse moment
$M_{\dot{\gamma}}$	rotational damping coefficient
n	flow behaviour index of power law fluid
p	pressure in the fluid film
p_1	pressure at the inner periphery
p_2	pressure at the outer periphery

P	pressure in the porous shell
Q	leakage across the boundary
(r,θ,z)	cylindrical coordinates system
r_1	inner radius of the seal rings
r_2	outer radius of the seal rings
s	measure of the flexibility, i.e. $s = \frac{f}{E'}$
v	velocity in r direction
w	velocity in y direction
W	load capacity
(Y,X,Z)	cartesian coordinates system
α	a measure of the porosity of seal faces, i.e. $\alpha = 12\frac{\varphi H}{c^3}$
β	angle of coning
γ	angle of tilt
δ	non-dimensional coning parameter, i.e. $\delta = \frac{r_2}{c}$
ε	non-dimensional tilt parameter i.e. $\varepsilon = \frac{\gamma r_2}{c}$
λ	inertia parameter depending upon angular velocity
ν	poisson's ratio
τ	shear stress
φ	permeability
ω	angular velcoty

The quantity carrying a bar denotes the corresponding non-dimensional form.

CHAPTER I

GENERAL INTRODUCTION

In any lubricating system the purity and the maintenance of the quantity of lubricant is highly desirable. 'Sealing in' the lubricant and 'sealing out' the contaminating foreign material are the measures that serve this purpose. The function of seal is to separate pressurized fluid where, for instance, a moving shaft passes through a machine housing or passes from one part of the machine to another. This requires prudent designing of the seal arrangements and the selection of the seal material. In the selection of any combination of seal arrangements and material the objective should be to obtain a design which will show the least amount of wear in service. It is also to be stressed upon that the designing may be of such a form that whatever wear takes place should be on the seal and not on the shaft. In other words the amount of wear on the lubricating system should lessen on account of sealing. For example, a leather seal will wear depending on the quality of the material of seal. But the wear on the seal can be reduced in those design where it is possible to fit a spring with the seal mounted on it to hold the seal close to the shaft.

1.1 SEAL DESIGNING

Since the lubricant in a mechanical system may have to operate under certain conditions, the arrangements of any

seal for the mechanical system calls for the consideration of all such conditions by a designer. Some of the important conditions are discussed as follows.

1.1.1 Temperature : It is well known that higher temperature of the lubricant results in higher fluidity. Thus if the seal is not sufficiently tight the leakage of the lubricant will be enhanced. Thus a seal designed for a low-temperature operating condition will fail to sufficiently seal in the fluid when the lubricant has to function under high temperature. The seal designer, therefore, considers the operating conditions when choosing the seal material and planning the spring arrangements, for high temperature may adequately influence the characters of the material used.

1.1.2 Pressure : Under most conditions of service in a pump or gearhousing or a roller bearing some pressure will prevail within the lubrication region. This means that in operation there will be more of a tendency for the lubricant to leak out than for dust or dirt to be drawn in. On shutdown, however, a partial vacuum may develop in some lubricating system upon cooling and cause dust laden air to be drawn in. In view of this ,it is not always possible to seal all types of bearings outright against the leakage or the infiltration of dust or foreign matter. Thus some designers make additional arrangements for more

effectiveness overall performance of the system. The use of external flingers is one of such additional arrangements. External flingers are useful where water may run down (or along) the shaft. They are also helpful in providing security to the bearing seal against the wear-borne effect of contaminating particles.

1.1.3 Wear : To design a seal that lessens the wear it is required that the material comprising seal-faces should be properly chosen. In the case of unsuitable combination of face material the wear may reach disastrous proportions. In practice, a badly designed seal which has a good combination of face material is often preferable to a better designed seal with unsuitable face material. The porosity of the material, for instance, is harmless as long as the pores are not interconnected. Such hollow pores have the advantage that they may store lubricants and may therefore have improved performance. Examples of such materials are metal oxides, steel containing graphite, and castings. A similar effect is produced through the action of wear on unhomogeneous materials with particles of varying thickness in the matrix or differing in thermal conductivities and expansion coefficient.

1.1.4 Type of Lubricant : The type of lubricant to be used sufficiently influences the kind of designing a seal

really requires. Fluid oils operating at temperatures within average limits (from 50°C to 150°C) require tighter sealing than greases which are made from oils of approximately the same viscosity. The soap content in the average bearing grease has a certain amount of restraining effect in itself.

Thus the designer of the seal must have beforehand sufficient information regarding the type of lubricant to be used, viscosity of the lubricant , the operating temperature, the dust density of the surrounding or the other contaminating outer materials, the operating speed of the system, the kind of products that might be ruined by the lubricant in case of its leakage, e.g. textiles by the lubricants, etc. It is also important to remember that for any seal to be effective the surfaces against which it rubs must be smooth and well polished.

1.2 TYPES AND CLASSIFICATION OF SEALS

In Industry a large number of seals are used to meet the many and varying problems presented by fluid sealing needs. Depending on the operating conditions and requirements, gaskets , O-rings and welds are used for sealing stationary machine joints ; soft packings, moulded elastomeric rings, piston rings, metal bushings and diaphragm seals are used for backward and forward movements.

Seals mounted on springs, stuffing boxes, lip seals, bushings, spiral groove seals and mechanical seals made out of a very large number of materials are the systems that are commonly used for sealing rotating shafts. Bearing engineers, group seals into the following three broad classifications according to the principles of design involved:

(1) Those involving actual frictional or sliding contact with the shaft. These require a relatively flexible sealing material such as leather, felt, cork or some synthetic material which can be pressfitted into the closure so that light contact prevails with the shaft.

(2) Those involving grooves or metallic devices such as stuffing boxes which require a certain amount of running clearance between the shaft, and make use of capillary attraction to keep a film of lubricant in the clearance space.

(3) Those which utilize the effect of centrifugal force by providing flingers which will keep dirt from entering the housing.

When the leakage flow is radial between plane surfaces the mechanical seal is termed as 'radial face seal'' and when the leakage flow is axial between the cylindrical surfaces the mechanical seal is termed as 'bushing seal'.

Axial forces control the leakage in radial face seals and the size of the radial clearance between bushing and shaft controls the leakage in bushing seals. The face seal is more and more replacing stuffing boxes for rotating shafts, having the advantages of smaller leakage losses, reduced maintenance and longer life.

1.3 FIELD OF APPLICATION

It was the automobile industry that recognized the advantages of mechanical seals and first used them in the water pumps of internal combustion engines. Today automobile water pumps are all fitted with face seals. After face seals had proved themselves in the motor industry, the pump manufacturers and the large chemical firms began to install an ever-increasing number of mechanical seals in a rapidly expanding range of applications. The petroleum industry went so far as to prescribe the exclusive use of mechanical seals in some refineries, pumping stations and tankers for reasons of safety and economy.

In the motor industry, face seals are used in abundance. They serve to seal crankshafts, water pumps and auxiliary pumps in motor vehicles, diesel engines and ships - engines. They seal bearings in tracked and cross-country vehicles, preventing the extrusion of grease and oil and the ingress of foreign bodies or dirty water. The

operating requirements for motor vehicles lie mainly in the low and middle range of pressure, speed and load.

Face seals are frequently used in household machinaries such as washing machines, driers, spin-driers, dish-washers and meat-mincers, as well as pumps for oil heaters and hot water distribution. Power and pump industries are also greatly benifited by the use of seals. Here, seals are used in water turbines, boiler feed pumps, gas circulators and to an increasing extent in nuclear reactor technology on high pressure rotary pumps and other control rod mechanisms. Furthermore, fans, compressors, refrigerators and vacuum pumps are fitted with face seals.

In the petroleum and chemical industries mechanical seals find wide applications and are required for the shafts of agitators, sprinkler systems and mixers, steam heated calenders, centrifuges, blowers and pumps for varied chemical products. In aircrafts and rockets, mechanical seals are used for sealing gas turbine shafts, turboserper chargers, hydraulic units and booster pumps for fuel and liquid gas. Here the rubbing speed can be very high. Apart from this, seals find applications in many other industries.

1.4 EXPLORATIVE DEVELOPMENTS

The first simple face seal appeared in about 1900 when very little information about functioning of seals was available. Although the use of seal dates back to a period far more prior to 1900, but this simple face seal was an improvement over all previous face seals e.g. traditional shaft packing and stuffing box.

Over the past several years advances in contacting mechanical face seal technology have been promising, but considerable work still needs to be done. Further improvement in seal design to increase seal life and reliability would result in a sufficient cost saving to the users. Also, it is known that the amount of energy consumed for pumping purposes due to seal friction losses can be significant. With the present state of the art of contacting face seal design, it is difficult to design a seal with low leakage, low friction, high reliability and long life. Considerable explorative work has been done over the past three decades. Judging by the progress hitherto one may expect continued exploration and increasing knowledge leading to evolution of still better seal design technology.

The earliest available literature dates back to 1946 when Fogg's experiments [1] on simple parallel face thrust bearings showed that considerable load could be

carried by flat faces without physical contact. Four years later, in 1950, Brkich [2] found out that the surface tension acting at the interface between liquid and air, at the low pressure edge of the seal faces, created a pressure differential to contain the liquid. The sealing pressure so created can be computed knowing the surface tension and assuming that the maximum gap between the seal faces is equal to the sum of the waviness of two face surfaces. In 1950 itself Salama [3] investigated that surface roughness produced by machining has significant bearings on pressure producing mechanism. In 1954 a paper by Wood [4] appeared in which exploration about seal-life was discussed. In conservative refinery practice, typical seal-life was noted as being about 2000-8000 hours. In domestic water pumps, life is probably of the order of 15000 hours, i.e. two years of continuous service. It was also investigated that for very high face velocities and poor lubrication, life may be only a matter of minutes. In 1957 Zienkiewics [5] found that for some configurations, thermal and pressure deformations of the bearing surface produce a convergent film which is load bearing. Surface tension as the means of sealing was discussed by Jagger [6] in the same year. He showed that the maximum pressure that could be sealed by this method was in the range of 25 to 50 psi for common

fluids assuming a 20 microinch gap between the seal faces. Whitley [7], in 1959, used grooves and slots in the seal faces to generate fluid pressure to maintain a full fluid film and thereby supporting load and minimising friction.

Thus, although 1950s witnessed a considerable work on face seals, yet the theory of face seal did not progress to the point of providing a general useable design of face seals. Still more investigations followed in 1960s especially after Denny [8] had carried out some experiments with plain thrust surfaces of the type used in radial face seals. In the range of conditions covered by these experiments, fluid pressures between the rotating annular surfaces were always greater than those predicted on the basis of laminar flow between parallel surfaces. He inferred that the factors contributing to this were as follows.

(a) Fluid pressures were generated between the faces by the shaft rotation.

(b) Wear of the faces tended to produce a convergent gap in the direction of flow.

Both effects resulted in stabilising action to prevent the faces from separating inadvertently. It was tentatively suggested that the generated pressures were due to vibration of the faces and the wear was due to impurities in the liquid. A centripetal pumping action of

appreciable magnitude was shown to occur under some conditions, so that the flow against a pressure gradient is possible.

Nahaldi and Osterle [9] studied the effects of face misalignment using different analytical techniques and found that axial vibrations increased or decreased the load bearing ability depending upon particular example. In 1960 Tanner [10,11]showed that the fact that the average pressure over the seal faces was greater than the oil pressure as was pointed out by Jagger [6]was unlikely to be explained by the effects of non-Newtonian behaviour of the fluid. Instead, as he suggested, it is possible that elastic deformation with this factor and surface tension may give a different result. He further mentioned that non-Newtonian effects do exist but the small order of magnitude of these effects will render them unimportant. In 1961 a number of papers [12-17] were presented in BHRA International Conference on Fluid Sealing. Both theoretical and experimental investigations were performed to have insight into the effects of frictional forces and surface roughness on sealing. Here the findings by Mayer [15] shares quite a significant contribution in that he found that higher pressure could be sealed with balanced seals than with unbalanced seals. This originally raised the question of why relatively small changes in balancing can alter the

maximum sealing pressure. This difference could be ascribed to the different lubricating regimes that might have existed between the seal faces.

Whitelay [18], in 1962 , brought out that the performance of seals is improved by using grooves. In 1963 Davies [19] and Lyman and Saibel [20] considered the effects of surface deformation and face misalignment respectively on leakage and axial forces. In 1967, some papers [21-23] presented in the Third International Conference on Fluid Sealing [BHRA] dealt amply with the hydrodynamic aspects of face seal lubrication. The pressure distribution in high pressure face seal was also touched upon. In 1968, the papers bearing the reference [24-27] discussed the hydrostatic and hydrodynamic large scale waviness and microasperities. The papers [28-35] published in 1969 further considered misalignment and vibrations of seal faces and microasperities of seals and demonstrated that these can cause hydrodynamic load support.

The period during 1970s can be cited as to have drawn appreciable amount of attention of various researchers to the functioning of a mechanical face seal. The effects of waviness, coning, misalignment, flexibility, roughness on leakage, axial and radial forces and moments

were mainly studied. Gibson et.al. [36] studied, in 1970, the elastohydrodynamic problem of reciprocating rubber seals for hydraulic actuators. The problem was that of a lubricated highly elastic surfaces in pure sliding. In 1971, Iny et.al. [37,38,39] presented a comprehensive theory of sealing based on the principles of hydrodynamic lubrication with the faces separated by a fluid film. He established that the hydrodynamic theory can be applied to the design of mechanical seals for more severe operating conditions. Field and Nau [40] in 1972 measured experimentally the oil film thickness and pressure distribution under an actual rectangular piston seal. He concluded that there is considerable difference in the behaviour of O-ring seals and rectangular seals. Lohou and Godet [41], in 1973 found that misalignment in radial face seal can cause hydrodynamic fluid pressure load support. Stanghan-Batch et.al. [42] applied hydrodynamic lubrication theory to an idealized wavy face seal. Extending the theory to cover radial flows in the fluid film the author indicated that the hydrodynamic film pressure combines with the curvature of the seal faces to induce an inward flow of fluid across the faces. The frequently observed inward flow phenomenon may be utilized to assist sealing. Under certain circumstances, however, the inward pumping effect can be a cause of seal failure, particularly at low fluid

pressures, and the choice of an inside or outside seal arrangement should be made to suit the duty required. The results of his work suggest that mechanical seal faces should not be lapped flat, but one of the faces should be given a deliberately wavy surface.

In all conditions of seal functioning the hydrodynamic effects are not the only ones that maintain lubricated gap in the face seals. This has led to the study of hydrostatic load support. Its significance impelled several researchers to use new techniques of predicting and controlling the radial face seal profile . Snapp and Sasdelli [43], assumed that the hydrostatic pressure drop across the seal faces is highly influenced by the gross deformation of the seal rings. In 1973 itself Metcalfe[44] carried out his work on pressure caused effects and found that pressure caused deformation resulted in divergent seal profile. An account of various developments have been embodied into the book by Mayer [45]. Radial variations in seal clearance affects both hydrodynamic and hydrostatic behaviour of primary seal ring. Moreover, the existence of full fluid film depends on both hydrodynamic and hydrostatic components of pressure. These investigations have been made by Zuk [46], Shapiro and Colsher [47] and Haardt [48] in 1974. In the same year Ruskell and Westcott [49] gave an account of analysis

made on the performance characteristics of thin lipped metal seals as compared to that of piston-ring seals. The work carried out in 1975 bears the reference [50-53] which, apart from discussing the seal dynamics , involves the effects of vibrations of seal ring in one degree of freedom. Field and Nau [53] also presented solution of elastohydrodynamic equations based on iteration scheme for a rectangular rubber seal.

In 1976 Ludwig [54] , Ludwig and Allen [55] and Metcalfe[56] studied further hydrodynamic pressure load support and pressure and thermal caused distortions. It was found that thermally caused rotation from friction results in a convergent seal profile and pressure caused deformation results in a divergent seal profile. Thermal deformation was further studied by Li [57] and Kilaparti [58], which led to the inference that thermal deformation prevents seal faces from remaining flat. To have better prediction of seal performance the consideration of face misalignment was deemed to be necessary. Ruskell [59] made a significant comparision between theoretical and experimental results for elastohydrodynamic lubrication of metal seals. It was demonstrated that an unusual seal profile is caused by the deformation of the seal. It was also predicted that thermal effects, non-Newtonian behaviour and thermoelastic effects have possible relevance to seals.

As in the case of microasperities and misalignment, large scale waviness can cause hydrodynamic fluid pressure load support. This was amply supported by the investigations of Lebeck et.al [61]and Lebeck [61,62] in 1977. Lebeck et.al [63], in 1978, gave experimental account of the effects of asperity on leakage and seal profile. Etsion [64,65] showed that the effect of curvature of a radial face seal is negligible. The effect of non-axisymmetric hydrostatic pressure due to radial variations in the film thickness is considerable, which in turn influences seal stability and wear of the outer and inner diameter. Hughes et.al [66] modeled a seal with a phase change using an idealized heat transfer model. Their results showed that the hydrostatic load support in a two phase seal is greater than for an all liquid or all gas seal . Patir and Cheng [67] suggested for incompressible flow that the flow equation should be multiplied by a factor ϕ depending on operational conditions. Metcalfe et.al [68] indicated that to improve seal performance in some cases the flatness of faces is deliberately disturbed. Wobble observation of primary seal ring is reported in [69].

In 1979 Lebeck [70,71] presented a mixed friction model including thermal rotation from frictional heating. Thermal and pressure caused rotation greatly alter face seal performance in the short run whereas after a period

of steady operation, the seal faces were parallel regardless of initial rotation. Thus this model can be applied to determine the effects of pressure and thermal rotation from frictional heating on performance of a face seal. In the same year Etsion and Etsion et.al [72-78] analysed the effects of coning misalignment and squeezing on the performance of a radial face seal considering both hydrodynamic and hydrostatic situation. .

A strong coupling was found between angular misalignment and transverse moment in both low and high pressure seals. Such coupling is a possible source of dynamic instability and can result in a wobbling of the primary seal ring. Hence, it can be concluded that the hydrodynamic transverse moment, which was overlooked in the past can affect mainly the dynamic stability of radial face seals and hence, has to be considered in any dynamic analysis of these seals. Further, the interaction between coning and diametral tilt has profound influence on seal performance. The axial separating force can be either positive or negative depending on the relation between the angle of tilt and the angle of coning. The same is true for tilting moment which can be either restoring or nonrestoring, and for the axial and angular stiffness of the sealing gap. Two different modes of

operation exist. In the first mode, contact between the mating faces, at maximum tilt, occurs on the outer diameter of the primary seal ring. In this case, high pressure on the inner diameter is needed for the stable operation. In the second mode, contact at maximum tilt is on the inner diameter of the seal ring, and high pressure on the outer diameter is needed for stable operation. Ruskell [79] found that with suitable geometry good lubrication for face seal is possible. He carried out experiments also for describing the lubrication of these seals.

In 1980 , Lebeck [80] and Young [81] brought out their experimental results showing how surface roughness and wear influence: load, seal-profile and leakage. Etsion et.al [82] analysed the effects of motion in 3 degrees of freedom of flexibly mounted seal ring on its stability and performance. A condition for angular stability is derived relating seal-operation-condition to its geometry and other design parameters. Walowit and Pinkus [83] gave a quantitative basis for the design and optimization of shrouded pocket face seals. It has been shown that for low seal pressures both hydrodynamic and squeeze film effects are important.

Suyanami and Masuda [84], in 1982, studied the behaviour of seal-ring in the shaft seal which operates on oil film to seal high pressure gas. The experiment was

performed on the 60 cm diameter seal ring. The analytical model is formulated and predicts the oval deformation of seal ring due to hot spots and that the oval shape rotates slowly but periodically according to the shift of hot spots. Theoretical predictions are confirmed to agree with experimental results. Krauter [85] described an experimental programme concerned with the elastohydrodynamic behaviour of sliding elastomeric seals for the stirling engine. During this programme an experimental apparatus was designed, built and used to measure oil film thickness distribution. For this oil film thickness measurement an optical interferometeric procedure was developed.

Etsion [86] analysed the Dynamic behaviour of a noncontacting face seal for the case of a rigidly mounted rotating seat and a flexibly mounted stationary ring taking into account various design parameters and operating conditions . The equations involved are non linear and solved numerically. The effects of various parameters (for instance, radii ratio and coning) on seal stability is discussed and an expression for critical stability is formulated.

1.5 PRESENT WORK

At one time it was commonly believed that leakage flow across the faces of a mechanical seal was prevented

by intimate contact between the two surfaces. Consequently seal design was oriented towards ensuring that face contact takes place over the whole face area and that wear is minimal under dry rubbing conditions which is achieved by rendering the faces as flat as possible. In addition to this one face was flexibly mounted in order to follow the inevitable run-out of the other. Majority of seals also have one of the faces made of carbon, which shows a considerable reluctance to seizure when in sliding contact with most engineering materials. Seal designs incorporating these features performed more or less satisfactorily for decades [39]. However, in recent years duty requirements have grown more severe such as higher pressure and temperature leading to face distortions,

It is now well established that for reliable operation over a long period, a radial-face mechanical seal must operate with its faces separated by a film of fluids [38]. But the present day requirements necessitate face seals to function under different conditions. Seal leakage and short seal life are frequently observed in the equipments associated with seals. Sudden seal failure has made mechanical face seals most unpredictable element. Thus in recent years a host of aspects influencing the operation of face seals have been studied.

Surface waviness, thermal distortions, surface roughness, vibrations etc. have been amply studied but we still fall short of adequate knowledge that may provide a better seal design.

Both hydrodynamic and hydrostatic effects were shown to have enormous influence over various seal characteristics [74,65] . Misalignments of the faces and coning are no less important in this regards [73]. Also, radial forces and squeeze effects are reported to be important in producing effects on seal performance [76,77]. In addition to this non-Newtonian effects do exist. Although non-Newtonian effects were reported to be insignificant [10,11], yet it is expected that a study of these effects when coupled with surface misalignment and flexibility of faces may lead to additional information that may help design a seal in a better way.

The present work is designed to study some of these aspects of radial face seals. The seal faces are assumed to be narrow in that it renders Reynolds equations worth yielding an analytical solution in some cases, as a consequence of elimination of circumferential pressure gradient from the original Reynolds equation. In fact circumferential pressure gradient becomes insignificant when compared with radial pressure gradient [38]. Also this assumption renders the

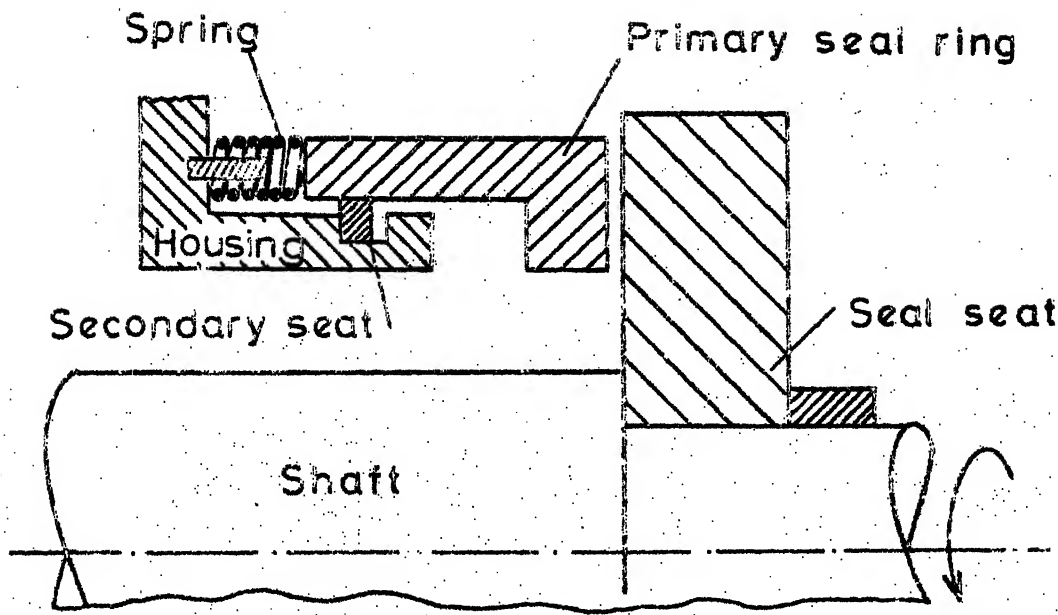

Fig. 1.1 End-face seal.

curvature effects insignificant, as has been pointed out in [64]. Thus the present work may be divided into two parts - Newtonian effects and non-Newtonian effects. These effects have been coupled with porosity, flexibility and squeeze effects. Misalignment and coning have also been studied simultaneously. Centrifugal inertial effects and effects of radial forces have also been discussed. Most of the discussion is centered on the axial forces and tilting moments. These are really vital for the stability and durability of face seals.

The Schematic of end-face seal is given in figure 1.1 .

CHAPTER II

CENTRIFUGAL INERTIA EFFECT IN A PARALLEL FACE SEAL

2.1 INTRODUCTION

It is now well established that, for a reliable operation of a radial face seal over a long period, it must be operated with its faces properly separated by a film of fluid. A proper gap is required to be maintained because too small a gap will enhance the wear of the faces and too big a gap will produce massive leakage. In both the cases the problem of early seal failure is encountered. Also significant is the dynamic instability which is wrought by the vibrational motion of the primary seal ring. Dynamic instability has been observed experimentally by Haardt and Godet [50] and Etsion and Burton [75]. Investigators have considered several factors that may influence the performance of a face seal which continues to be an unpredictable element in the absence of sufficient information. Lohou and Godet [41], Lebeck et.al [60] and Lebeck [61,62] and Etsion [72-78] considered the effects of misalignment. Surface waviness [42], thermal effect [54,55,57] , elastohydrodynamic effect [53,59], surface roughness [80,81] and squeeze effect [76] have already been studied, but there is no general theory as yet which can explain the strange behaviour of a radial face seal.

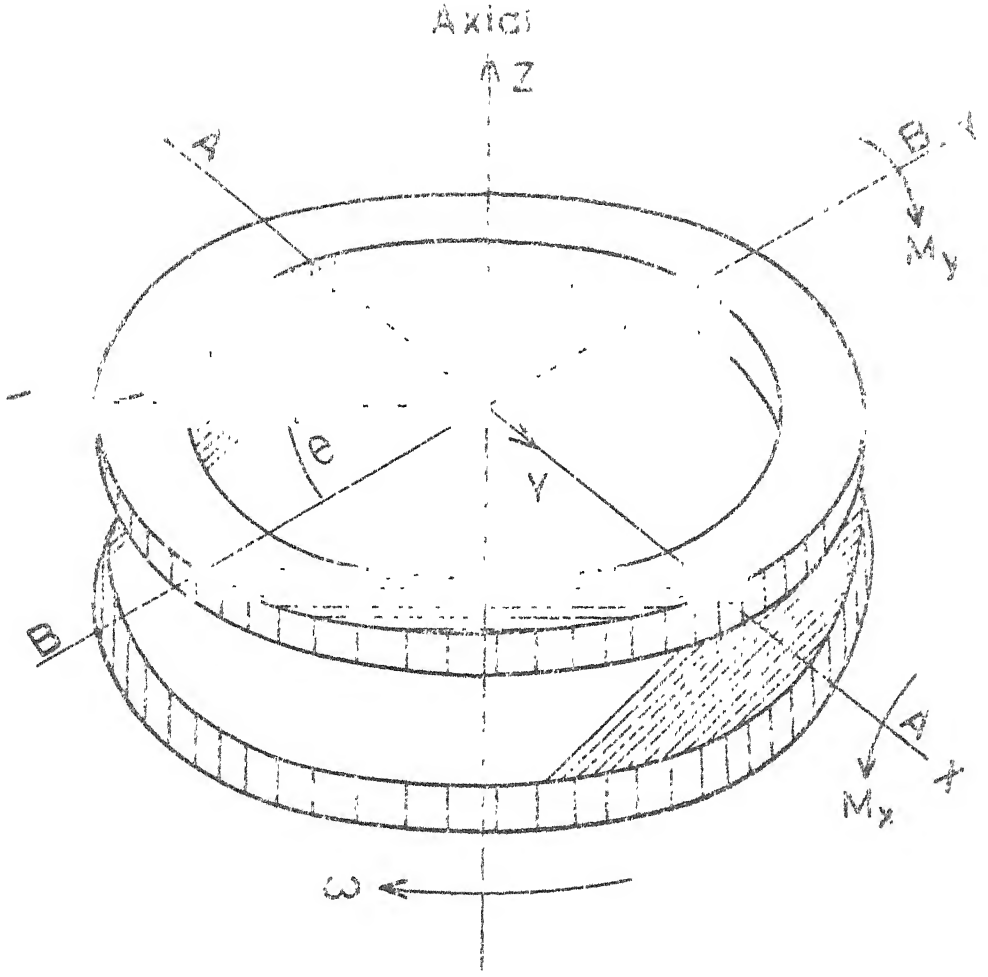

Fig 2.1 Parallel face seal

Primary seal ring, being flexibly mounted on a support, remains sensitive to a very small variation in the operational conditions. The secondary seal, on account of its high speed, may generate unavoidable amount of centrifugal inertia which in turn may well influence the performance of a face seal.

Therefore in this chapter we start with a simple parallel face seal and analyse the variation of axial force, transverse moment and leakage after including the centrifugal inertia term in the equation of motion.

2.2 MATHEMATICAL ANALYSIS

Figure 2.1 is the configuration of a parallel face seal. It is considered that the flow is laminar and axisymmetric, the fluid is incompressible and the viscosity is constant. Further, in accordance with the theory of lubrication, all inertia terms have been neglected except that of centrifugal inertia. It is also assumed that the pressure is independent of the z-coordinate.

The equations of motion, including the term of centrifugal inertia in it, are

$$\frac{dp}{dr} = \mu \frac{\partial^2 v}{\partial z^2} - \rho \frac{u^2}{r} \qquad (2.1)$$

and

$$\frac{\partial^2 u}{\partial z^2} = 0 \qquad (2.2)$$

where μ is the viscosity ρ is the density and (u,v) the components of velocity in (θ,r) directions respectively. p is the pressure at (r,θ).

The equation of continuity in the cylindrical coordinates is

$$\frac{1}{r}\frac{\partial}{\partial r}(rv) + \frac{1}{r}\frac{\partial u}{\partial \theta} + \frac{\partial w}{\partial z} = 0 \qquad (2.3)$$

where w is the velocity in the z direction.

The boundary conditions for the velocity components are (ω is the angular velocity of the rotor).

$$v = 0,\ u = 0 \text{ at } z = 0 \qquad (2.4)$$

$$v = 0,\ u = r\omega \text{ at } z = h \qquad (2.5)$$

The solutions for u and v are obtained by solving equations (2.1) and (2.2), using boundary conditions in equations (2.4) and (2.5). Finally we get

$$u = \frac{r\,\omega z}{h} \qquad (2.6)$$

and

$$v = \frac{1}{2\mu}\frac{dp}{dr}z(z-h) - \frac{\rho r\omega^2}{12\mu h^2}(z^4 - zh^3) \qquad (2.7)$$

Integrating the equation of continuity (2.3) across the film using the boundary conditions

$$w = 0 \text{ at } z = 0 \qquad (2.8)$$

$$w = 0 \text{ at } z = h \qquad (2.9)$$

we obtain

$$\frac{1}{r}\frac{\partial}{\partial r}\left(\int_o^h r\, v\, dz\right) + \frac{1}{r}\frac{\partial}{d\theta}\left(\int_o^h u\, dz\right) = -\left[w\right]_{z=o}^{z=h} \qquad (2.10)$$

where $\left[\ w\ \right]_{z=o}^{z=h}$ represents the value of w at z = 0 and z = h.
On further simplification, equation (2.10) reduces to

$$\frac{1}{r}\frac{\partial}{\partial r}\left[\ r\left\{-\frac{h^3}{12\mu}\frac{dp}{dr} + \frac{3}{120}\rho\frac{\omega^2 h^3 r}{\mu}\right\}\right] = 0 \qquad (2.11)$$

Equation (2.10) is the final equation governing the flow of the fluid film between the faces of seal.
Since h = constant, equation (2.10) reduces to

$$\frac{\partial}{\partial r}\left[\ r\left(\frac{dp}{dr} - \frac{3}{10}\rho\omega^2 r\right).\right] = 0 \qquad (2.12)$$

Equation (2.11) is solved with the help of the following boundary conditions

$$p=p_1 \text{ at } r=r_1 \text{ and } p=p_2 \text{ at } r = r_2 \qquad (2.13)$$

where r_1 and r_2 are inner and outer radii respectively.
p_1 is the inner pressure and p_2 is the outer pressure.
Thus the pressure distribution is given by the following expression

$$p = \left[\log\left(\frac{r}{r_1}\right)(p_1-p_2)\left(\frac{1}{\log\left(\frac{r_1}{r_2}\right)}\right)\right.$$

$$-\left\{\frac{3}{20}\rho\omega^2(r_1^2-r_2^2)\right\}\left\{\log\left(\frac{r}{r_1}\right)\frac{1}{\log\left(\frac{r_1}{r_2}\right)}\right\}$$

$$\left. + p_1 - \left\{\frac{3}{20}\rho\omega^2(r_1^2-r^2)\right\}\right] \qquad (2.14)$$

2.2.1 Axial Force :

The axial force is defined by

$$F_z = \int_{r_1}^{r_2} p\, 2\pi\, r\, dr \qquad (2.15)$$

On substituting for p form equation (2.14) in equation (2.15) and integrating, we get the expression for F_z as below

$$F_z = \frac{\pi}{2}\left[\{ 2r_2^2 \log\left(\frac{r_2}{r_1}\right) - (r_2^2 - r_1^2)\}\{(p_1 - p_2) - \frac{3}{20}\rho\omega^2(r_1^2 - r_2^2)\}\left(\frac{1}{\log\left(\frac{r_1}{r_2}\right)}\right) + 2p_1(r_2^2 - r_1^2) - \frac{3}{20}\rho\omega^2(r_1^2 - r_2^2)\right] \qquad (2.16)$$

2.2.2 Restoring Moment : The tilting moment about x axis, also called restoring moment, is defined by

$$M_x = -\int_0^{2\pi}\int_{r_1}^{r_2} p\, r^2 \cos\theta\, d\theta\, dr \qquad (2.17)$$

The factor pr^2 in the integrand $pr^2\cos\theta$ in equation (2.17) is a function of r only. Further, when $\cos\theta$ is integrated between the limits 0 and 2π, the integral becomes zero. Therefore

$$M_x = 0 \qquad (2.18)$$

2.2.3 Transverse Moment :

The moment about y axis is called the transverse

moment and is defined by

$$M_y = \int_0^{\pi} \int_{r_1}^{r_2} pr^2 \sin\theta \, d\theta \, dr \qquad (2.19)$$

for half face.

Substituting for p from equation (2.14) in equation (2.19) and integrating, the expression for M_y becomes

$$M_y = 2 \left[-\frac{1}{3} \left\{ r_2^2 \log\left(\frac{r_2}{r_1}\right) \right\} \left\{ \frac{1}{\log\left(\frac{r_1}{r_2}\right)} \right\} \right.$$

$$- \frac{1}{9}(r_2^3 - r_1^3)\{(p_1 - p_2) - \frac{3}{20}\rho\omega^2(r_1^2 - r_2^2)\}$$

$$\left. + \frac{1}{3}p_1(r_2^3 - r_1^3) + \frac{1}{100}\rho\omega^2(3r_2^5 + 2r_1^5 - 5r_1^2 r_2^3) \right] \qquad (2.20)$$

2.2.4 Leakage :

The leakage is the flow across the seal ring and is defined as

$$Q = \int_0^{2\pi h} v \, r \, d\theta \, dz \qquad (2.21)$$

Substituting for v from equation (2.7) in equation (2.21) and integrating we get

$$Q = -\frac{\pi}{6}\frac{h^3}{\mu} \left[\left\{ \frac{1}{\log\left(\frac{r_1}{r_2}\right)} \right\} \{(p_1 - p_2) - \frac{3}{120}\rho\omega^2(r_1^2 - r_2^2)\} \right] \qquad (2.22)$$

2.3 NON-DIMENSIONAL SCHEME

We adopt the following non-dimensional scheme

$$\bar{r} = \frac{r}{r_2} \; ; \; \bar{p}_1 = \frac{p_1}{p_2} \; ; \; \lambda = \frac{\rho\omega^2 r_2^2}{p_2} \; ; \; \bar{r}_1 = \frac{r_1}{r_2} \; ;$$

$$\bar{F}_z = \frac{2F_z}{\pi p_2 r_2^2} \; ; \; \bar{M}_y = \frac{M_y}{2r_2^3 p_2} \; ; \; \bar{Q} = \frac{Q}{(\pi h^3/6p_2\mu)} \qquad (2.23)$$

The non-dimensional axial force becomes

$$\bar{F}_z = \left[\{2\log(\frac{1}{\bar{r}_1}) - (1-\bar{r}_1)\} \{ \frac{1}{\log(\bar{r}_1)} \} \{ (\bar{p}_1 - 1) - \frac{3}{20}\lambda(\bar{r}_1^2 - 1) \} \right.$$

$$\left. + 2\bar{p}_1(1-\bar{r}_1^2) - \frac{3}{20}\lambda(\bar{r}_1^{-2} - 1)^2 \right] \qquad (2.24)$$

The non-dimensional form of the transverse moment is :

$$\bar{M}_y = \left[\{ \frac{1}{3}\log(\frac{1}{\bar{r}_1}) - \frac{1}{9}(1-\bar{r}_1^3) \} \{ \frac{1}{\log(\bar{r}_1)} \} \times \{ (\bar{p}_1 - 1) \right.$$

$$- \frac{3}{20}\lambda(\bar{r}_1^{-2} - 1) \} + \frac{1}{3}\bar{p}_1(1-\bar{r}_1^3)$$

$$\left. + \frac{1}{100}\lambda(3 + 2\bar{r}_1^{-5} - 5\bar{r}_1^{-2}) \right] \qquad (2.25)$$

The dimensionless form of the side leakage is :

$$\bar{Q} = -\{ \frac{1}{\log(\bar{r}_1)} \} \left[(\bar{p}_1 - 1) - \frac{3}{20}\lambda(\bar{r}_1^2 - 1) \right] \qquad (2.26)$$

2.4 RESULTS AND DISCUSSION

The dimensionless axial force $\bar{F}_z$, the transverse moment $\bar{M}_y$ and the leakage $\bar{Q}$ are calculated from equations (2.24), (2.25) and (2.26) respectively. The results are presented in the form of graphs in the figures 2.2, 2.3 and 2.4.

Each of the quantities $\bar{F}_z$, $\bar{M}_y$ and $\bar{Q}$ is a function of the inertia parameter $\lambda = \frac{\rho\omega^2 r_2^2}{p_2}$ and the radii ratio $\bar{r}_1 = \frac{r_1}{r_2}$. λ, for a fixed value of r_2, p_2 and the density ρ, would depend on the angular velocity ω. Thus the minimum value of λ can be zero which corresponds to the hydrostatic situation. The maximum value of λ would depend on the value of ω. In the present chapter we have taken the maximum value of λ to be 350. It may be even greater. Further, the radii ratio $\bar{r}_1$ would increase or decrease according as r_1 increases or decreases, or r_2 decreases or increases. In each case increasing $\bar{r}_1$ would signify decreasing the thickness of the seal ring. The present analysis assumes the value of $\bar{r}_1$ between .80 and .95 which is in accordance with the real situation.

Figure 2.2 represents the variation of dimensionless axial force $\bar{F}_z$ with the inertia parameter λ. This figure shows that, for all values of radii ratio $\bar{r}_1$, the dimensionless axial force $\bar{F}_z$ increases as λ increases. However, $\bar{F}_z$ decreases with an increase in the value of $\bar{r}_1$. The increase in the value of $\bar{F}_z$ with λ is sharper for smaller value of $\bar{r}_1$ than for large value of $\bar{r}_1$.

Figure 2.3 represents the graph between the non-dimensional transverse moment $\bar{M}_y$ for various values of $\bar{r}_1$. This figure shows that the transverse moment

decreases with an increase in the value of both λ and $\bar{r}_1$. However, the rate of decline in the values of $\bar{M}_y$ with an increase in λ is less for larger values of $\bar{r}_1$ than for smaller values of $\bar{r}_1$. It tends to become almost constant with respect to λ as $\bar{r}_1$ approaches unity.

Figure 2.4 represents the variation of non-dimensional leakage $\bar{Q}$ with λ and indicates that $\bar{Q}$ increases with an increase in both λ and radii ratio $\bar{r}_1$.

The aforesaid discussion leads to the conclusion that for a fixed value of $\bar{r}_1$, higher angular velocity results in higher values of axial force and leakage. Thus unless additional devices are used, the lubrication system in which the rotor has very low angular velocity, would witness an early failure of face seal because of massive wear in the absence of adequate separating force. On the other hand the systems in which rotor has very high angular velocity will starve for lubricant because of the massive leakage it will have to undergo. Thus a proper angular velocity of rotor is required to be maintained to ensure smooth functioning of face seal for a long period.

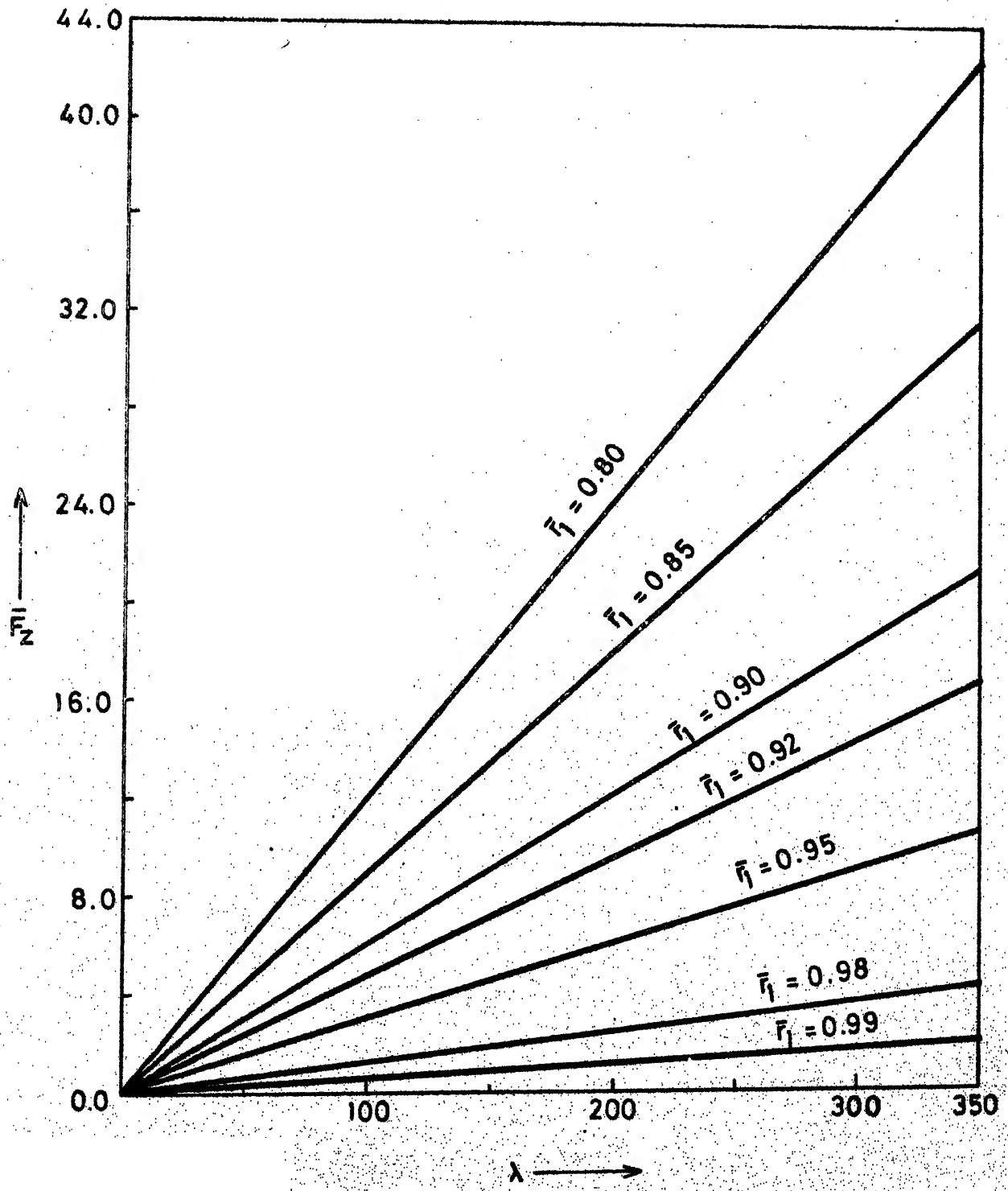

Fig. 2 2 Dimensionless axial force as a function of inertia parameter for various values of radii ratio.

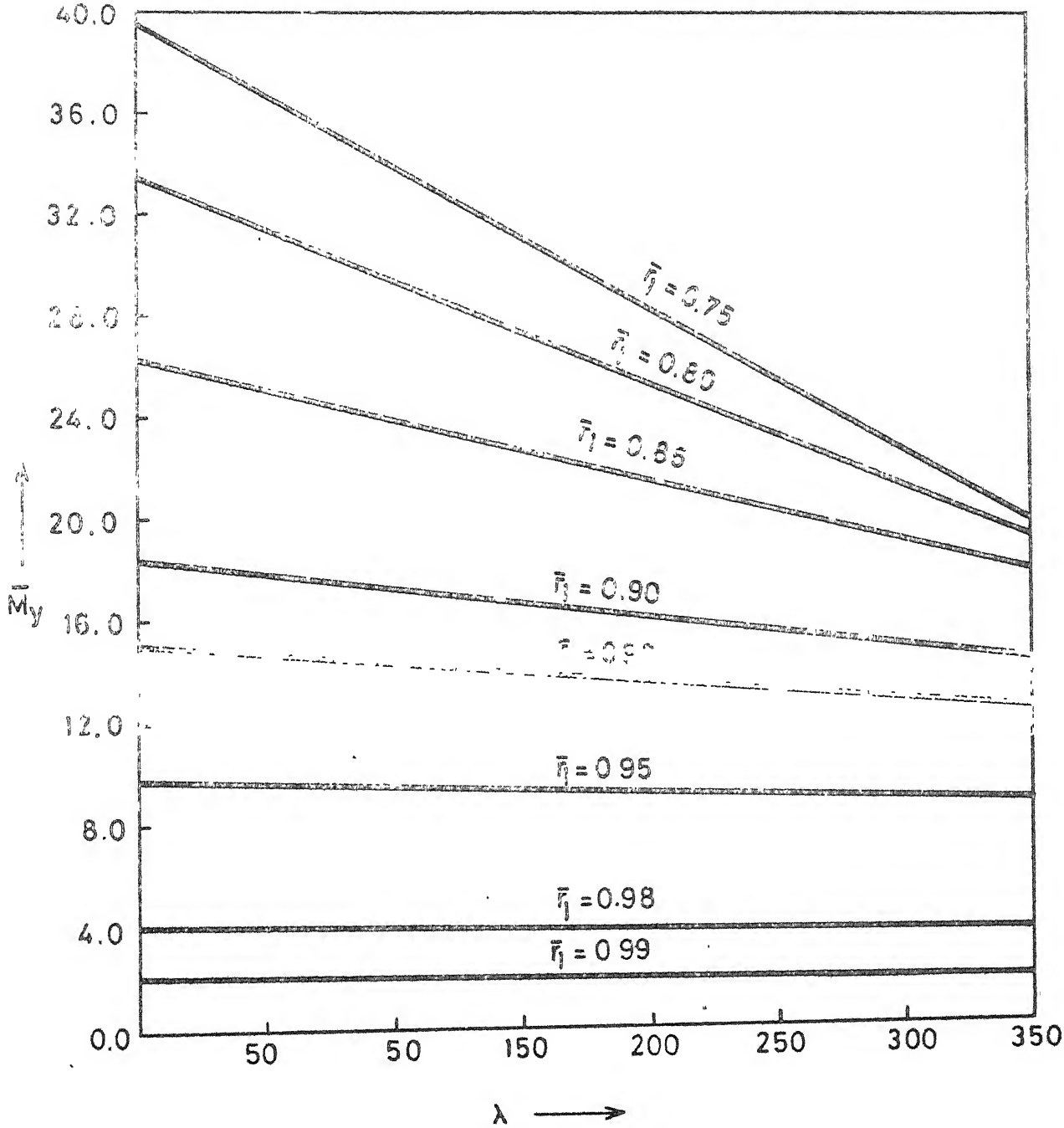

Fig. 2 3 Dimensionless transverse moment as a function of inertia parameter for various values of radii ratio.

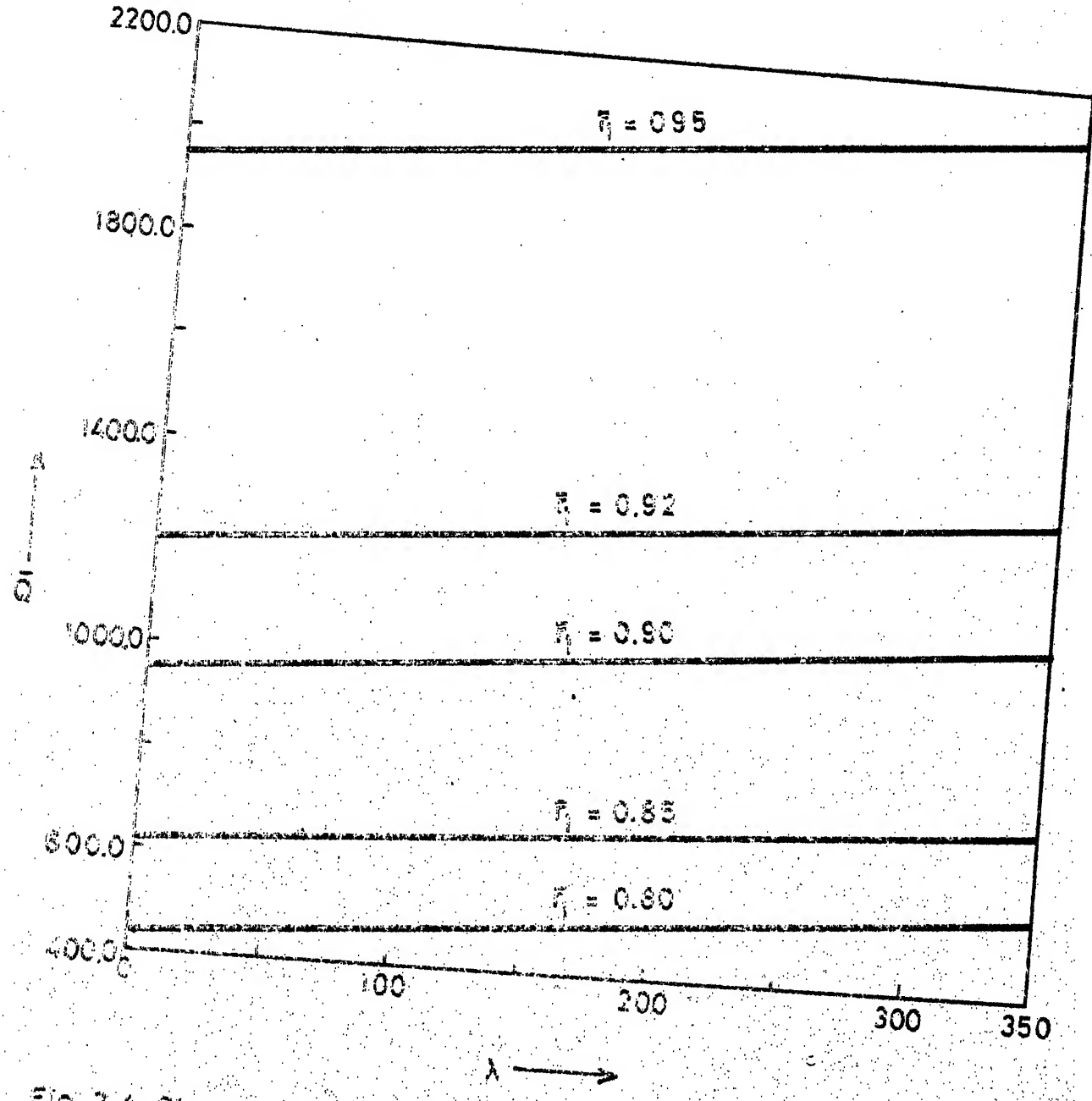

Fig 2.4 Dimensionless leakage as a function of inertia parameter fo various values of radii ratio.

CHAPTER III

SQUEEZE EFFECTS IN MISALIGNED RADIAL FACE SEALS WITH CONING

3.1 INTRODUCTION

The primary seal ring of an end-face seal is flexibly mounted on spring or bellows (Fig.1.1). Imperfections in the axisymmetry of such a support prevents the primary seal ring from being ideally perpendicular to the shaft. Since the clearance between primary real ring and seal seat is of the order of few micrometers, and since imperfections of this order of magnitude are almost inevitable in the flexible support, it is very likely that diametral tilt is inherent in end-face seals.

Coning of the mating faces is also inevitable due to thermal and mechanical distortions. Hence to predict accurately end-face seals' performance, both diametral tilt and coning have to be considered.

There is considerable scatter in the life of radial face seals. In an attempt to visuatize the crux of the problem, Sharoni and Etsion [72] considered the effects of coning on seal characteristics. Etsion [76]

This chapter has been published in the form of following research paper ''Squeeze Effect in Misaligned Radial Face Seal With Coning'', Wear, Vol.85,1983,p.143.

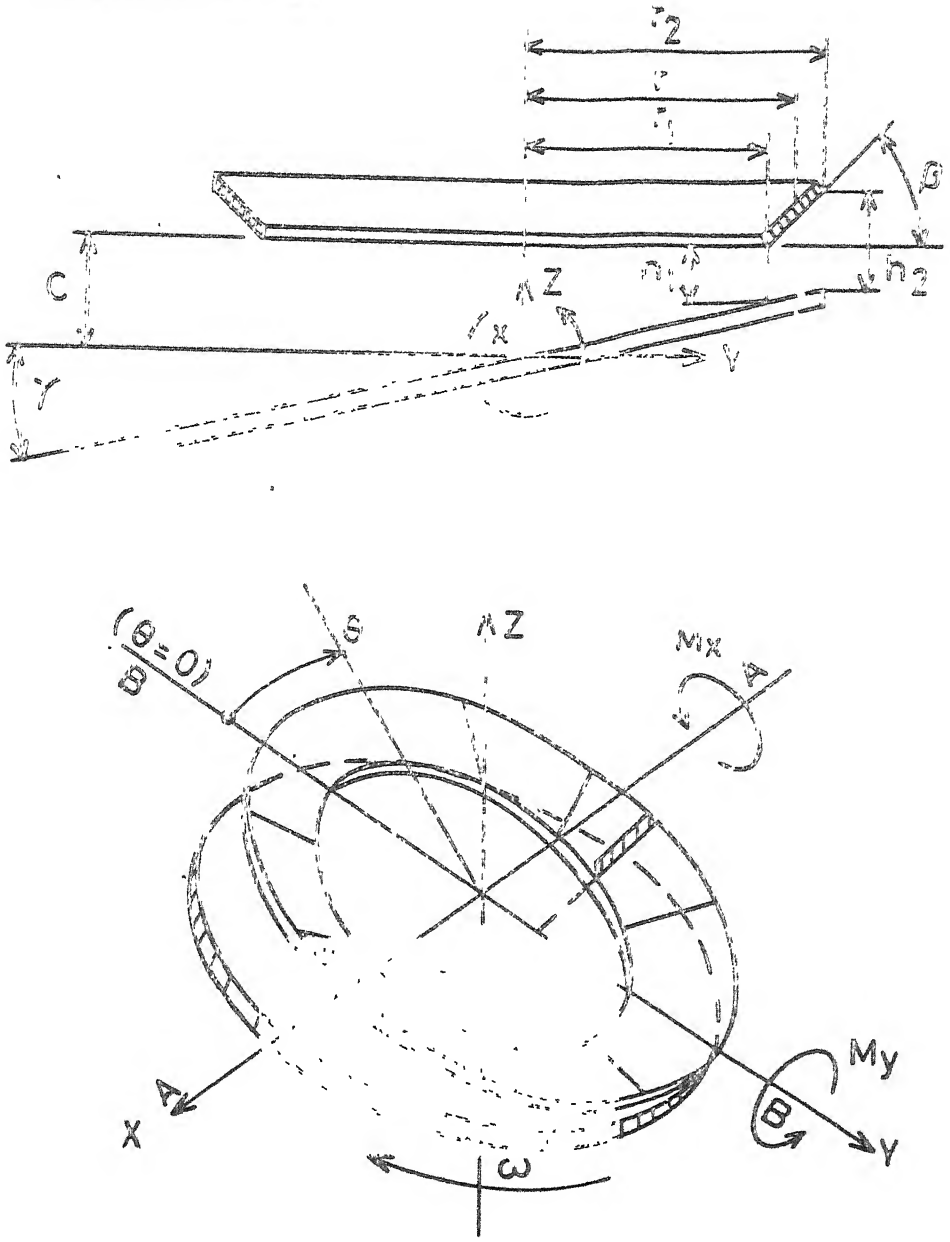

Fig 3.1 Face seal with diametral tilt and coning.

analysed radial face seals by treating the film thickness as time dependent and considering only misalignment of seal faces.

The analysis of ref. 72 has indicated that high pressure seal stability may be improved by coning. In the present chapter the squeeze effects in a misaligned high pressure radial face seal with coning is analysed. The film thickness was regarded as time-dependent and expressions for forces and moments have been obtained. Etsion's [76] analysis may be obtained as a special case of the present analysis.

3.2 MATHEMATICAL ANALYSIS

The Reynolds equation for a misaligned radial face seal (fig.3.1) using an incompressible fluid is

$$\frac{\partial}{\partial r}\left(rh^3 \frac{\partial p}{\partial r}\right) + \frac{1}{r}\frac{\partial}{\partial \theta}\left(h^3 \frac{\partial p}{\partial \theta}\right) = 6\mu r\left(\omega \frac{\partial h}{\partial \theta} + 2 \frac{\partial h}{\partial t}\right) \qquad (3.1)$$

where the film thickness h is (figure 3.1)

$$h = c + \gamma\, r \cos\theta + \beta(r - r_1) \qquad (3.2)$$

where c is the seal clearance along the central line joining the centres of seal faces, γ is the angle of tilt and (r,θ) is the coordinate of the point through which the thickness is measured, β is the angle of coning and r_1 is the inner radius of the seal ring.

Equation (3.1) may be solved separately for pure hydrodynamic, pure hydrostatic or pure squeeze effects but only the squeeze effects are considered here. Using the narrow seal approximation [64], equation (3.1) reduces to

$$\frac{\partial}{\partial r}\left(h^3 \frac{\partial p}{\partial r}\right) = 12\mu \frac{\partial h}{\partial t} \qquad (3.3)$$

where $\frac{\partial h}{\partial t}$ is obtained by differentiating the film thickness h in the equation (3.2). Thus

$$\frac{\partial h}{\partial t} = -v_c + \dot{\gamma}\ r_m \cos\theta \qquad (3.4)$$

where v_c is the velocity at the centre, i.e. $v_c = -\frac{\partial c}{\partial t}$, and $\dot{\gamma} = \frac{\partial \gamma}{\partial t}$. The symbol r_m denotes the mid radius i.e. $r_m = \left(\frac{r_1+r_2}{2}\right)$ where r_2 is the outer radius of the seal ring. By combining equations (3.3) and (3.4) we obtain

$$\frac{\partial}{\partial r}\left(h^3 \frac{\partial p}{\partial r}\right) = 12\mu\left(-v_c+\dot{\gamma}\ r_m \cos\theta\right) \qquad (3.5)$$

To integrate equation (3.5) the pressure boundary conditions are

$$p = 0 \text{ at } r = r_1 \text{ and at } r = r_2$$

$$\frac{\partial p}{\partial r} = 0 \text{ at some } r = r' \qquad (3.6)$$

where r' is the local radius corresponding to the pressure extremum.

Integration of equation (3.5) with respect to r gives

$$h^3 \frac{\partial p}{\partial r} = 12\mu(-v_c + \dot{\gamma} r_m \cos\theta)r + K_1(\theta) \qquad (3.7)$$

where $K_1(\theta)$ is the constant of integration which is a function of θ . To evaluate θ we make use of the second pressure condition given in the equation (3.6). Thus the value of $K_1(\theta)$ is obtained as

$$K_1(\theta) = -12\mu(-v_c + \dot{\gamma} r_m \cos\theta)r' \qquad (3.8)$$

On combining equation (3.7) and equation (3.8) we obtain final expression for the pressure gradient as the following

$$\frac{\partial p}{\partial r} = 12\mu \frac{(-v_c + \dot{\gamma} r_m \cos\theta)(r-r')}{h^3} \qquad (3.9)$$

Integrating equation (3.9) we get

$$p(r) = 12\mu(-v_c + \dot{\gamma} r_m \cos\theta)\int_{r_1}^{r} \frac{(r-r')}{h^3} dr + K_2(\theta) \qquad (3.10)$$

where $K_2(\theta)$ is the constant of integration which is a function of θ , Equation (3.10) and equation (3.6) together give $K_2(\theta) = 0$ and

$$r' = \left(\frac{\int_{r_1}^{r_2} \frac{r\,dr}{h^3}}{\int_{r_1}^{r_2} \frac{dr}{h^3}}\right) \qquad (3.11)$$

By solving equation (3.11) and then substituting the value

of r' in equation (3.10) and carrying out some algebraic manipulation we get the expression for the pressure as

$$p = \frac{6\mu\omega(v_c - \dot{\gamma}\, r_m \cos\theta)(r-r_1)(r_2-r)}{\{c+\gamma\, r\cos\theta + \beta(r-r_1)\}^2 \{c+\gamma\, r_m \cos\theta + \beta(r_m-r_1)\}} \qquad (3.12)$$

3.2.1 Axial Force :

The axial force is defined as [76]

$$F_z = 2\, r_m \int_0^{\pi} \int_{r_1}^{r_2} p\, dr\, d\theta \qquad (3.13)$$

3.2.2 Restoring Moment :

The restoring moment about x axis is defined as

$$M_x = -2 r_m^2 \int_0^{\pi} \int_{r_1}^{r_2} \cos\theta\, p\, dr\, d\theta \qquad (3.14)$$

3.2.3 Translational Damping Coefficient :

F_z is a function of both v_c and $\dot{\gamma}$ as does M_x. The translational damping coefficient F_v is defined as the value of axial force F_z when we put $\dot{\gamma} = 0$ in the expression of F_z. Thus

$$F_v = F_z \ (\dot{\gamma} = 0) \qquad (3.15)$$

3.2.4 Cross-coupled Damping Coefficient :

The cross-coupled damping coefficient $F_{\dot{\gamma}}$ is defined as the value of axial force F_z when we put $v_c = 0$ in the expression of F_z. Thus

$$F_{\dot{\gamma}} = F_z (v_c = 0) \qquad (3.16)$$

3.2.5 Rotational Damping Coefficient :

The rotational damping coefficient $M_{\dot{\gamma}}$ is defined as the value of the restoring moment M_x when we put $v_c = 0$ in the expression for M_x. Thus

$$M_{\dot{\gamma}} = M_x(v_c = 0) \tag{3.17}$$

3.3 NON-DIMENSIONAL SCHEME

The following substitutions are used

$$\bar{r} = \frac{r}{r_2} ; \bar{r} = \frac{r_1}{r_2} ; \bar{r}_m = \frac{r_m}{r_2} ; \varepsilon = \frac{\gamma r_2}{c} ; \delta = \frac{\beta r_2}{c}$$

$$\bar{F}_v = \frac{F_v}{24\mu v_c r_2 (\frac{r_2}{c})^3} ; \quad \bar{F}_{\dot{\gamma}} = \frac{F_{\dot{\gamma}}}{24\mu\dot{\gamma} r_2^2 (\frac{r_2}{c})^3} \tag{3.18}$$

$$\bar{M}_{\dot{\gamma}} = \frac{M_{\dot{\gamma}}}{24\mu\dot{\gamma} r_2^3 (\frac{r_2}{c})^3} ; \quad \bar{M}_v = \frac{M_v}{24\mu v_c r_2^2 (\frac{r_2}{c})^3}$$

Using this scheme to obtain the dimensionless pressure as the following

$$\bar{p} = \frac{6\mu (\frac{r_2}{c})^3 (\frac{v}{r_2} - \dot{\gamma}\bar{r}_m \cos\theta)(\bar{r}-\bar{r}_1)(1-\bar{r})}{\{1+\varepsilon\bar{r}\cos\theta + \delta(\bar{r}-\bar{r}_1)\}^2 \{1+\varepsilon\bar{r}_m\cos\theta + \delta(\bar{r}_m-\bar{r}_1)\}} \tag{3.19}$$

Now let us suppose

$$I = \int_{\bar{r}_1}^{1} \bar{p}\, d\bar{r} = \frac{1}{(\varepsilon\cos\theta)^3} \left[\log\left\{\frac{1+\varepsilon\cos\theta+\delta(1-\bar{r}_1)}{1+\varepsilon\bar{r}_1\cos\theta}\right\} - \left\{\frac{(1-\bar{r}_1)(\varepsilon\cos\theta+\delta)}{1+\varepsilon\bar{r}_m\cos\theta+\delta(\bar{r}_m-\bar{r}_1)}\right\}\right] \tag{3.20}$$

Using equation (3.20) in the formula for the translational damping coefficient F_v, the rotational damping coefficient $\bar{M}_{\dot{\gamma}}$ and the cross-coupled damping coefficient $F_{\dot{\gamma}}$, we obtain the non-dimensional integrals for their expressions as the following

$$\bar{F}_v = \bar{r}_m \int_o^\pi I \, d\theta$$

$$= \bar{r}_m \int_o^\pi \frac{1}{(\varepsilon\cos\theta)^3} \left[\log\left\{\frac{1+\varepsilon\cos\theta+\delta(1-\bar{r}_1)}{1+\varepsilon\bar{r}_1\cos\theta}\right\}\right.$$

$$\left. -\left\{\frac{(1-\bar{r}_1)(\varepsilon\cos\theta+\delta)}{1+\varepsilon\bar{r}_m\cos\theta+\delta(\bar{r}_m-\bar{r}_1)}\right\}\right] d\theta \qquad (3.21)$$

and

$$\bar{F}_{\dot{\gamma}} = \bar{M}_v$$

$$= -\bar{r}_m^2 \int_o^\pi \frac{1}{\varepsilon^3\cos^2\theta} \left[\log\left\{\frac{1+\varepsilon\cos\theta+\delta(1-\bar{r}_1)}{1+\varepsilon\bar{r}_1\cos\theta}\right\}\right.$$

$$\left. -\left\{\frac{(1-\bar{r}_1)(\varepsilon\cos\theta+\delta)}{1+\varepsilon\bar{r}_m\cos\theta+\delta(\bar{r}_m-\bar{r}_1)}\right\}\right] d\theta \qquad (3.22)$$

and

$$\bar{M}_{\dot{\gamma}} = -\bar{r}_m^3 \int_o^\pi I\cos^2\theta \, d\theta$$

$$= \bar{r}_m^3 \int_o^\pi \frac{1}{\varepsilon^3\cos} \left[\log\left\{\frac{1+\varepsilon\cos\theta+\delta(1-\bar{r}_1)}{1+\varepsilon\bar{r}_1\cos\theta}\right\}\right.$$

$$\left. -\left\{\frac{(1-\bar{r}_1)(\varepsilon\cos\theta+\delta)}{1+\varepsilon\bar{r}_m\cos\theta+\delta(\bar{r}_m-\bar{r}_1)}\right\}\right] d\theta \qquad (3.23)$$

3.4 RESULTS AND DISCUSSION

The dimensionless translational damping coefficient $\bar{F}_v$, the cross-coupled damping coefficient $\bar{F}_{\dot{\gamma}}$ or $\bar{M}_v$ and the dimensionless rotational damping coefficient $\bar{M}_{\dot{\gamma}}$ are evaluated by numerical integration of equations (3.21), (3.22) and (3.23) respectively. Each of $\bar{F}_v$, $\bar{M}_{\dot{\gamma}}$, $\bar{F}_{\dot{\gamma}}$ is a function of tilt parameter ε and coning parameter δ. The minimum value for both $\varepsilon = \frac{\gamma r_2}{c}$ and $\delta = \frac{\beta r_2}{c}$ is equal to zero. This corresponds to the cases of no angular misalignment and no coning respectively. The expression for the film thickness from equation (3.2) can be written as

$$\frac{h}{c} = 1+\varepsilon\bar{r}\cos\theta +\delta(\bar{r}-\bar{r}_1)$$

$\theta = \pi$ corresponds to minimum film thickness (figure 3.1). Thus when $\theta = \pi$, the film thickness, because of the misalignment, is minimum only if $\varepsilon \leq 1$. But if $\varepsilon > 1$, a negative film thickness is obtained which is meaningless. Thus the maximum value that ε can take is 1. Further, when $r = r_2$, $\theta = \pi$ and $\varepsilon = 1$, the non-dimensional film thickness $\frac{h}{c} = \delta(1-\bar{r}_1)$. For all practical purposes the value of $\bar{r}_1$ can be as near to 1 as .98 (this means the thickness of seal ring is very small). Thus when $\bar{r}_1 = .98$, $\frac{h}{c} = \delta \times .02$. Further, $\frac{h}{c} < 1$ at the end where $\theta = \pi$ and $r = r_2$. Therefore, the maximum value that δ can assume

is the one which keeps the value of $\frac{h}{c} = \delta(1-\bar{r}_1)$ smaller than 1. Which is possible when $\delta \leq 10$. Thus in present discussion the maximum value of δ is taken to be 10.

Each of the characteristics has been plotted as a function of the tilt parameter ε, the value of which vary between 0 and 1, for the values of δ varying between 0 and 10.

The positive values of the coefficients $\bar{F}_v$ and $\bar{M}_{\dot{\gamma}}$ indicate that if the seal ring is disturbed from a certain position (c,γ), the response F_v and $M_{\dot{\gamma}}$ restrict the disturbance.

The cross-coupled damping coefficient shows a tendency to restore any given tilt of the faces, that is a positive $\dot{\gamma}$ which increases the tilt angle γ, generates a separating force $F_{\dot{\gamma}}$ this in turn increases the clearance c. A positive v which decreases the clearance c, produces a moment M_v which reduces the tilt γ. In both cases, the result is a stabilizing effect tending to prevent any contact between mating faces.

Figures 3.2 and 3.3 indicate that the translational damping coefficient remains almost constant at small tilts and increases sharply as the tilt parameter approaches unity.

Figures 3.4 and 3.5 show that the cross-coupled damping coefficient depends strongly on the tilt parameter. At small values of tilt parameter ε, which results from small tilt angle γ, or large seal clearance c, the coupling effects are small. As ε increases and approaches unity, the cross-couple damping coefficient registers a sharp increase.

Figure 3.6 and 3.7 indicate that the behaviour of the rotational damping coefficient is essentially the same as that of the translational damping coefficient.

All of the graphs show that as δ increases, the values of forces and moments decrease. They decrease with an increase in the value of radius ratio.

Finally, it may be concluded that squeeze with coning may be desirable where the large values of the separating forces produce leakage, because coning causes a reduction in these forces.

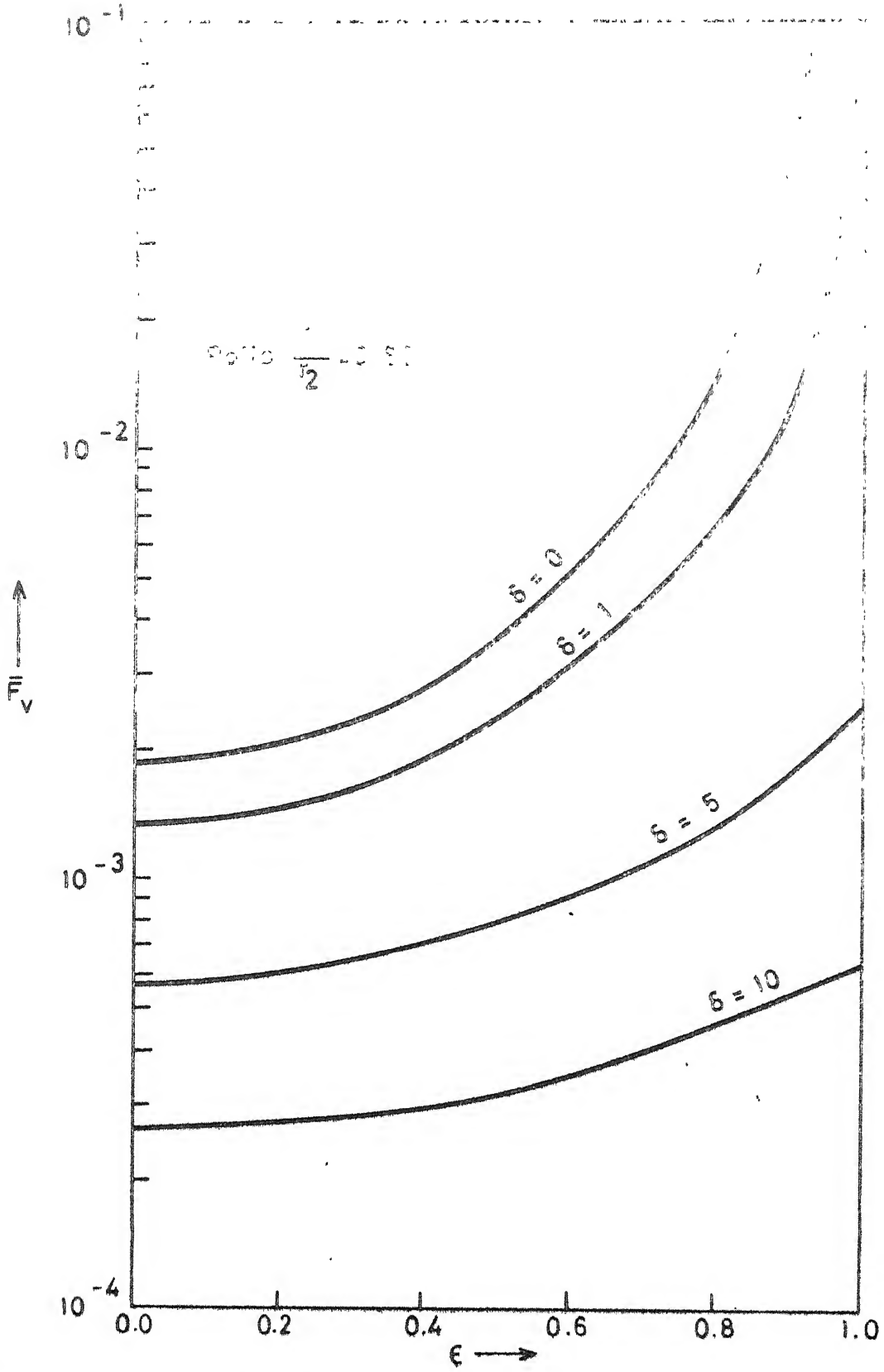

Fig. 3.2 Dimensionless translational damping coefficient as a function of tilt parameter for various values of coning parameter

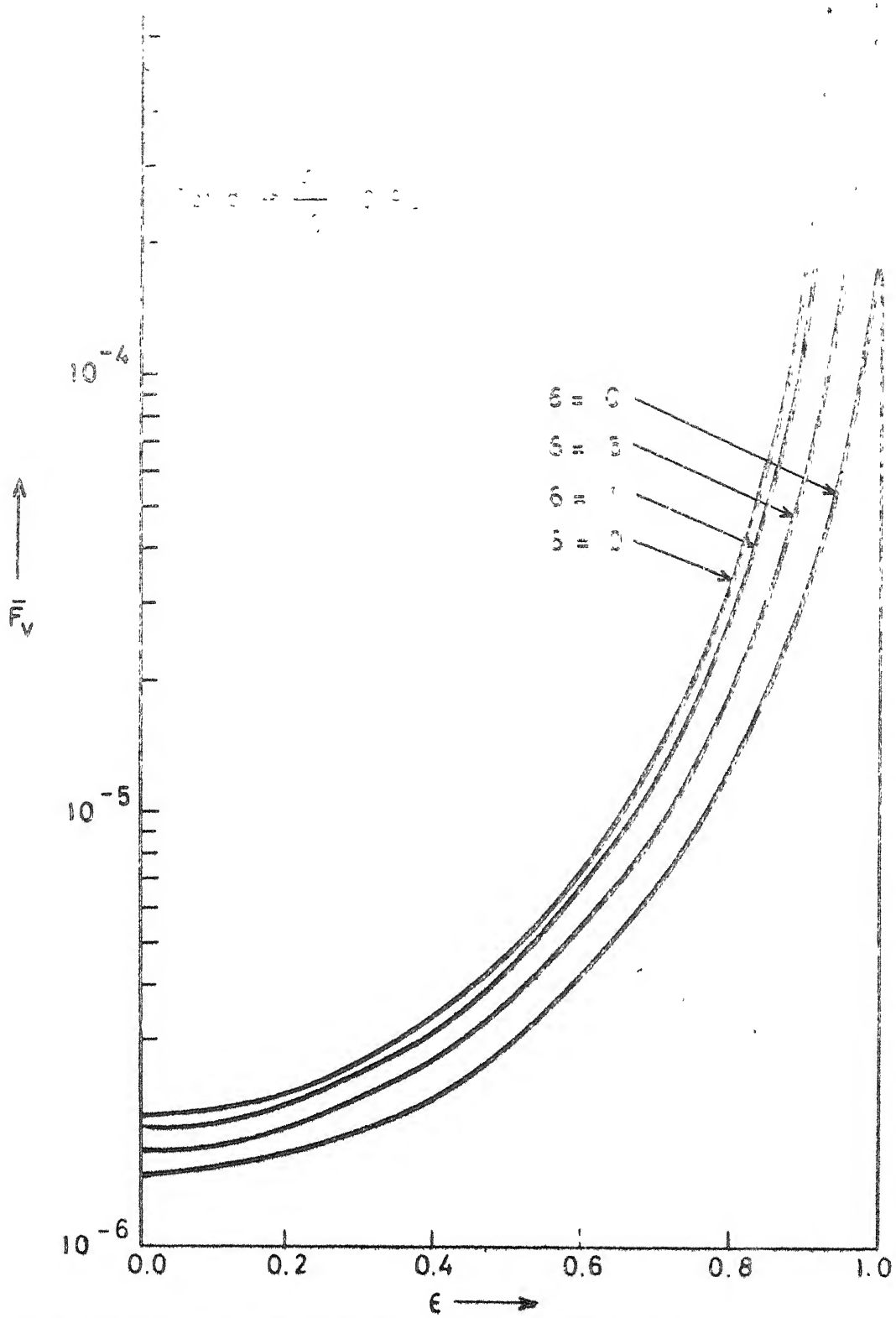

Fig. 3.3 Dimensionless translational damping coefficient as a function of tilt parameter for various values of coning parameter

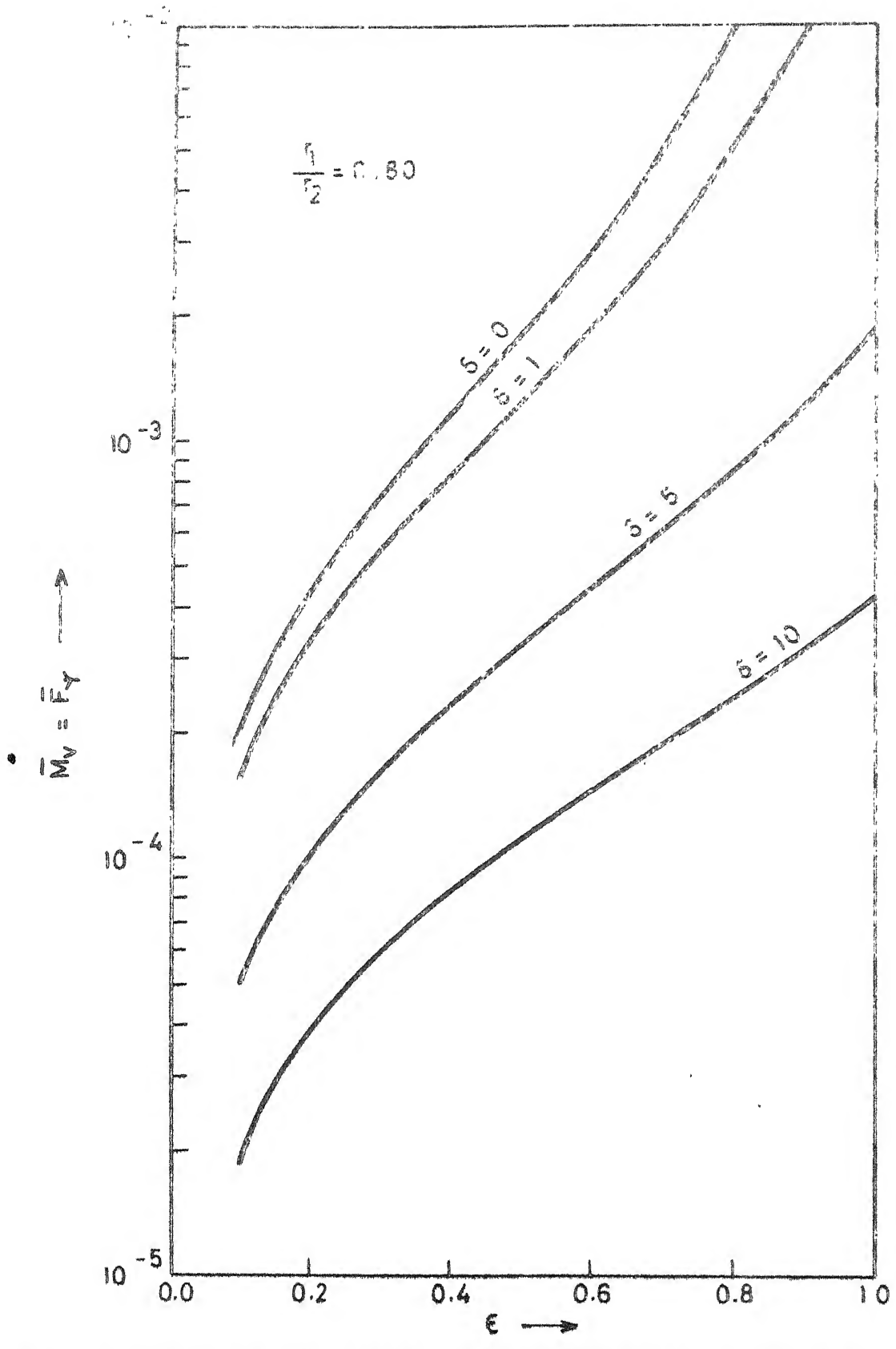

Fig. 3.4 Dimensionless cross-coupled damping coefficient as a function of tilt parameter for various values of coning parameter.

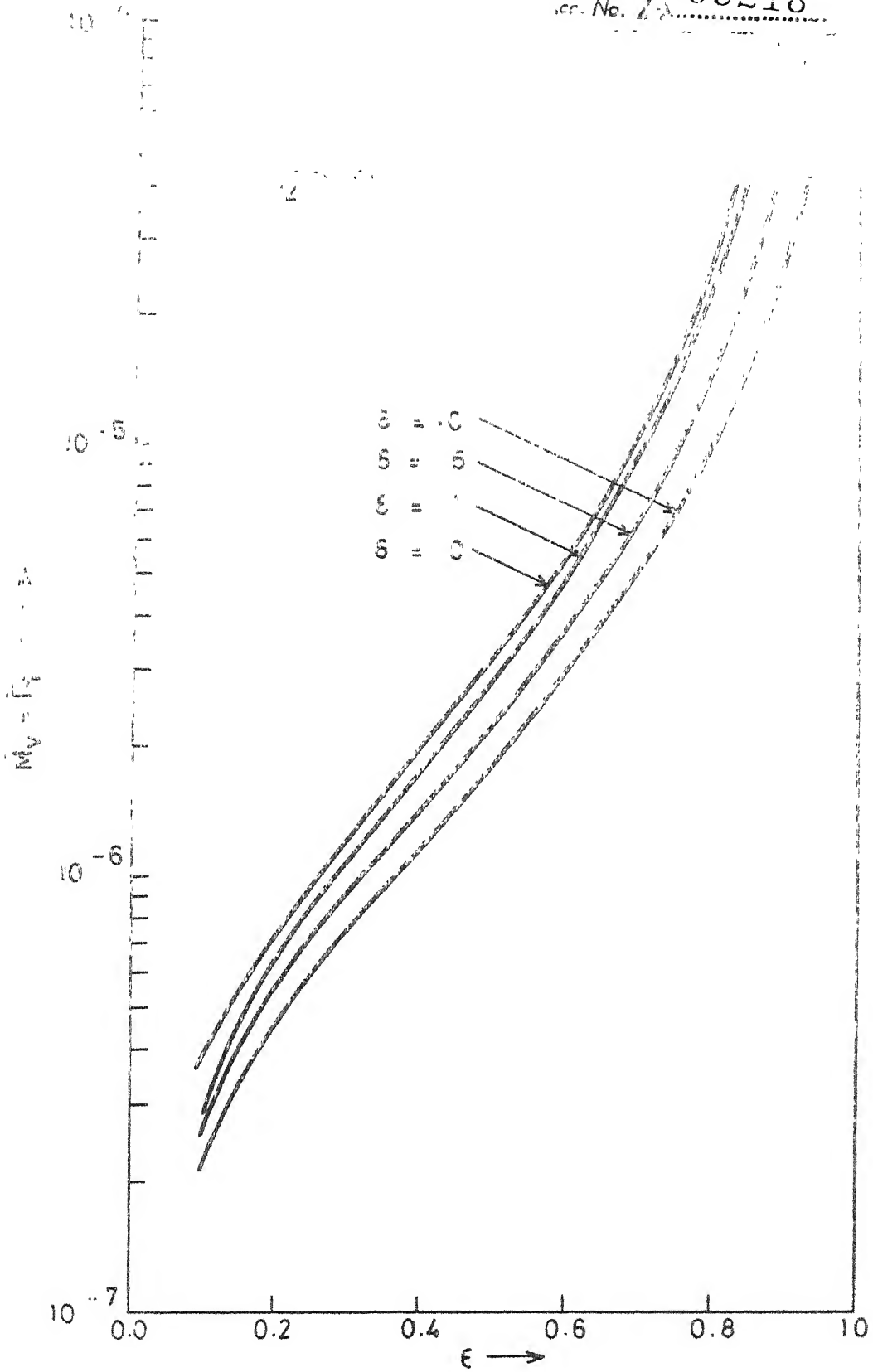

Fig 3 5 Dimensionless cross-coupled damping coefficient as a function of tilt parameter for various values of coning parameter

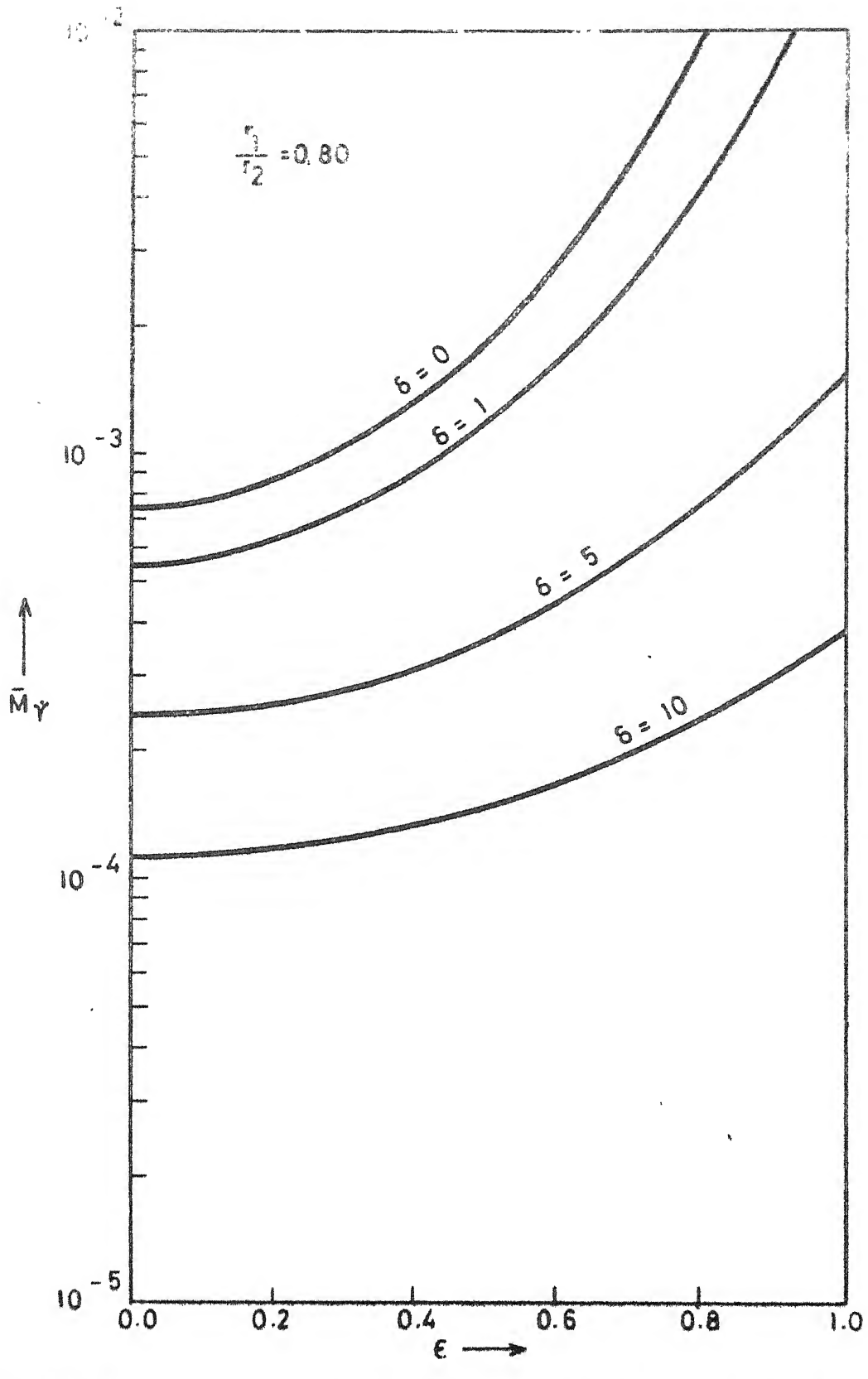

Fig. 3.6 Dimensionless rotational damping coefficient as a function of tilt parameter for various values of coning parameter

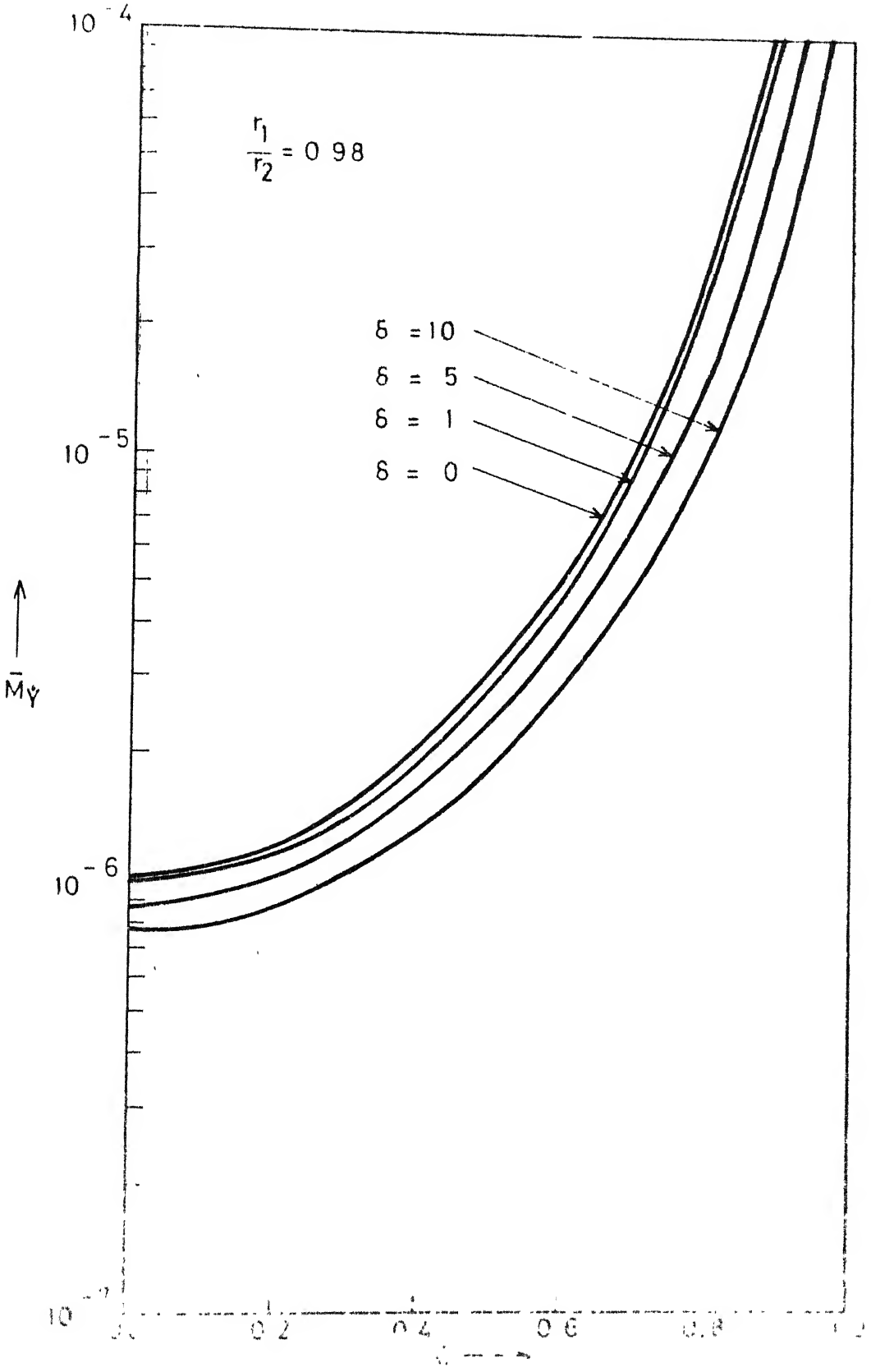
10^{-4}
$\frac{r_1}{r_2} = 0.98$
δ = 10
δ = 5
δ = 1
δ = 0
10^{-5}
10^{-6}
$\bar{M}\dot{\gamma}$
0.2
0.4
0.6
0.8

CHAPTER IV

HYDRODYNAMIC EFFECTS IN POROUS RADIAL FACE SEALS WITH MISALIGNMENT

4.1 INTRODUCTION

A radial face seal (fig.4.1) is probably the most non-predictable machine element. However, face seals are widely used in a host of industrial equipment and in other applications. The inability to predict seal life within reasonable accuracy is a major disadvantage and seal failure is a common problem. Recently many investigators have treated the problem and there have been several hypotheses put forth to explain the mechanism responsible for the development of lubricating film pressure that acts to separate the primary seal faces. These hypotheses include surface angular misalignment [28,29], surface waviness [27,42], microasperities [30] and thermal deformation [57,58]. Inspite of these investigations, the theory of face seal lubrication demands still more attention.

The restoring moment which is an important factor for stabilising or destabilising the seal-function has been discussed in [52,55,65]. The transverse moment that leads the angular misalignment vector by 90° is generated by hydrodynamic effects [74]. The author

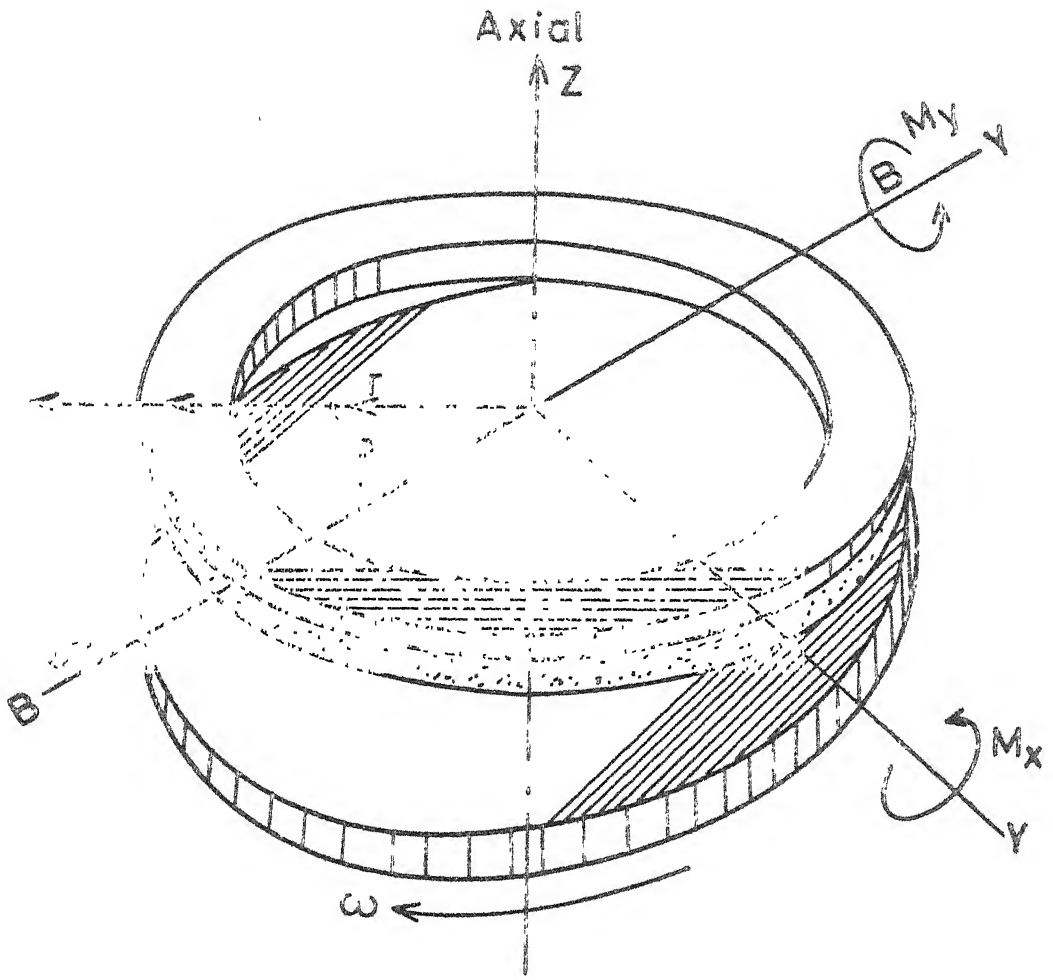

Fig 4.1 Porous face seal with angular misalignment

has shown that the transverse moment due to the angular misalignment of the seal faces can result in a wobbling of the primary seal ring. It is further concluded that the hydrodynamic transverse moment certainly plays an important role in radial face seal operation.

The analysis made by [74] include only angular misalignment. However, a face seal may be sufficiently influenced by several other factors depending on the operational conditions and nature of the face material of a face seal. This is significant because, apart from influencing other seal characteristics, these may influence transverse moment also which determines dynamic stability of a face seal. One of several factors is the porosity of the seal faces.

The porosity of the faces, which has not yet been analysed for misaligned face seals, constitute the main objective of this chapter. The primary seal ring is considered to be coated with a porous material (figure 4.1) and the faces are considered to be misaligned.

4.2 MATHEMATICAL ANALYSIS

The Reynolds equation for a narrow seal with incompressible fluid as lubricant is :

$$\frac{\partial}{\partial r}(r\, h^3\, \frac{\partial p}{\partial r}) = 6\mu\omega r\frac{\partial h}{\partial \theta} + 12\,\mu r(v_h - v_o) \qquad (4.1)$$

where h is the film thickness, v_h is the velocity of fluid at the face of secondary seal at z = h and v_o is the velocity of the fluid at z = 0 i.e. at the face of primary seal ring which is porous. p is the pressure of the fluid between the faces at a pt. (r,θ).

Assuming that the flow in the porous shell in fig. 4.1 is governed by Darcy's law [87]

$$q_\theta = -\frac{\varphi}{\mu}\frac{1}{r}\frac{\partial P}{\partial \theta} \qquad (4.2)$$

$$q_r = -\frac{\varphi}{\mu}\frac{\partial P}{\partial r} \qquad (4.3)$$

and

$$q_z = -\frac{\varphi}{\mu}\frac{\partial P}{\partial z} \qquad (4.4)$$

where φ is the permeability, μ is the viscosity of the fluid P is the pressure in the porous medium q_θ, q_r and q_z are the respective flux of the fluid in the θ, r and z directions.

The equation of continuity in cylindrical coordinates system is :

$$\frac{\partial v_r}{\partial r} + \frac{v_r}{r} + \frac{1}{r}\frac{\partial v_\theta}{\partial \theta} + \frac{\partial v_z}{\partial z} = 0$$

Equation of continuity may also be written as :

$$\frac{\partial}{\partial r}(q_r) + \frac{\partial}{r\partial\theta}(q_\theta) + \frac{\partial}{\partial z}(q_z) = 0 \qquad (4.5)$$

Since the circumferential pressure gradient in annular cases are much smaller than other pressure gradients [38], the term involving q_θ can be neglected in the equation of continuity (4.5) because $\frac{\partial p}{\partial \theta}$ is neglegible as compared to $\frac{\partial p}{\partial r}$. Thus on putting the values of q_r and q_z from equations (4.3) and (4.4) in equation (4.5), the equation of continuity reduces to

$$\frac{\partial^2 P}{\partial r^2} + \frac{\partial^2 P}{\partial z^2} = 0 \qquad (4.6)$$

(ρ and μ are independent of r and z).

It is reasonable to assume that $\frac{\partial P}{\partial z}$ is linear across the porous matrix [87]. Finally from equation (4.4) we have $\frac{\partial P}{\partial z} = 0$ at the outer surface of the porous shell, since there is no axial flow of the lubricant there.

These assumptions can be expressed as

$$\frac{\partial P}{\partial z} = \xi(z+H) \text{ and } \frac{\partial P}{\partial z}\Big|_{z=-H} = 0 \qquad (4.7)$$

where ξ is a constant depending on r only and H is the thickness of the porous shell, i.e., z = -H refers to a point on the outer surface and

$$V_o = -\frac{\rho}{\mu}\frac{\partial P}{\partial z}\Big|_{z=0} \qquad (4.8)$$

From equation (4.7) we have

$$\frac{\partial^2 P}{\partial z^2} = \xi = \frac{1}{(z+H)} \frac{\partial P}{\partial z} \tag{4.9}$$

On using equation of continuity (4.6) here, we obtain

$$\frac{\partial P}{\partial z} = (z+H) \frac{\partial^2 P}{\partial z^2} = -(z+H) \frac{\partial^2 P}{\partial r^2} \tag{4.10}$$

Furthermore, we have $v_h = 0$ at $z = h$ because secondary real seat is not supposed to be porous. Also, the pressure is continuous at the interface, i.e. $p = P$ at $z = 0$.

In view of equations (4.8) and (4.10) we have

$$V_o = \frac{\alpha}{\mu} H \frac{\partial^2 p}{\partial r^2} \tag{4.11}$$

Also, equations (4.6) and (4.9) together give

$$\frac{\partial^2 P}{\partial r^2} = - \frac{\partial^2 P}{\partial z^2} = -H - \xi \tag{4.12}$$

On using equation (4.11) in equation (4.1) we have the final governing equation as :

$$\frac{\partial}{\partial r}\left(rh^3 \frac{\partial p}{\partial r}\right) = 6\mu\omega r \frac{\partial h}{\partial \theta} - 12\rho Hr \frac{\partial^2 p}{\partial r^2} \tag{4.13}$$

Using the analysis for narrow seals in [64], equation (4.13) further reduces to the following

$$\frac{\partial}{\partial r}\left[(h^3+12\rho H) \frac{\partial p}{\partial r}\right] = 6\mu\omega \frac{\partial h}{\partial \theta} \tag{4.14}$$

where h, the film thickness, is expressed as

$$h = c + \gamma\, r \cos\theta$$

where c is the clearance of the seal faces along the line joining their centres and γ is the angle of tilt.

Now

$$\frac{\partial h}{\partial \theta} = -\gamma\, r \sin\theta \qquad (4.15)$$

Substituting for $\frac{\partial h}{\partial \theta}$ from equation (4.15) in equation (4.14), we obtain

$$\frac{\partial}{\partial r}\left[(h^3+12\eta H)\,\frac{\partial p}{\partial r}\right] = -6\mu\,\omega\,\gamma r \sin\theta \qquad (4.16)$$

Integrating equation (4.16) with respect to r we get

$$\frac{\partial p}{\partial r} = \frac{-3\mu\,\omega\,\gamma r^2 \sin\theta + K(\theta)}{(h^3+12\eta H)} \qquad (4.17)$$

where $K(\theta)$ is the constant of integration which is a function of θ .

Therefore

$$p(r) = \int_{r_1}^{r} \frac{\left[(-3\mu\,\omega\,\gamma r^2 \sin\theta\,) + K(\theta)\,\right]}{(h^3+12\eta H)}\, dr \qquad (4.18)$$

We have the following boundary conditions :

$$p(r_1) = 0 = p(r_2)$$

Therefore

$$p(r_2) = 0 = \int_{r_1}^{r_2} \left[\frac{(-3\mu\,\omega\,\gamma r^2 \sin\theta + K(\theta)}{(h^3+12\eta H)}\right] dr$$

which yields the value of $K(\theta)$ as :

$$K(\theta) = \frac{\int_{r_1}^{r_2} \frac{3\mu\omega\gamma r^2 \sin\theta}{(h^3+12\phi H)}\, dr}{\int_{r_1}^{r_2} \frac{dr}{(h^3+12\phi H)}} \qquad (4.19)$$

In view of [74] , in the absence of hydrostatic component, cavitation is assumed to occur in the region where $\frac{\partial h}{\partial \theta} > 0$ i.e. when $\theta > \pi$ and thus pressure is assumed to be zero for $\theta > \pi$. But when the hydrostatic component does exist, the extent of cavitation is dependent on the pressure differential across the seal boundaries. The cavitation zone decreases as the sealed pressure increases until a full fluid film condition is reached. We shall now consider the cavitation flow.

4.3 CAVITATION FLOW

4.3.1 Axial Force :

In the case of very small pressure differential across the seal boundaries, the axial force is defined as [74].

$$F_z = \int_0^{\pi} \int_{r_1}^{r_2} pr\, dr\, d\theta$$

Integrating the right hand side of the equation by parts we get a more simple form for F_z as the following:

$$F_z = -\frac{1}{2}\int_0^{\pi}\int_{r_1}^{r_2} \frac{\partial p}{\partial r}\, r^2\, dr\, d\theta \qquad (4.20)$$

On putting the value of $\frac{\partial p}{\partial r}$ from equation (4.17) in equation (4.20)

$$F_z = -\frac{1}{2}\int_0^{\pi}\int_{r_1}^{r_2} \left[\frac{-3\mu\,\omega\, r^2\,\gamma\,\sin\theta + K(\theta)}{(c+\gamma\, r\cos\theta)^3 + 12\,\text{Ø}H)}\right] r^2\, dr\, d\theta \qquad (4.21)$$

4.3.2 Transverse Moment :-

The moment about y-axis is given by

$$M_y = \int_0^{\pi}\int_{r_1}^{r_2} p\, r^2\, \sin\theta\, dr\, d\theta$$

Integrating this with respect to r, by parts, and then using equation (4.17) we get

$$M_y = -\frac{1}{3}\int_0^{\pi}\int_{r_1}^{r_2} \left[\frac{-3\mu\,\omega\,\gamma\, r^2\,\sin\theta + K(\theta)}{(c+\gamma\, r\cos\theta)^3 + 12\,\text{Ø}H)}\right] r^3\,\sin\theta\, dr\, d\theta \qquad (4.22)$$

4.3.3 Restoring Moment :-

The restoring moment is the moment about x-axis and is given by

$$M_x = -\int_0^{\pi}\int_{r_1}^{r_2} p\, r^2\, \cos\theta\, dr\, d\theta$$

$$= \frac{1}{3}\int_0^{\pi}\int_{r_1}^{r_2} \left[\frac{-3\mu\,\omega\,\gamma\, r^2\,\sin\theta + K(\theta)}{(c+\gamma\, r\cos\theta)^3 + 12\,\text{Ø}H}\right] r^2\,\cos\theta\, dr\, d\theta \qquad (4.23)$$

4.4. NON-DIMENSIONAL SCHEME

Various non-dimensional quantities are defined below :

$$\bar{r} = \frac{r}{r_2} \; ; \; \bar{r}_1 = \frac{r_1}{r_2} \; ; \; \bar{p} = \frac{pc^2}{\mu \omega r_2^2} \; ; \; K(\theta) = \frac{K(\theta)\, c^2}{\mu \omega r_2^2}$$

$$\varepsilon = \frac{\gamma r_2}{c} \; ; \; \bar{\alpha} = \frac{12 \mathcal{O} H}{c^3} \; ; \; \bar{F}_z = \frac{F_z c^2}{\mu \omega r_2^4} \; ; \; \bar{M}_Y = \frac{M_y c^2}{\mu \omega r_2^5}$$

$$\bar{M}_x = \frac{M_x c^2}{\mu \omega r_2^5} \; ; \; \frac{\partial \bar{p}}{\partial \bar{r}} = \frac{c^2}{\mu \omega r_2} \frac{\partial p}{\partial r} = \frac{-3\varepsilon \bar{r}^2 \sin\theta + \bar{K}(\theta)}{(1 + \varepsilon \bar{r} \cos\theta)^3 + \bar{\alpha}}$$

(4.24)

$$\text{Thus} \quad \bar{K}(\theta) = \frac{\int_{\bar{r}_1}^{1} \frac{3\varepsilon \sin\theta \bar{r}^2 \, d\bar{r}}{[(1+\varepsilon \bar{r} \cos\theta)^3 + \bar{\alpha}]}}{\int_{\bar{r}_1}^{1} \frac{dr}{(1+\varepsilon \bar{r} \cos\theta)^3 + \bar{\alpha}}} \qquad (4.25)$$

and

$$\bar{p}(\bar{r}) = \int_{\bar{r}_1}^{\bar{r}} \left[\frac{(-3\varepsilon \bar{r}^2 \sin\theta + \bar{K}(\theta)}{(1+\varepsilon \bar{r} \cos\theta)^3 + \bar{\alpha}} \right] d\bar{r} \qquad (4.26)$$

The non-dimensional axial force becomes

$$\bar{F}_z = \frac{F_z c^2}{\mu \omega r_2^4} = \frac{1}{2} \int_0^{\pi} \int_{\bar{r}_1}^{1} \left[\frac{3\varepsilon \bar{r}^2 \sin\theta - \bar{K}(\theta)}{(1+\varepsilon \bar{r} \cos\theta)^3 + \bar{\alpha}} \right] \bar{r}^2 \, d\bar{r} \, d\theta$$

(4.27)

The non-dimensional form of the transverse moment is given as below

$$\bar{M}_Y = \frac{1}{3} \int_0^{\pi} \int_{\bar{r}_1}^{1} \left[\frac{3\varepsilon \bar{r}^2 \sin\theta - \bar{K}(\theta)}{(1+\varepsilon \bar{r} \cos\theta)^3 + \bar{\alpha}} \right] \bar{r}^3 \sin\theta \, d\bar{r} \, d\theta \qquad (4.28)$$

The non-dimensional form of the restoring moment becomes

$$\bar{M}_x = \frac{1}{3}\int_0^{\pi}\int_{\bar{r}_1}^{1}\left[\frac{-3\varepsilon\,\bar{r}^2\sin\theta + \bar{K}(\theta)}{(1+\varepsilon\,\bar{r}\cos\theta)^3 + \bar{\alpha}}\right]\bar{r}^3\cos\theta\,d\bar{r}\,d\theta \qquad (4.29)$$

Equations (4.27), (4.28) and (4.29) when evaluated give the values of the seal charactaristics to be considered for cavitation case. When full fluid film prevails, the component of restoring moment becomes zero whereas that of the transverse moment is doubled.

4.5 REDUCTION OF DOUBLE INTEGRALS TO SINGLE INTEGRALS

To find out an expression for $p(\bar{r})$, let us assume

$$I = \int \frac{(-3\varepsilon\,\bar{r}^2\sin\theta + \bar{K}(\theta)}{(1+\varepsilon\,\bar{r}\cos\theta)^3 + \bar{\alpha}}\,d\bar{r} \qquad (4.30)$$

Let $\alpha^3 = \bar{\alpha}$, $1 + \varepsilon\,\bar{r}\cos\theta = u$ $d\bar{r} = \frac{du}{\varepsilon\cos\theta}$ and $\bar{r} = \frac{u-1}{\varepsilon\cos\theta}$ (4.31)

With these substitutions our integral I reduces to

$$I = -\frac{3\sin\theta}{\varepsilon^2\cos^3\theta}\left[\int\frac{u^2}{u^3+\alpha^3}du + \int\frac{1+M-2u}{u^3+\alpha^3}du\right] \qquad (4.32)$$

where $M = -\frac{\bar{K}(\theta)\varepsilon\cos^2\theta}{3\sin\theta}$.

On integrating (4.32) we obtain

$$I = \frac{-3\sin\theta}{\alpha^2\,\varepsilon\cos^3\theta}\left[I_1 + MI_2\right] \qquad (4.33)$$

where

$$I_1 = \alpha^2 \log(u^3+\alpha^3)+\frac{(1+2\alpha)}{2} \log \left(\frac{(u+\alpha)^2}{u^2-\alpha u+\alpha^2}\right)+\frac{(1+4\alpha)}{\sqrt{3}} \tan^{-1}\frac{(2u-\alpha)}{\sqrt{3}\ \alpha} \tag{4.34}$$

and

$$I_2 = \log \frac{(u+\alpha)^2}{u^2-\alpha u+\alpha^2} + \frac{1}{\sqrt{3}} \tan^{-1} \frac{(2u-\alpha)}{\sqrt{3}\alpha} - \tag{4.35}$$

Thus using equations (4.26),(4.33),(4.34),(4.35), we can evaluate $p(\bar{r})$ easily for various values of $\bar{\alpha}$ and ε.

Proceeding in the same way, we can reduce the double integrals in equation (4.25),(4.26) and (4.27) to single integrals by integrating these integrals w.r.t. $\bar{r}$. Thus the single integral expressions for separating force, transversse moment and restoring moments are as the following

$$\bar{F}_z = \frac{3}{2\varepsilon^4} \int_0^{\pi} \tan\theta \sec^4\theta \left[\frac{u^2}{2} - 4u + \frac{(6-M)}{3} \log(u^3+\alpha^3) \right.$$

$$+ Q_1 \log(u+\alpha) + \frac{Q_2}{2} \log(u^2-\alpha u+\alpha^2)$$

$$\left. + \frac{(2Q_3+Q_2\alpha)}{\sqrt{3}\ \alpha} \tan^{-1} \frac{(2u-\alpha)}{\sqrt{3}\ \alpha} \right]_{u_1}^{u_2} d\theta \tag{4.36}$$

where $Q_1 = \frac{L_2-L_1\alpha}{3\alpha^2}$; $Q_2 = \frac{L_1\alpha-L_2}{3\alpha^2}$; $Q_3 = \frac{L_1\alpha+2L_2}{3\alpha}$;

$L_1 = -(4-2M+\alpha^3)$; $L_2=(4\alpha^3+1-M)$; $u=1+\varepsilon\ \bar{r}\cos\theta$;

$u_1 = 1 + \varepsilon\ \bar{r}_1 \cos\theta$; $u_2 = 1 + \varepsilon \cos\theta$

And

$$\bar{M}_x = -\frac{1}{\varepsilon^5}\int_0^{\pi} \tan^2\theta \sec^4\theta \left[\frac{u^3}{3} - \frac{5u^2}{2} + (10+M)u \right.$$

$$-\frac{(10+3M+\alpha^3)}{3}\log(u^3+\alpha^3) + \frac{Q_{22}}{2}\log(u^2-\alpha u+\alpha^2)$$

$$+ Q_{11}\log(u+\alpha)$$

$$\left. + \frac{1}{\sqrt{3}\alpha}\frac{(2Q_{33}+Q_{22}\alpha)}{\sqrt{3}\alpha}\tan^{-1}\frac{(2u-\alpha)}{\sqrt{3}\alpha} \right]_{u_1}^{u_2} \qquad (4.37)$$

And

$$\bar{M}_y = \frac{1}{\varepsilon^5}\int_0^{\pi} \tan\theta \sec^5\theta \left[\frac{u^3}{3} - \frac{5u^2}{2} + (10+M)u \right.$$

$$-\frac{(10+3M+\alpha^3)}{3}\log(u^3+\alpha^3) + \frac{Q_{22}}{2}\log(u^2-\alpha u+\alpha^2)$$

$$\left. +Q_{11}\log(u+\alpha)+\frac{(2Q_{33}+Q_{22}\alpha)}{\sqrt{3}\alpha}\tan^{-1}\frac{(2u-\alpha)}{\sqrt{3}\alpha} \right]_{u_1}^{u_2}$$

(4.38)

where $Q_{11} = \frac{L_{22}-L_{11}\alpha}{3\alpha^2}$; $Q_{22} = \frac{L_{11}\alpha-L_{22}}{3\alpha^2}$; $Q_{33} = \frac{L_{11}\alpha+2L_{22}}{3\alpha}$;

$L_{11} = (5+3M+5\alpha^3)$; $L_{22} = -\{(1+M)+(10+M)\alpha^3\}$.

3.5 RESULTS AND DISCUSSION

These are two expressions for each of the quantities separating force, restoring moment and transverse moment. In each case one expression involves double integration and the other involves single integration. Each of the expressions (equations (4.36) , (4.37) and (4.38)) involving single integration also carries a factor of some power of $\cos\theta$ in the denominator of the integrand. Since the

integrand has to be integrated between the limits $\theta = 0$ and $\theta = \pi$, the integrand becomes indefinitely large in the neighbourhood of and at the value of $\theta = \pi/2$. Thus numerical integration of these expressions results in frequent messages of overflow. Thus double integration of equations (4.27), (4.28) and (4.29) is performed to obtain the numerical values of the axial force and moments.

Before performing numerical integrations, a value of the porosity parameter $\bar{\alpha} = \frac{12\phi H}{c^3}$ is required. Various porous materials have permeabilities ranging from 100×10^{-12} cm^2, to about 2000×10^{-12} cm^2. Thus for a bearing material having $\phi = 1500 \times 10^{-12}$ cm^2, H = 0.508 cm and $c = 2.54 \times 10^{-3}$ cm, $\frac{12\phi H}{c^3}$ is about 0.54. Thus the values of $\bar{\alpha} = \frac{12\phi H}{c^3}$ are taken between 0.25 and 1.0.

The axial force $\bar{F}_z$ is presented in figures 4.2 and 4.3, the restoring moment $\bar{M}_x$ in figures 4.4 and 4.5 and the transverse moment $\bar{M}_y$ in figure 4.6 and 4.7. Each of these quantities is plotted against the values of ε ranging between 0 and 1, for wide range of values of porosity parameter $\bar{\alpha}$. An increase in the value of $\bar{\alpha}$ may either be caused by an increase in the value of permeability ϕ or by a decrease in the value of seal clearance.

Figure 4.2 and 4.3 indicate that the value of axial force increases sharply for an increase in the value of tilt parameter ε till it attains some value about

.25. For $\varepsilon > .25$, an increase in the value of ε is followed by an increase in the value of axial force but less sharply. Figure 4.4 and 4.5 show that the value of restoring moment increases very sharply with ε but the sharpness slackens as ε approaches unity. Transverse moments [figs. 4.6 and 4.7] behaves essentially as the restoring moment does.

Each of the figures indicate that each of these three quantities decrease with an increase in the value of $\bar{\alpha}$. Thus when there is a case of excessive leakage and it is sought to lessen the transverse moment to bring about stability in a face seal, the porosity of face material may serve the purpose, since it tends to decrease them. Also, when compared with $\bar{\alpha} = 0$, i.e., a case when no porosity is there, the porous face seal has a tendency to undergo less shooting increments in the values of these characteristics with ε.

It has been established [74] that the hydrodynamic transverse moment which can affect the dynamic stability of radial face seals has to be considered in any dynamic analysis of seals. It is , therefore, concluded on the basis of present analysis that the porosity of face material has important influence on the stability of radial face seals because porosity as such significantly

influences the dynamic transverse moment. Further reducing the hydrodynamic transverse moment to a minimum may result in more stable seals.

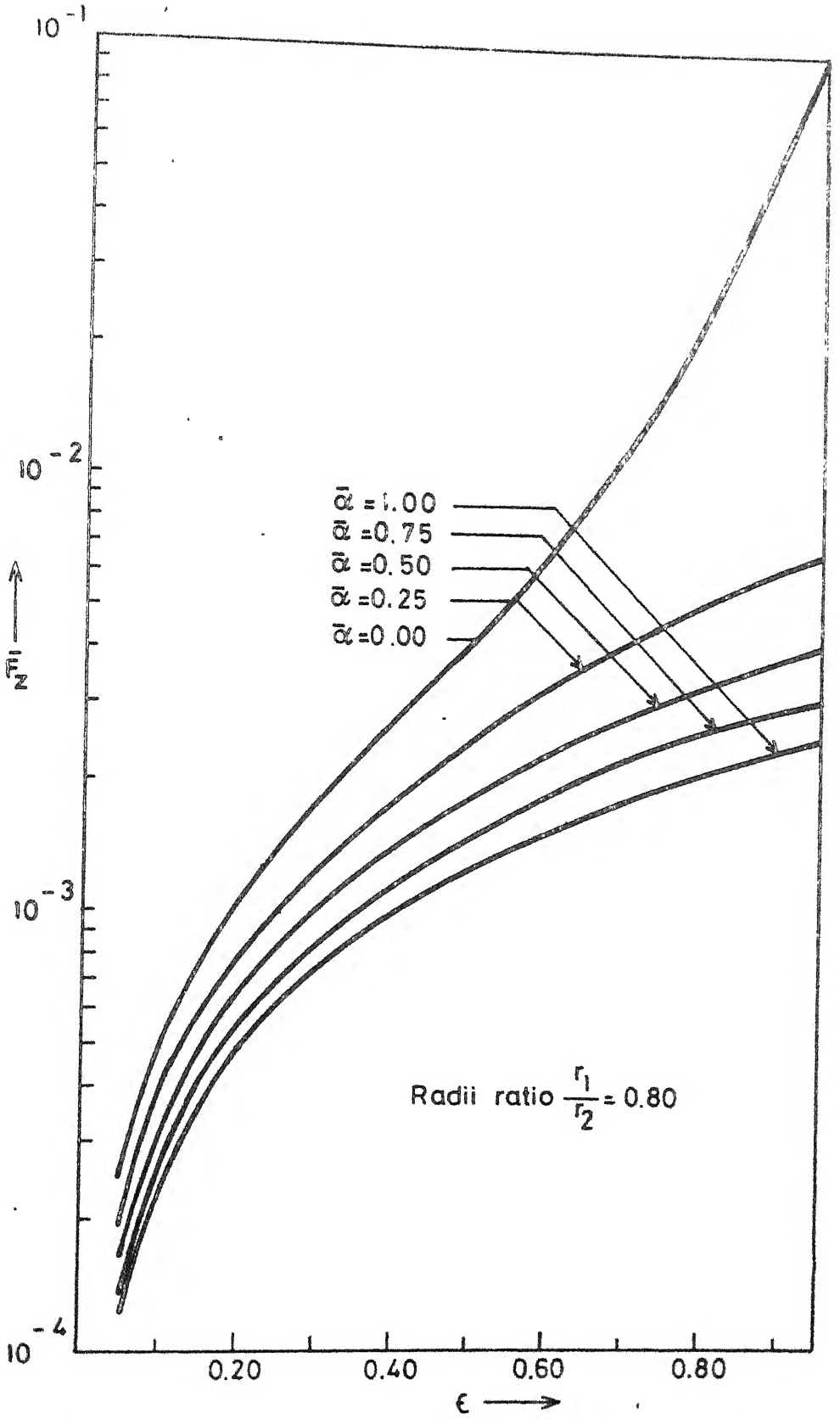

Fig 4.2 Dimensionless axial force as a function of tilt parameter for various values of porosity parameter.

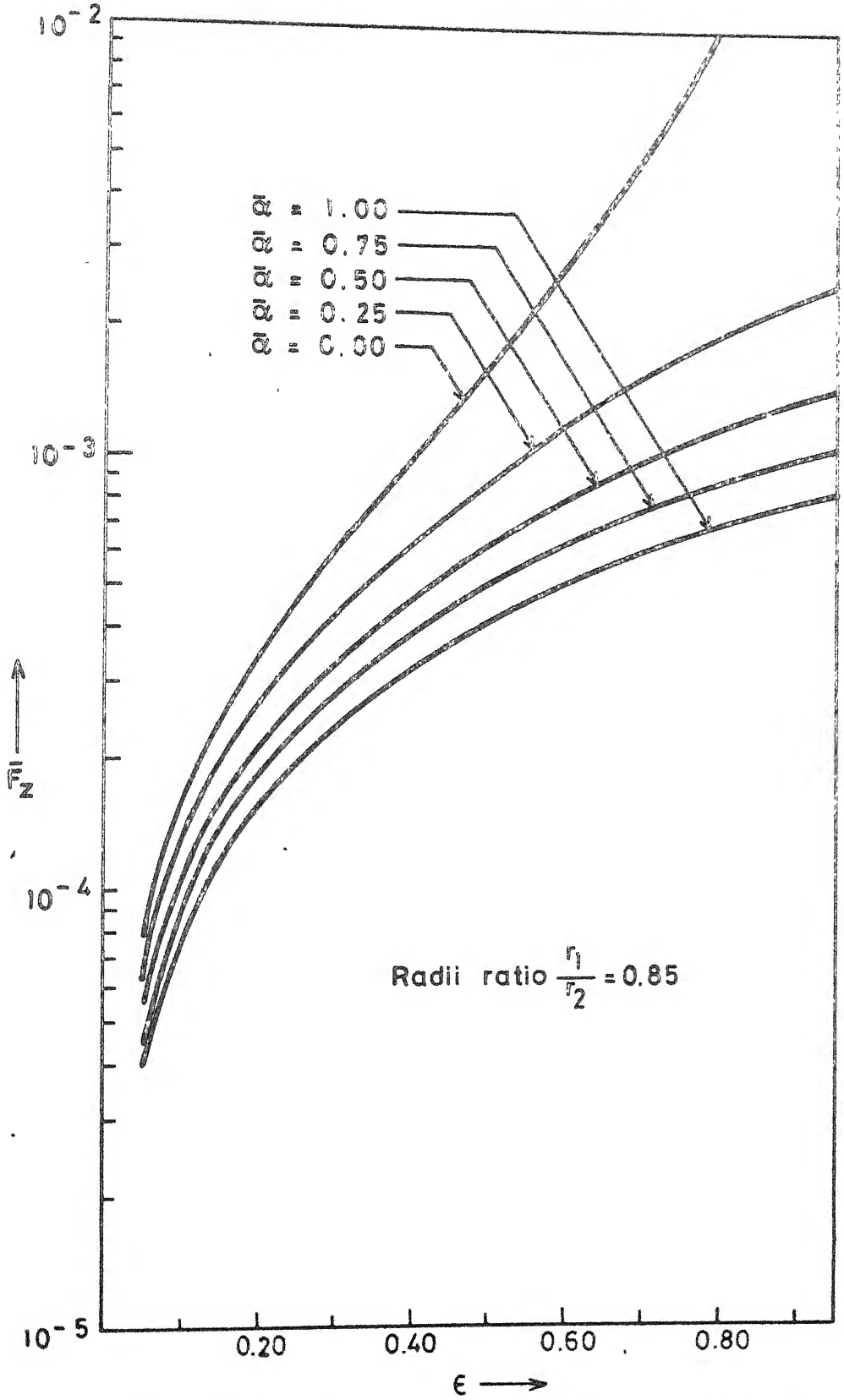

Fig. 4 3 Dimensionless axial force as a function of tilt parameter for various values of porosity parameter

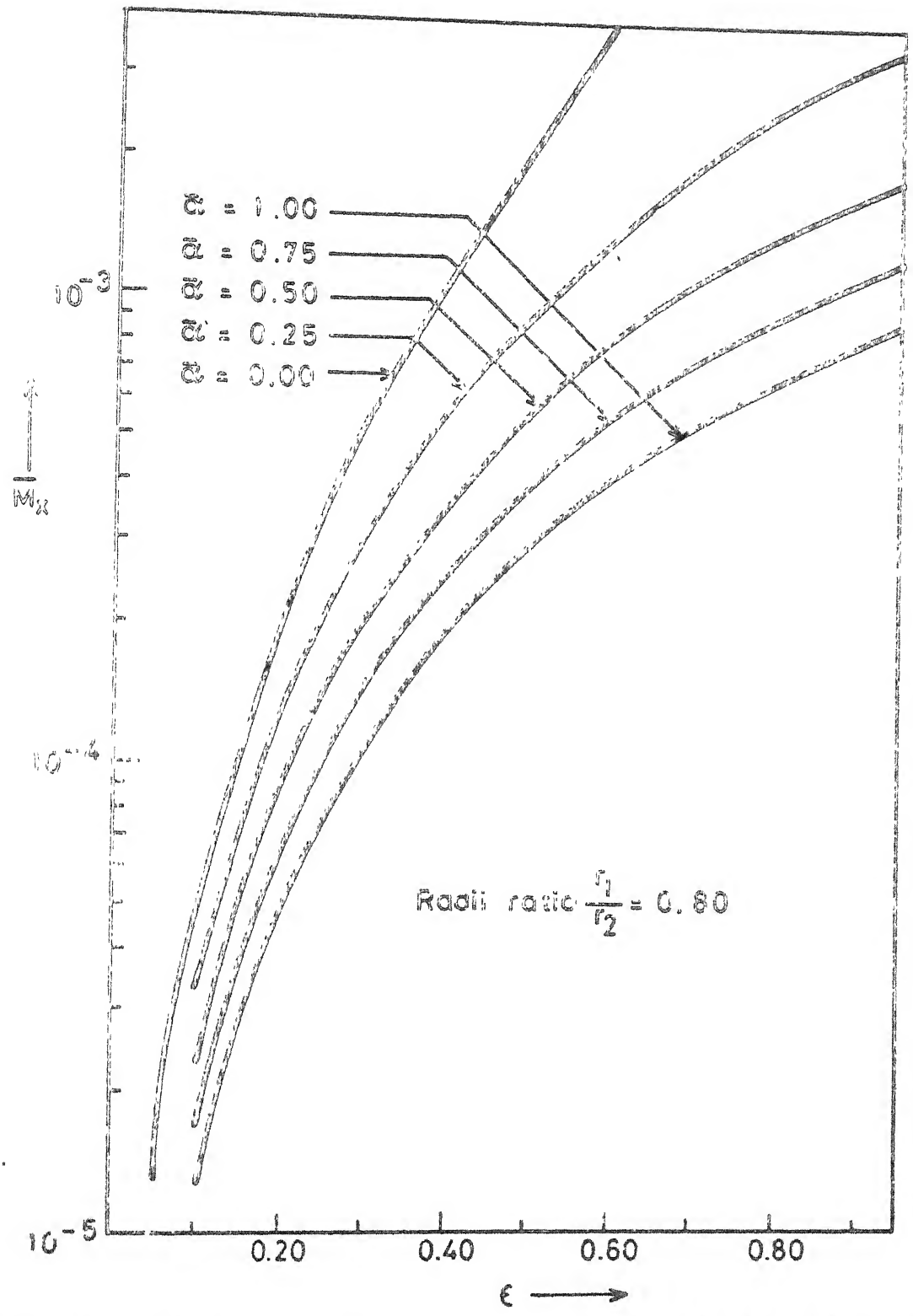

Fig 4.4 Dimensionless restoring moment as a function of tilt parameter for various values of porosity parameter.

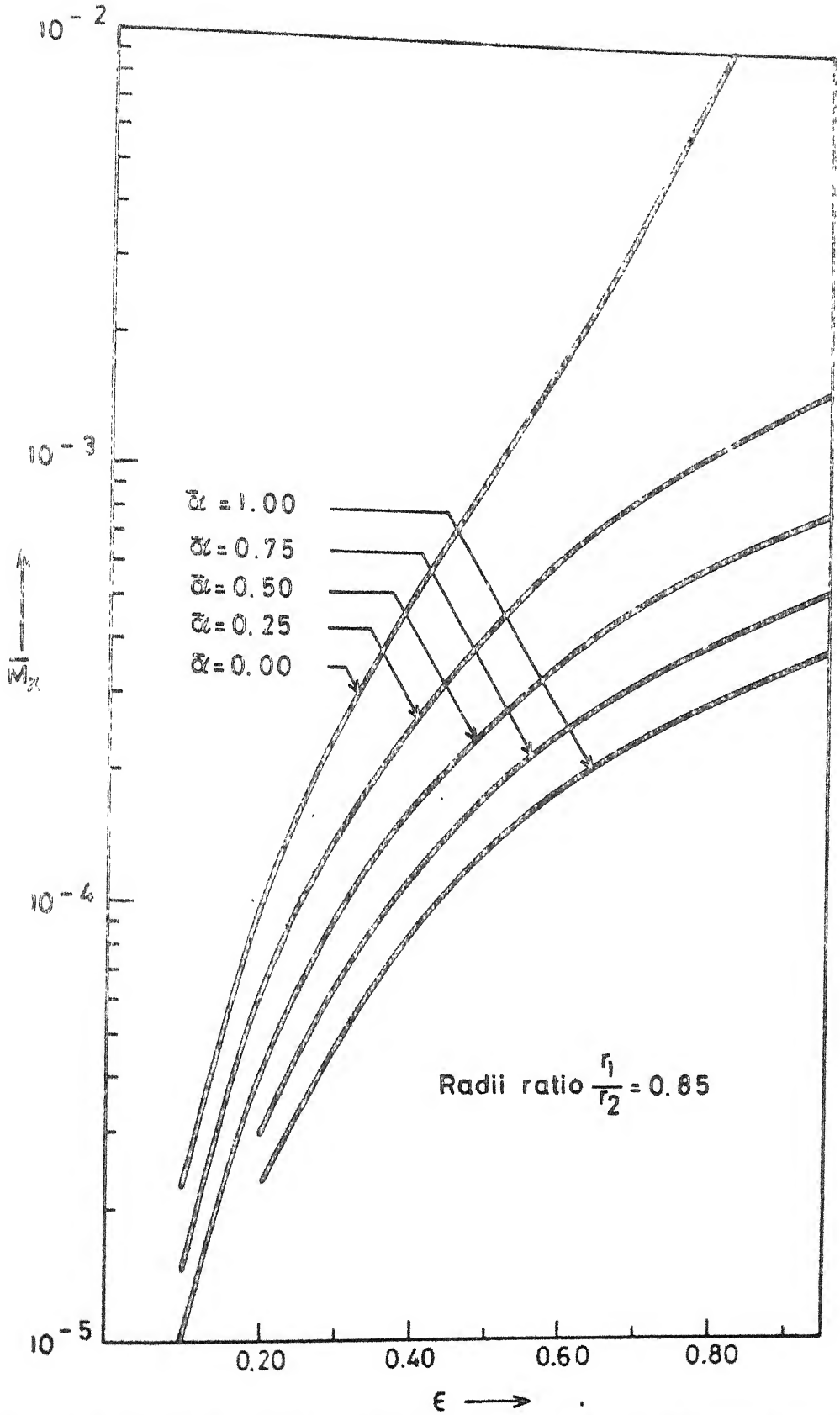

Fig 4.5 Dimensionless restoring moment as a function of tilt parameter for various values of porosity parameter.

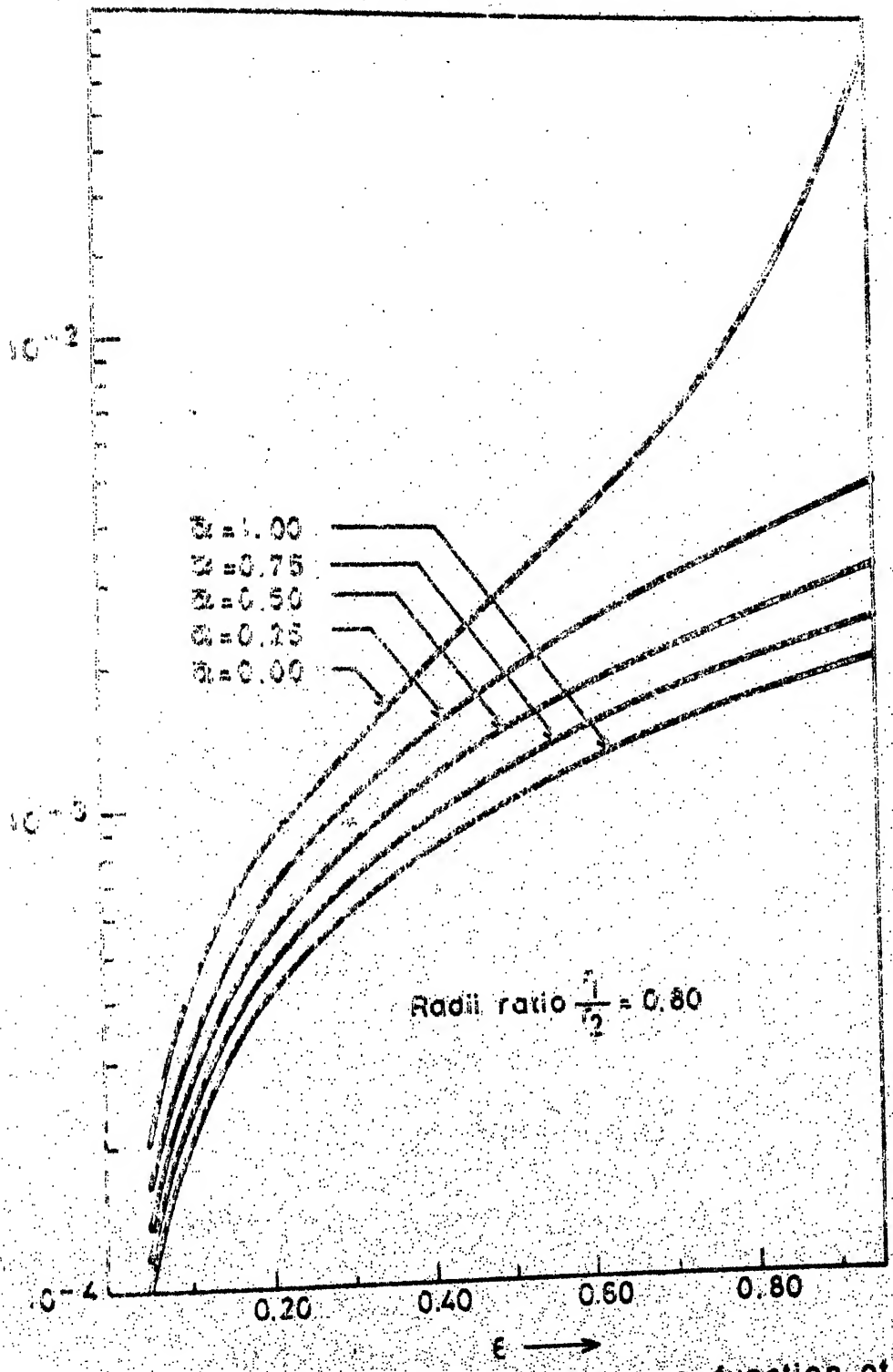

Fig 4.6 Dimensionless transverse moment as a function of tilt parameter for various values of porosity parameter.

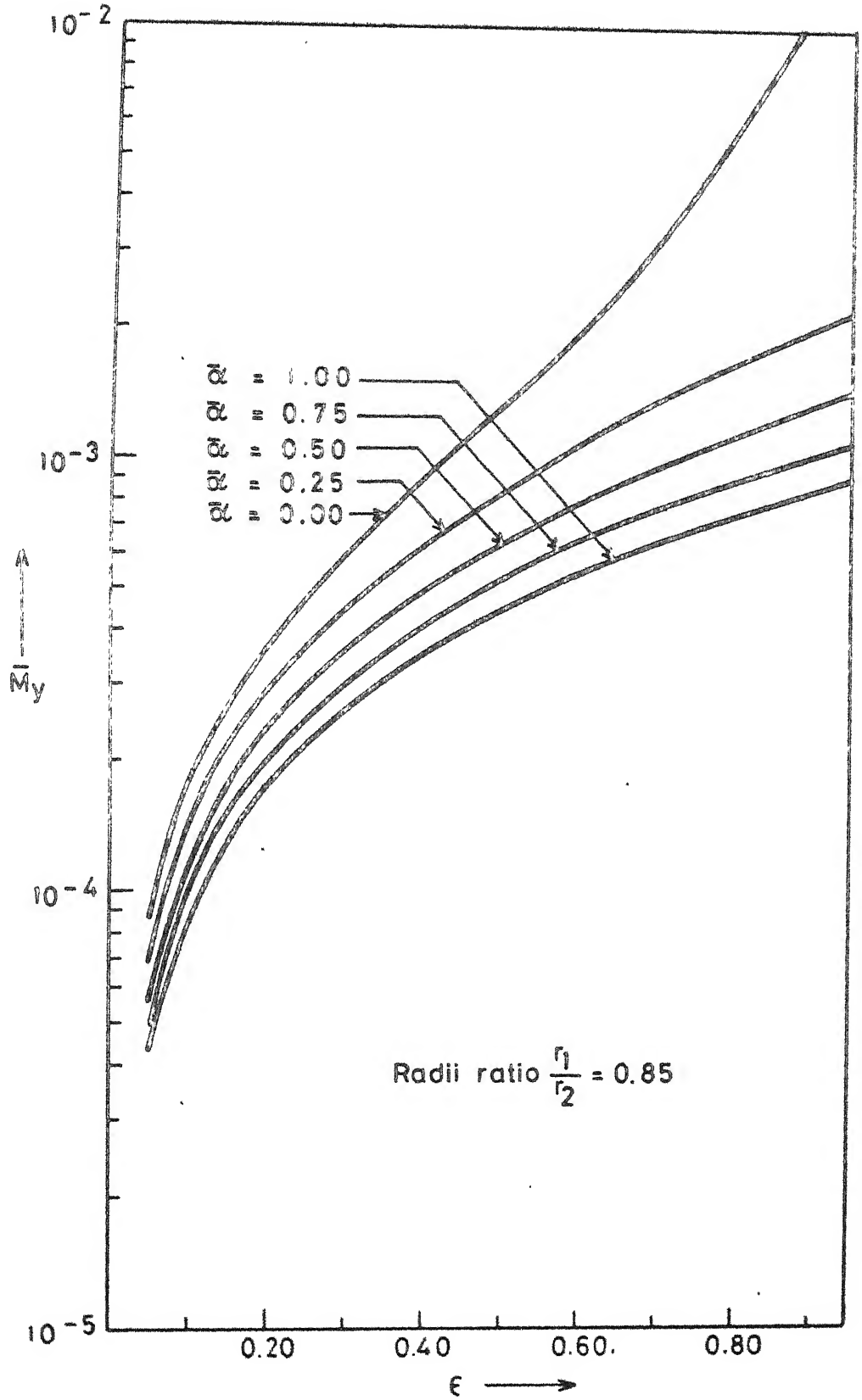

Fig 4.7 Dimensionless transverse moment as a function of tilt parameter for various values of porosity parameter

CHAPTER V

ELASTOHYDROSTATIC RADIAL AND AXIAL FORCES IN A MISALIGNED RADIAL FACE SEAL

5.1 INTRODUCTION

The secondary seal in a radial face seal is usually an elastic member such as an O ring or a piston ring. Its main task is to prevent leakage via the radial clearance between the primary seal ring and the seal housing. Since the primary seal ring is flexibly mounted on a support, it has five degrees of freedom [86] out of which two are the two perpendicular radial directions. Further, since the leakage highly depends on the eccentricity between the seal seat and the primary seal ring [28,31], a shifting of primary seal ring in the radial direction is followed by a heavy leakage which in turn brings about seal failure.

Both hydrodynamic and hydrostatic effects can produce radial forces in a misaligned radial face seal. The hydrodynamic component is due to nonaxisymmetric tangential and radial shear and the hydrostatic component is mainly due to nonaxisymmetric hydrostatic pressure distribution [65].

In order to provide a better understanding of radial face seal mechanism Etsion and Sharoni [77] and

Etsion [78] have studied the effects of radial forces combined with the effects of coning on a radial face seal. It has been shown that radial forces have direct influence on the stability of the seal. Axial forces, which have impact on leakage and wear, have also been studied for various cases [64,65,72,73,74,75,76,86]. But these analyses ignored the consideration of the elastic nature of the seal faces which may be considerably deformed elastically under high pressure. As a mater of fact,the film thickness undergoes a change and accordingly the radial and axial forces follow suit.

It is thus the objective of thischapter to study the effect of elasticity of seal faces by considering film thickness as a linear function of pressure. The influence on the radial force, which is so much vital for the stability of a seal, has been discussed in detail. In addition to this,the changes in the axial force have also been discussed.

5.2 MATHEMATICAL ANALYSIS

Figure 4.1 depicts the geometry of a misaligned radial face seal. The Reynolds equation for a narrow seal with an incompressible lubricant is :

$$\frac{\partial}{\partial r}\left(r\, h'^{3}\, \frac{\partial p}{\partial r}\right) = 6\mu\, \omega\, r\, \frac{\partial h'}{\partial \theta} \qquad (5.1)$$

where h' is the film thickness when the pressure is p. In fact

$$h' = h + sp \tag{5.2}$$

where h is the film thickness when no elastic effect is produced. h for a narrow seal is given by

$$h = c + \gamma\, r_m \cos\theta \tag{5.3}$$

s is the parameter which is inversely proportional to the modulus of elasticity of the face material. Further, c is the clearance along the centres of the faces of a seal and γ and r_m are the angle of tilt and the mid radius respectively.

For a solution which deals with the hydrostatic component only and for a narrow seal [64] equation (5.1) reduces to

$$\frac{\partial}{\partial r}\left(h'^3 \frac{\partial p}{\partial r}\right) = 0 \tag{5.4}$$

The pressure boundary conditions are

$$\begin{aligned} p &= p_1 \quad \text{when } r = r_1 \\ p &= p_2 \quad \text{when } r = r_2 \end{aligned} \tag{5.5}$$

$\frac{\partial p}{\partial r} = 0$ at some $r = r'$.

Integrating equation (5.4) and using equation (5.2), we get

$$\frac{\partial}{\partial r}\left[\,(h+sp)^4\,\right] = B \tag{5.6}$$

Integrating this equation we get

$$(h + sp)^4 = Br + C \tag{5.7}$$

where B and C are constants of integration depending only on θ. These constants are determined with the help of the boundary conditions in the equation (5.5). Thus we have

$$B = \frac{[(h+sp_1)^4-(h+sp_2)^4]}{(r_1-r_2)} \tag{5.8}$$

and

$$C = \frac{[r_1(h+sp_2)^4-r_2(h+sp_1)^4]}{(r_1-r_2)} \tag{5.9}$$

Now for a narrow seal [64], equation (5.7) may be approximated as

$$(h+sp)^4 = Br_m+C$$

$$= \frac{[(h+sp_1)^4-(h+sp_2)^4]r_m+[r_1(h+sp_2)^4-r_2(h+sp_1)^4]}{(r_1-r_2)} \tag{5.11}$$

or

$$p = \frac{1}{s}\left(\left[\frac{\{(h+sp_1)^4-(h+sp_2)^4\}\, r_m+\{r_1(h_1+sp_2)^4-r_2(h+sp_1)^4\}}{(r_1-r_2)}\right]^{\frac{1}{4}}-h\right) \tag{5.11}$$

5.2.1. Axial Force :

The axial force is given by

$$F_3 = 2 \int_0^{\pi} \int_{r_1}^{r_2} r_m \, d\theta \, dr \qquad (5.12)$$

On substitution of the value of p from equation (5.11) into equation (5.12) we obtain

$$F_z = 2 \int_0^{\pi} \int_{r_1}^{r_2} \frac{1}{s} \left[\frac{\{\{(h+sp_1)^4-(h+sp_2)^4\}r_m}{(r_1-r_2)} + \frac{r_1(h+sp_2)^4-r_2(h+sp_1)^4\}\}^{1/4} - h(r_1-r_2)}{(r_1-r_2)} \right] r_m \, d\theta \, dr$$

$$= \frac{2r_m}{s} \int_0^{\pi} [\{\{-(h+sp_1)^4-(h+sp_2)^4\} r_m - r_1(h+sp_2)^4-r_2(h+sp_1)^4\}\}^{1/4}-(r_2-r_1)h] \, d\theta \qquad (5.13)$$

Now

$$\int_0^{\pi} h \, d\theta = \int_0^{\pi} (C+\gamma \, r_m \cos\theta) d\theta = c\pi \qquad (5.14)$$

Using equation (5.14) in equation (5.13), we get more simplifed form for axial force F_z as :

$$F_z = \frac{2r_m}{s} [\pi c(r_1 - r_2) - \int_0^{\pi} [\{\{ (h+sp_1)^4-(h+sp_2)^4 \} r_m + \{r_1(h+sp_2)^4-r_2(h+sp_1)^4\}\}^{1/4}] d\theta] \qquad (5.15)$$

on further simplification F_z becomes

$$F_z = \frac{2r_m(r_2-r_1)}{s} \left[-\pi c + \frac{1}{2^{1/4}} \int_0^{\pi} \{(h+sp_1)^4+(h+sp_2)^4\}^{1/4} d\theta \right] \qquad (5.16)$$

5.2.1.1 Axial Force For No Flexibility Case :

The axial force for the case when none of the faces is flexible is given by

$$F_z(s=0) = 2r_m(r_2-r_1)\int_0^{\pi} \frac{(p_1h_1 + p_2h_2)}{(h_1 + h_2)}d\theta$$

5.2.2 Radial Force :

The radial force is given by

$$F_R = -2\int_0^{\pi}\int_{r_1}^{r_2} \tau_r \cos\theta \; r \; d\theta \; dr \qquad (5.17)$$

where

$$\tau_r = -\frac{h'}{2}\frac{\partial p}{\partial r} \qquad (5.18)$$

From equation (5.6), the value of τ_r becomes

$$\tau_r = -\frac{\{(h+sp_1)^4-(h+sp_2)^4\}}{8s(r_1-r_2)(h+sp)^2} \qquad (5.19)$$

Using equation (5.8) and (5.9) and equation (5.18) in equation (5.17) and then integrating, we get

$$F_R = \frac{1}{6s}\int_0^{\pi} I_1 \cos\theta \; d\theta + \frac{1}{3s}\int_0^{\pi} I_2 \cos\theta \; d\theta \qquad (5.20)$$

where

$$I_1 = (h_2+sp_2)^2 \; r_2 - r_1(h_1+sp_1)^2 \qquad (5.21)$$

and

$$I_2 = \frac{r_1(h_2+sp_2)^4 - r_2(h_1+sp_1)^4}{(h_1+sp_1)^2+(h_2+sp_2)^2} \qquad (5.22)$$

where

$$h_1 = c + \gamma\, r_1 \cos\theta$$

$$h_2 = c + \gamma\, r_2 \cos\theta$$

5.2.2.1 Radial Force For No-Flexibility Case :

When faces are not flexible, i.e. s = 0 the radial force is given by

$$F_R(s=0) = 2r_m \int_0^{\pi} \frac{(p_2-p_1)(h_1h_2)}{(h_1+h_2)}\, d\theta \qquad (5.23)$$

5.3 NON-DIMENSIONAL SCHEME

We resort to the undermentioned non-dimensional scheme

$$\bar{r}_m = \frac{r_m}{r_2} ; \bar{r}_1 = \frac{r_1}{r_2} ; \varepsilon = \frac{\gamma\, r_2}{c} ; \bar{F}_R = \frac{F_R}{p_2 r_2 c} ; \bar{F}_z = \frac{F_z}{p_2 r_2^2} ;$$

$$\bar{h}_1 = \frac{h_1}{c} = 1 + \varepsilon \bar{r}_1 \cos\theta ; \bar{h}_2 = \frac{h_2}{c} = 1+\varepsilon\cos\theta ; s = \frac{sp_2}{c} \qquad (5.24)$$

Using equation (5.24) in equation (5.16) and equation (5.19) we get the non-dimensional forms of the axial force and the radial force as given below :

$$\bar{F}_z = \frac{2\bar{r}_m(1-\bar{r}_1)}{\bar{s}}\Big[-\pi + \frac{1}{2^{1/4}} \int_0^{\pi} \{(1+\varepsilon\, \bar{r}_m \cos\theta + \bar{s}\bar{p}_1)^4 (1+ \varepsilon\, \bar{r}_m \cos\theta + \bar{s})^4 \}^{1/4}\, d\theta\Big] \qquad (5.25)$$

and

$$\bar{F}_R = \frac{1}{6\bar{s}} \int_0^{\pi} \bar{I}_1 \cos\theta \, d\theta + \frac{1}{3\bar{s}} \int_0^{\pi} \bar{I}_2 \cos\theta \, d\theta \qquad (5.26$$

where

$$\bar{I}_1 = (\bar{h}_2 + \bar{s})^2 - \bar{r}_1 (\bar{h}_1 + \bar{s}\bar{p}_1)^2 \qquad (5.27$$

and

$$\bar{I}_2 = \frac{(\bar{h}_2 + \bar{s})^4 \bar{r}_1 - (\bar{h}_1 + \bar{s}\bar{p}_1)^4}{(\bar{h}_1 + \bar{s}\bar{p}_1)^2 + (\bar{h}_2 + \bar{s})^2} \qquad (5.28)$$

Further, we calculate non-dimensional axial and radial forces abinitio to find expressions for these forces for a case where no elastic deformation occurs, i.e. when s = 0. Thus

$$\bar{F}_z \ (s=0) = \frac{F_z(s=0)}{p_2 r_2^2} = 2\bar{r}_m (1-\bar{r}_1) \int_0^{\pi} \left(\frac{\bar{h}_2 + \bar{p}_1 \bar{h}_1}{\bar{h}_2 + \bar{h}_1} \right) d\theta \qquad (5.29)$$

and

$$\bar{F}_R (s=0) = \frac{F_R(s=0)}{p_2 r_2 c} = 2\bar{r}_m \int_0^{\pi} \frac{(1-\bar{p}_1)\bar{h}_1 \bar{h}_2}{(\bar{h}_1 + \bar{h}_2)} \, d\theta \qquad (5.30)$$

Now we define the following quantities :

$$F_1 = \left\{ \frac{\bar{F}_z - \bar{F}_z(s=0)}{\bar{F}_z(s=0)} \right\} \times 100 \qquad (5.31)$$

and

$$F_2 = \left\{ \frac{\bar{F}_R - \bar{F}_R(s=0)}{\bar{F}_R(s=0)} \right\} \times 100 \qquad (5.32)$$

From definitions in equations (5.29) and (5.30) it is clear that F_1 and F_2 refer to the percentage difference in the values of the axial and the radial forces respectively, in the present case from their corresponding values when $s = 0$.

5.4 RESULT AND DISCUSSION

The values of F_1 and F_2 are obtained by integrating equations (5.31) and (5.32) numerically by Romberg method. Both F_1 and F_2 are functions of $\bar{p}_1 = p_1/p_2$ (inner to outer pressure ratio), $\bar{r}_1 = \frac{r_1}{r_2}$ (radii ratio), $\bar{s}$ (elastic parameter) and ε (tilt parameter). The curves for F_1 and F_2 are plotted against the tilt parameter ε (figures 5.1 to 5.4). The value of $\bar{r}_1$ is fixed at 0.9.

Figure 5.1 represents the graph between F_1 and ε at a fixed value of $\bar{p}_1$, i.e., $\bar{p}_1 = 0$. This figure indicates that the percentage difference F_1 increases slowly with an increase in the value of tilt parameter when it is less than .8 (approx.) but for $\varepsilon > .8$, the rate at which F_1 increases with ε is faster. The three different curves in figure 5.1 make it clear that the value of axial force increases with an increase in the value of elastic parameter $\bar{s}$. Since $\bar{s} = \frac{sp_2}{c}$, an increase in $\bar{s}$ may either be due to a

decrease in the value of the clearance c of the centres of seal faces or an increase in the value of s or both. Initial decrease in the value of c will come about following the shifting of the flexibly mounted face towards the secondary seal ring whereas an increase in the value of s is done by a more flexible nature of the face material. This happens due to a decrease in the modulus of elasticity of face material. It can thus be interpreted from figure 5.1 that for a seal with a more flexible face material , the percentage difference in the value of axial force is higher.

Figure 5.2 corresponds to the case when $\bar{p}_1 = 1000$. This indicates that the pressure at the inner boundary, p_1, is higher than the pressure at the outer boundary, p_2. Whereas in figure 5.1 p_1 is less than p_2. This figure 5.2 depicts a behaviour of F_1 similar to that of Figure 5.1, i.e., the percentage difference in the axial force increases with $\bar{s}$. However, there are significant quantitative differences. For $\bar{p}_1 = 0$, the maximum percentage difference is of the order 14 o/o, whereas for $\bar{p}_1 = 1000$, this difference goes as high as 60 o/o , Also, for $\bar{p}_1 = 1000$, the behaviour of F_1 with ε is quite different from that of F_1 for $\bar{p}_1 = 0$ F_1, for $\bar{p}_1 = 1000$, remains almost constant with ε till

$\varepsilon < .6$ (approx.). But F_1 decreases with a further increase in ε.

Each of the figures 5.3 and 5.4 represents curves of the percentage difference in the radial force, F_2, versus the tilt parameter ε, for various values of $\bar{s}$. Figure 5.3 is a graph with $\bar{p}_1 = 0$. This figure reveals that the value of F_2 is less than zero and they show a very little variation with $\bar{s}$. This is a very remarkable result in that it indicates that the flexibility of face material does not have a very significant impact on the radial forces. Moreover , a negative value of F_2 indicates that the radial force infact decreases when seal faces become flexible. Thus in view of [77,78] the flexibility reduces slightly the inward pumping that is generated by the radial force. Also, when ε increases the radial force increases (from fig.5.4) which is in perfect agreement with the behaviour of radial force with misalignment shown by Etsion and Sharoni [77] and Etsion [78].

Figure 5.4 is a graph between F_2 and ε for $\bar{p}_1$=1000. The qualitative behaviour is reversed as compared to that in figure 5.4. This figure indicates that F_2 increases as $\bar{s}$ increases which implies that the radial force increases with the flexibility of the face material. However, the percentage difference is not very high. Also, for every

value of $\bar{s}$, the percentage difference F_2 decreases with an increase in the angular misalignment parameter ε.

The hydrostatic component of the radial force F_R acts along the line BB which connects the highest and the lowest points of the primary seal ring. When the high pressure is on the inside periphery of the seal (as is the case presented in the figure 5.4), the radial force F_R is directed towards the point of maximum film thickness. On the other hand, when the high pressure is on the outer periphery, the radial force F_R acts in the direction of minimum film thickness (this has been presented in the figure 5.3). Thus the percentage difference F_2 has opposite behaviour in both the cases (fig.5.3 and 5.4).

Radial force effects appear to be more pronounced when the high pressure is on the outside periphery of the seal [78]. This is because such an arrangement is inherently unstable [65] due to nonrestoring hydrostatic moment which tends to increase any angular misalignment and thereby raise the magnitude of radial forces. From figure 5.4, it is clear that in case of higher pressure on the outer periphery radial forces are decreased because of flexibility of a seal which implies that the damage to the stability of the

seal is lessened. Moreover the radial displacement of the primary seal ring becomes less following which the leakage through the secondary seal, which is generated due to inward pumping in such cases, is also lowered.

It may thus be concluded that rendering the faces flexible is in the interest of stability of a radial face seal which is having high pressure on the outer periphery and operating under indequate separating force.

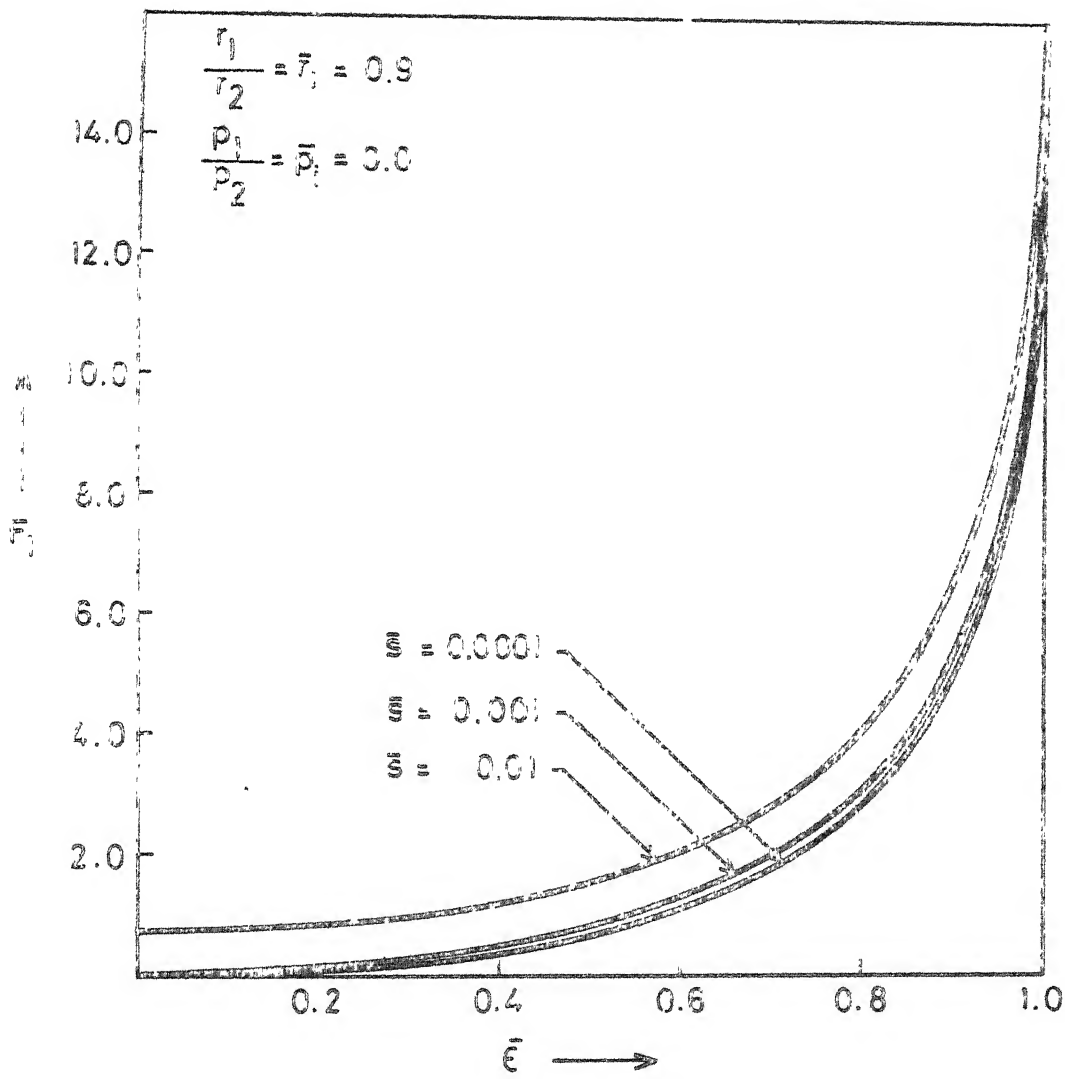

Fig. 5.1 Variation of the percentage difference in the axial forces with the tilt parameter for various values of elasticity parameter

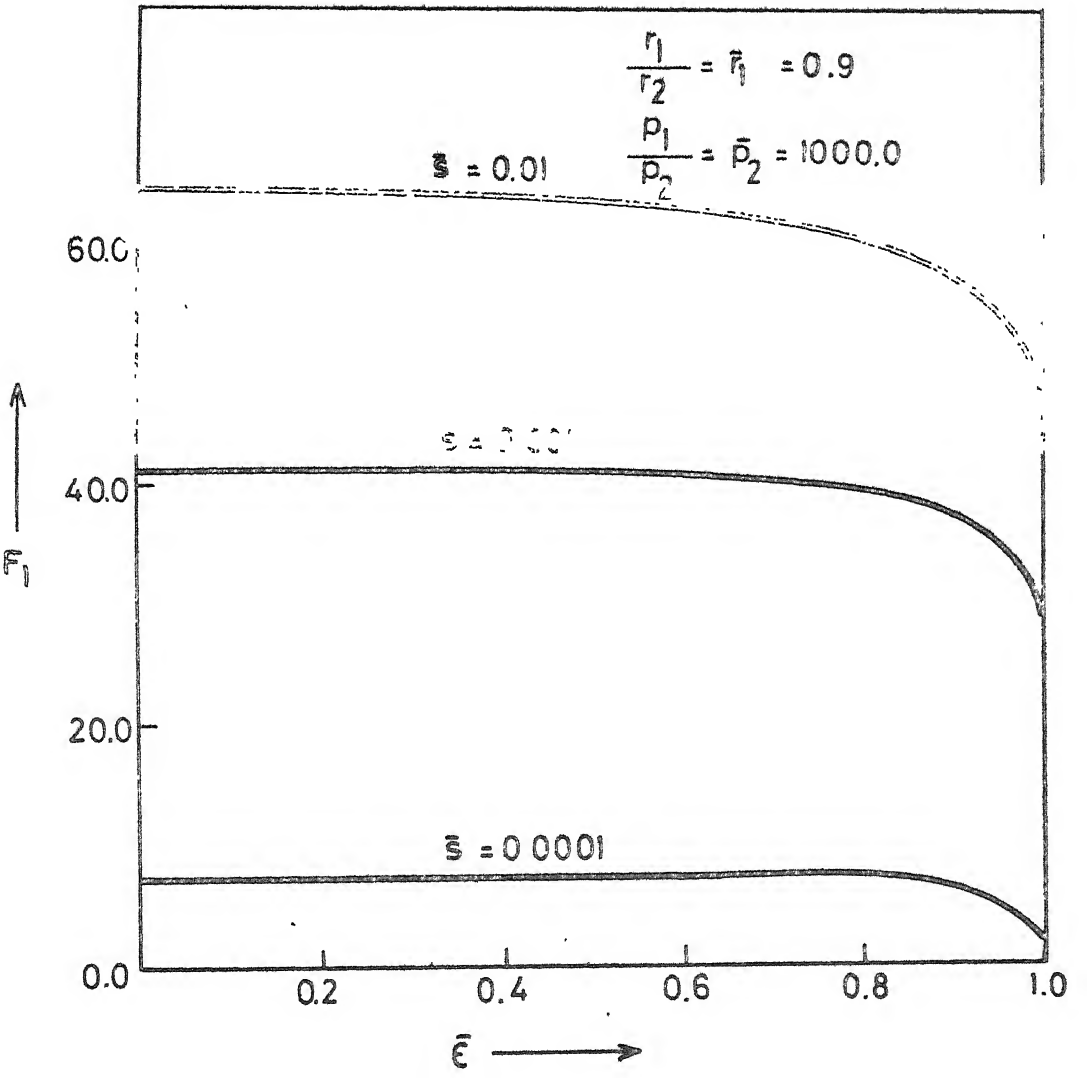

Fig. 5.2 Variation of the percentage difference in the axial forces with the tilt parameter for various values of elasticity parameter.

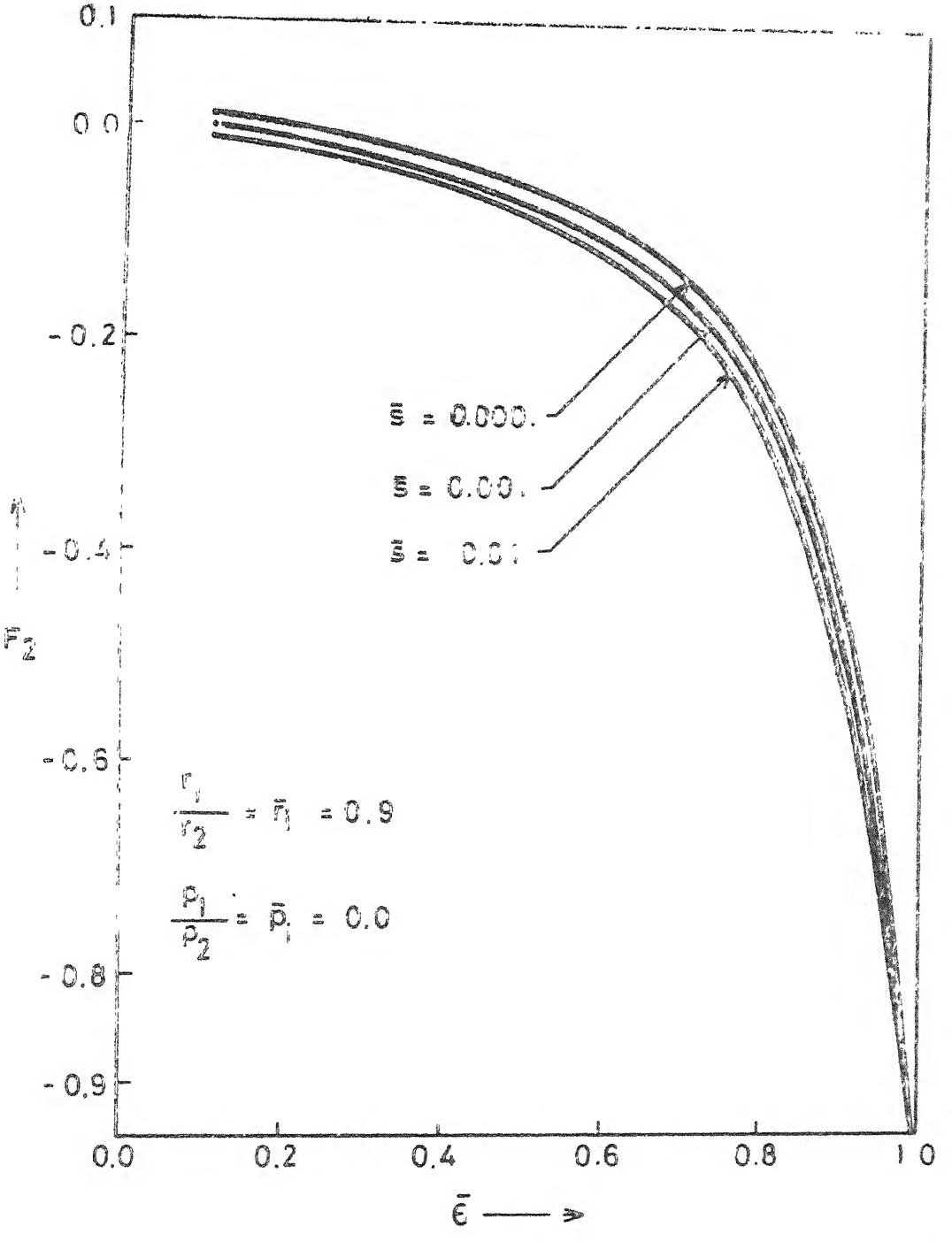

Fig. 5.3 Variation of the percentage difference in the radial forces with the tilt parameter for various values of elasticity parameter.

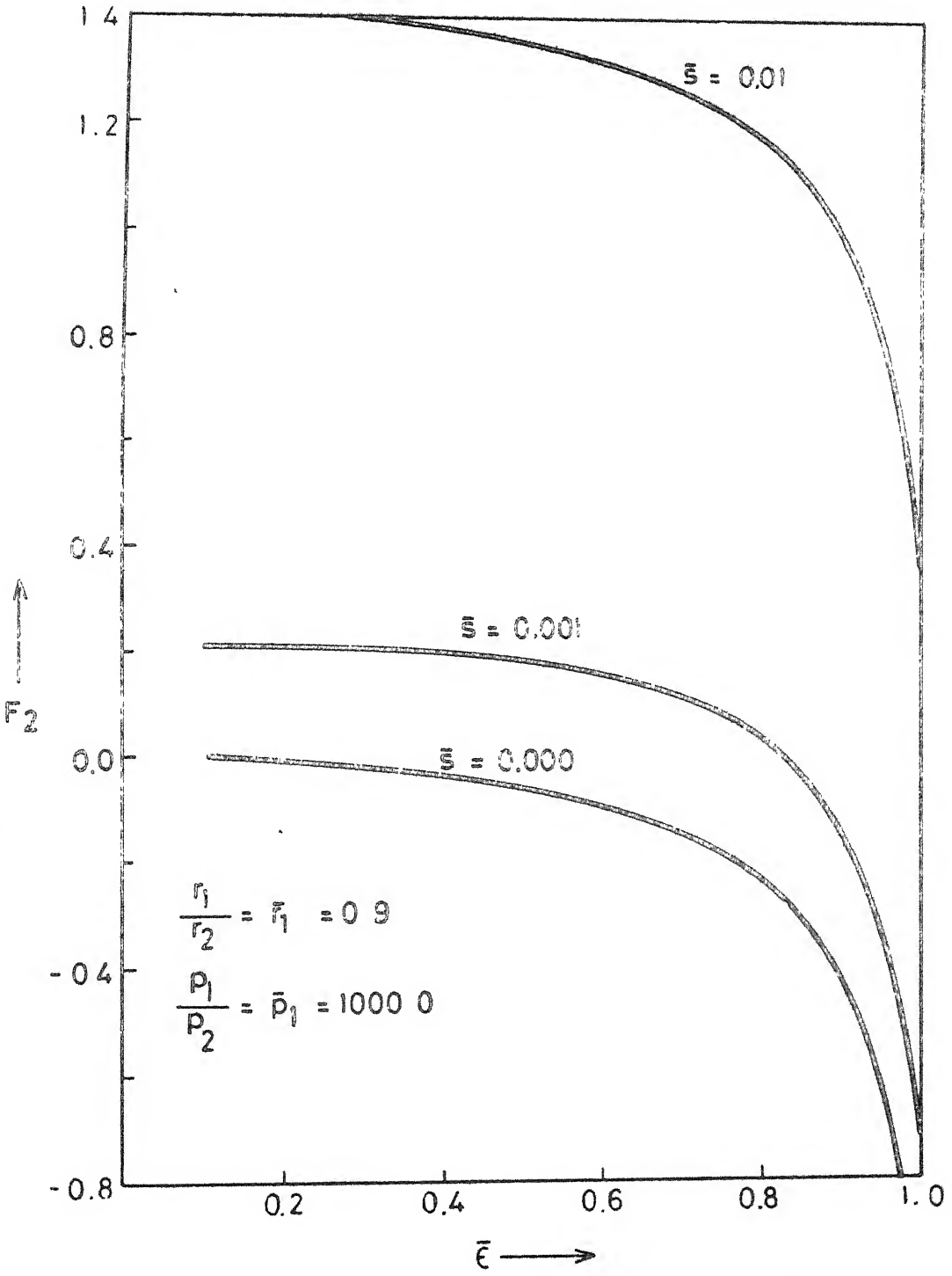

Fig 5.4 Variation of the percentage difference in the radial forces with the tilt parameter for various values of elasticity parameter

CHAPTER VI

HYDROSTATIC PRESSURE EFFECTS IN A MISALIGNED RADIAL FACE SEAL WITH A NON-NEWTONIAN FLUID

6.1 INTRODUCTION

Axial forces in excess of those theoretically predicted for aligned flat seal faces are now well established [8,27,42]. These axial forces are crucial in providing the mechanism that separates the seal faces and controls the gap between them. Several different mechanisms have been proposed to understand the origin of these forces. Of these mechanisms, hydrostatic pressure which is most important.

Several investigators, including Cheng and Snapp [23], Snapp and Sasdelli [43], Metcalfe [44], Mayer [45], Metcalfe[56], Etsion [64,65], Lebeck [70], Etsion [73], Etsion and Burton [75] and Etsion [76] have refined the techniques of determining the radial face profile and the hydrostatic pressure distribution. In most of the earlier investigations, the lubricant was treated essentially to be a Newtonian. However, the non-Newtonian behaviour is almost invariably observed in most lubricating processes. This may be a consequence of the fact that the fluids such as plastics, greases,

slurries etc. are being produced indurtrially in increasing quantities and these fluids are finding use in the lubrication systems. This non-Newtonian behaviour of the lubricant may also become prominant because of the contamination and the other severe operational requirements. In such situations, the Newtonian postulate,which assumes a linear relationship between the shear stress and the rate of strain, is violated.

Various theories have been developed in recent years to describe the flow behaviour of a non-Newtonian fluid based upon the fundamental constitutive relation that the shear stress is equal to the product of consistency and the rate of strain where the consistency itself may be a function of both shear stress and rate of strain. One such model is that of the 'power law' fluid in which shear stress varies as some power of strain rate. The power index, say n, is of immense significance in the study of the power law fluid flow problems. Its deviation from unity determines the change in the Newtonian behaviour of the lubricant. For $n = 1$, the fluid is Newtonian ; for $n < 1$, it characterizes a pseudoplastic behaviour and for $n > 1$, it is a dilatant fluid.

The value of the flow behaviour index and consitency for some non-Newtonian fluids which obey the power law model are listed below in table 6.1 Ref.[88,89].

Table 6.1 Typical values of the flow behaviour index and consistency variable for some well known non-Newtonian fluids.

Composition of fluid	Flow behaviour index	Consistency
23.3 per cent Illinois yellow clay in water	0.229	0.863
67 per cent Carboxy-methyl-cellulose (CMC) in water	0.716	0.121
3.0 per cent CMC in water	0.566	2.80
23 per cent lime in water	0.178	1.04
4 per cent paper pulp in water	0.575	6.13
54.3 per cent cement rock in water	0.153	0.331
14.3 per cent clay in water	0.350	0.0344
25.0 per cent clay in water	0.185	0.204
40.4 per cent clay in water	0.132	2.30
27 per cent Titanium dioxide water suspension (0.2-1.0 micron, particle size)	1.41	Data not available

In recent years, this non-Newtonian model has found extensive application in various lubrication problems. See reference [88] for detail. However, it has not been applied to the case of a misaligned radial face seal. Tanner [10,11] did study the effects of non-Newtonian fluid for seals but his model dealt with the viscoelastic fluids without considering the misalignment of the faces.

It is thus likely that the study of radial face seals when coupled with the concepts of misalignment and flexibility of faces may lead to significant non-Newtonian effects. Hence the study of these non-Newtonian effects through the power law model may yield additional information which will help in the designing of face seals.

In this chapter, therefore, power law model is used to investigate the effects of misalignment and flow behaviour index on axial forces and tilting moments. The curvature effects that were neglected by Etsion [65] are also given due considerations. Seal characteristics such as axial force, tilting moment and side leakage are obtained as functions of the flow behaviour index and the tilt parameter. Apart from this, a comparision has also been performed between the Newtonian and non-Newtonian cases.

6.2 MATHEMATICAL ANALYSIS

In this section, the mathematical analysis for hydrostatic face seals is developed considering the lubricant as power law fluid. The schematic of the misaligned face seal is given in figure 3.1. It is assumed that the power law fluid enteres between the faces, whose inner radii is r_1 each, at a pressure p_1. h is the film thickness which depends upon the angle of tilt γ and the variables r and θ .

We shall first derive the generalized Reynolds equation applicable to the model under consideration and then apply this to study the seal behaviour.

The stress strain relation for the motion of a power law fluid is given by

$$\tau_{ij} = m \left| \sqrt{e_{ij}\, e_{ji}} \right|^{n-1} e_{ij} \quad ; \; i,j=1,2,3 \qquad (6.1)$$

(The origin of coordinates system lies at c/2)

where τ_{ij} is the stress tensor, e_{ij} is the rate of deformation tensor, m is the consistency and n is the flow behaviour index. The consistency m, in general, can be a function of both shear stress and shear rate. The consistency may be interpreted as a parameter depending upon the viscosity of the fluid. For a Newtonian fluid (n=1), the consistency is identical to

the fluid viscosity. The dimensions and the numerical values of m depends upon n.

For one dimensional case, equation (6.1) reduces to

$$\tau = m \left| \frac{\partial v}{\partial z} \right|^{n-1} \frac{\partial v}{\partial z} \qquad (6.2)$$

The equation of motion and the equation of continuity governing the flow of incompressible fluid, in one-dimensional case, one given by

$$\frac{\partial p}{\partial r} = \frac{\partial \tau}{\partial z} \qquad (6.3)$$

$$\frac{\partial p}{\partial z} = 0 \qquad (6.4)$$

and

$$\frac{1}{r} \frac{\partial}{\partial r}(rv) + \frac{\partial w}{\partial z} = 0 \qquad (6.5)$$

respectively.

Substituting for τ from equation (6.2) in equation (6.3), we get

$$\frac{\partial p}{\partial r} = \frac{\partial}{\partial z} \left[m \left| \frac{\partial v}{\partial z} \right|^{n-1} \frac{\partial v}{\partial z} \right] \qquad (6.6)$$

Since the flow that occurs is pressure induced, with a constant pressure in the axial direction, the flow will be symmetrical about the film thickness. In view of this the boundary conditions can be stated as follows

$$z = 0, \quad \frac{\partial v}{\partial z} = 0, \tag{6.7}$$

$$z = h/2, \quad v = 0 \text{ and } w = 0 \tag{6.8}$$

Integration of equation (6.6), using the boundary conditions (6.7) and (6.8), yields the velocity distribution v, in the small gap between the mating faces of seal, as follows

$$v = \left(\frac{n}{n+1}\right)\left(-\frac{1}{m}\frac{\partial p}{\partial r}\right)^{1/n}\left[\left(\frac{h}{2}\right)^{\left(\frac{n+1}{n}\right)} - z^{\left(\frac{n+1}{n}\right)}\right] \tag{6.9}$$

Substituting for v from equation (6.9) in equation of continuity (6.5) and then integrating we get

$$\frac{1}{r}\frac{\partial}{\partial r}\left[r\left(\frac{2n}{2n+1}\right)\left(-\frac{1}{m}\frac{\partial p}{\partial r}\right)^{\frac{1}{n}}\left(\frac{h}{2}\right)^{\left(\frac{2n+1}{n}\right)}\right] = 0 \tag{6.10}$$

For isoviscous fluids, equation (6.10) reduces to

$$\frac{\partial}{\partial r}\left[r\, h^{\left(\frac{2n+1}{n}\right)}\left(\frac{\partial p}{\partial r}\right)^{\frac{1}{n}}\right] = 0 \tag{6.11}$$

Integrating equation (6.11) we get

$$p = B(\theta)\int_{r_1}^{r}\frac{dr}{r^n\, h^{(2n+1)}} + C(\theta) \tag{6.12}$$

where B and C are the constant of integration and are probably the functions of θ only.

The film thickness h for a misaligned radial face seal is

$$h = c + \gamma\, r\cos\theta \tag{6.13}$$

The pressure boundary conditions as per the situation quoted earlier are

$$p = p_1 \text{ at } r = r_1 \tag{6.14}$$

$$p = 0 \text{ at } r = r_2 \tag{6.15}$$

Substituting for h from equation (6.13) in equation (6.12) and integrating, using the boundary conditions (6.14) and (6.15), we get

$$p = B(\theta) \int_{r_1}^{r} \frac{dr}{r^n (c + \gamma\, r \cos\theta)^{(2n+1)}} + C(\theta) \tag{6.16}$$

where

$$C(0) = p_1 \tag{6.17}$$

and

$$B(\theta) = \frac{-p_1}{\int_{r_1}^{r_2} \frac{dr}{r^n (c+\gamma\, r \cos\theta)^{(2n+1)}}} \tag{6.18}$$

For n = 1

$$p = -p_1 \frac{\int_{r_1}^{r} \frac{dr}{r(c+\gamma\, r \cos\theta)^3}}{\int_{r_1}^{r_2} \frac{dr}{r(c+\gamma\, r \cos\theta)^3}} \tag{6.19}$$

6.2.1. Axial Force :

The axial force, which provides separation mechanism, is given by

$$F_z = \int_0^{2\pi} \int_{r_1}^{r_2} p\, r\, d\theta\, dr \tag{6.20}$$

Integrating this equation by parts, we obtain simpler formula for F_z as follows

$$F_z = -\pi r_1^2 p_1 - \frac{1}{2}\int_0^{2\pi}\int_{r_1}^{r_2} \frac{\partial p}{\partial r} r^2 \, dr \, d\theta \qquad (6.21)$$

Supstituting for $\frac{\partial p}{\partial r}$ from equation (6.12), we get

$$F_z = -\pi r_1^2 p_1 + \frac{1}{2} p_1 \int_0^{2\pi} \left(\frac{\int_{r_1}^{r_2} \frac{dr}{r^{(n-2)}(c+\gamma\, r\cos\theta)^{(2n+1)}}}{\int_{r_1}^{r_2} \frac{dr}{r^n (c+\gamma\, r\cos\theta)^{(2n+1)}}} \right) \qquad (6.22)$$

For Newtonian case (n=1)

$$F_z(n=1) = -\pi p_1 r_1^2 + \frac{1}{2} p_1 \int_0^{2\pi} \left(\frac{\int_{r_1}^{r_2} \frac{r\, dr}{(c+\gamma\, r\cos\theta)^3}}{\int_{r_1}^{r_2} \frac{dr}{(c+\gamma\, r\cos\theta)^3}} \right) \qquad (6.23)$$

6.2.2 Tilting Moment :

Tilting moment, the moment about x axis, is given by (also called the restoring moment)

$$M_x = -\int_0^{2\pi}\int_{r_1}^{r_2} p\, r^2 \cos\theta \, d\theta \, dr \qquad (6.24)$$

where (-) sign is used in order to obtain the positive value of restoring moment.

Integrating equation (6.24) by parts we get

$$M_x = \frac{1}{3}\int_0^{2\pi} \frac{\partial p}{\partial r} r^3 \cos\theta \; dr \, d\theta \qquad (6.25)$$

Substituting for $\frac{\partial p}{\partial r}$ from equation (6.12) in equation (6.25) we get

$$M_x = -\frac{1}{3}\int_0^{2\pi}\left(\frac{\int_{r_1}^{r_2}\frac{dr}{r^{(n-3)}(c+\gamma\, r\cos\theta)^{(2n+1)}}}{\int_{r_1}^{r_2}\frac{dr}{r^{n}(c+\gamma\, r\cos\theta)^{(2n+1)}}}\right)\cos\theta\, d\theta \qquad (6.26)$$

6.2.3 Leakage :

The leakage across the seal is obtained from

$$Q = -2\int_0^{\pi}\left(\frac{2n}{2n+1}\right)\left(\frac{h}{2}\right)^{\left(\frac{2n+1}{n}\right)}\left(\frac{1}{m}\frac{\partial p}{\partial r}\right)^{1/n} r\, d\theta \qquad (6.27)$$

Substituting for $\frac{\partial p}{\partial r}$ from equation (6.12) in equation (6.27), we get

$$Q = \left(\frac{n}{(2n+1)}\right)\left(\frac{p_1}{2m}\right)^{1/n}\int_0^{\pi}\frac{d\theta}{\left(\int_{r_1}^{r_2}\frac{dr}{r^{n}(c+\gamma\, r\cos\theta)^{(2n+1)}}\right)^{1/n}} \qquad (6.28)$$

6.3 NON-DIMENSIONAL SCHEME

For nondimensionalizing the various quantities involved, the undermentioned scheme is adhered to

$$\bar{r} = \frac{r}{r_1}\ ;\ \varepsilon = \frac{\gamma\, r_1}{c}\ ;\ \bar{r}_2 = \frac{r_2}{r_1}\ ;\ \bar{r}_1 = \frac{r_1}{r_2} = \frac{1}{\bar{r}_2}\ ;$$

$$\bar{F}_z = \frac{F_z}{p_1 r_1^2}\ ;\ \bar{p} = \frac{p}{p_1}\ ;\ \bar{M}_x = \frac{3M_x}{p_1 r_1^3} \qquad (6.29)$$

Thus the dimensionless pressure, force and tilting

moment assume the following forms

$$\bar{p} = \frac{\int_1^{\bar{r}} \frac{d\bar{r}}{\bar{r}^n(1+\varepsilon\ \bar{r}\cos\theta)^{(2n+1)}}}{\int_1^{\bar{r}_2} \frac{d\bar{r}}{\bar{r}^n(1+\varepsilon\ \bar{r}\cos\theta)^{(2n+1)}}} \tag{6.30}$$

$$\bar{F}_z = -\pi + \frac{1}{2}\int_0^{2\pi} \left(\frac{\int_1^{\bar{r}_2} \frac{\bar{r}^2\, d\bar{r}}{\bar{r}^n(1+\varepsilon\ \bar{r}\cos\theta)^{(2n+1)}}}{\int_1^{\bar{r}_2} \frac{d\bar{r}}{\bar{r}^n(1+\varepsilon\ \bar{r}\cos\theta)^{(2n+1)}}} \right) d\theta \tag{6.31}$$

and

$$\bar{M}_x = \int_0^{2\pi} \left(\frac{\int_1^{\bar{r}_2} \frac{d\bar{r}}{\bar{r}^{(n-3)}(1+\varepsilon\ \bar{r}\cos\theta)^{(2n+1)}}}{\int_1^{\bar{r}_2} \frac{d\bar{r}}{\bar{r}^n(1+\varepsilon\ \bar{r}\cos\theta)^{(2n+1)}}} \right) \cos\theta\, d\theta \tag{6.32}$$

where $\varepsilon = 0$, i.e. for parallel seals

$$\bar{F}_z\,(\varepsilon = 0) = -\pi + \left(\frac{1-n}{3-n}\right)\left(\bar{r}_2^{2} - 1\right)\pi \tag{6.33}$$

$$\bar{M}_x\,(\varepsilon = 0) = 0 \tag{6.34}$$

Now when $\varepsilon = 0$ and $n = 1$, i.e. for parallel seals with Newtonian lubricant

$$\bar{F}(n=1, \varepsilon=0) = \frac{\pi\,(\bar{r}_2^{2} - 3)}{2\ \log \bar{r}_2} \tag{6.35}$$

Nondimensional scheme for the leakage is complicated for power law model because the dimension of the consistency m depends on the flow behaviour index n. Therefore, we consider the ratio of tilted faces leakage to corresponding parallel faces leakage to study the behaviour of leakage. Thus we denote the ratio by

$$\bar{Q} = \frac{Q}{Q(\varepsilon=0)}$$

$$= \frac{\int_0^{\pi} \frac{d\theta}{\left(\int_1^{\bar{r}_2} \frac{d\bar{r}}{\bar{r}^n (1+\varepsilon\, \bar{r} \cos\theta)^{(2n+1)}} \right)^{1/n}}}{\int_0^{\pi} \frac{d\theta}{\left(\int_1^{\bar{r}_2} \frac{d\bar{r}}{\bar{r}^n} \right)^{1/n}}} \qquad (6.36)$$

6.4 RESULTS AND DISCUSSION

Equations (6.31) and (6.32) give expressions for the dimensionless axial separating force $\bar{F}_z$ and the dimensionless tilting moment $\bar{M}_x$ respectively. Each of them is a function of the flow behaviour index n and tilt parameter ε. Equation (6.33) represents the expression for separating axial force when $\varepsilon = 0$ and is positive. Equation (6.34) depicts, as expected, that the tilting moment vanishes for $\varepsilon = 0$.

These equations have been solved numerically using Romberg method, for inner-to-outer radii ratio equal

to 0.9. This is in accordance with Etsion [65] in that the author mentions that for all practical purposes the radii ratio is greater than 0.8 . The other two important parameters are the flow behaviour index n which is made to vary from 0.2 to 2.0 [89] and the tilt parameter which is made to vary from 0 to 1. Each of the quantities has been plotted against both the parameters n and ε.

Figure 6.1 is a graph between the non-dimensional axial force $\bar{F}_z$ and the tilt parameter ε, for various values of n. The value $\varepsilon = 0$ corresponds to the case when the faces are parallel. The figure indicates that as the value of ε increases the value of axial force $\bar{F}_z$ for pseudoplastics increases negligibly till $\varepsilon = 0.6$ (approx.). When ε 0.6 $\bar{F}_z$ increases more rapidly. For dilatant fluids, $\bar{F}_z$ decreases first reaches a minimum around $\varepsilon = 0.7$ and then increases.

Figure 6.2 shows the variation in the axial force $\bar{F}_z$ with n. This figure shows that for all values of ε the value of the axial force $\bar{F}_z$ decreases as the flow behaviour index n, increases.

We define a ratio $\dfrac{\bar{F}_z}{\bar{F}_{z(\varepsilon=0)}}$, i.e. the ratio of the axial force for misaligned radial face seal to the axial force for parallel face seal. This ratio has been plotted in figure 6.3 and 6.4 against ε and n respectively. It is

seen that for dilatant fluids ($n > 1.6$ approx.) this ratio decreases with ε first reaches a minimum around $\varepsilon = 0.7$ and then rises sharply. This indicates that a small angle of tilt has a determimental effect on the axial force. For fluids for which $n < 1.6$, the ratio is always greater than unity which signifies that the separating force is always larger for a misaligned face seal than for a parallel face seal. Similar interpretations can be made from figure 6.4.

From these figures it can be inferred that for a face seal that undergoes massive wear because of insufficient generation of separating force the use of pseudoplastics becomes favourable in that it increases these forces and helps in maintaining the faces apart. But for a face seal that starver for lubrication because of frequent huge leakage, the use of dilatant fluid will be beneficial.

Figures 6.5 and 6.6 represent the graphs of the tilting moment $\bar{M}_x$ against ε and n respectively. These figures together reveal that the tilting moment $\bar{M}_x$ increases as the value of ε and the flow behaviour index n increase. For a pseudoplastic fluid, $\bar{M}_x$ is much less than that for a Newtonian and a dilatant fluid. Thus the dilatant fluids are more useful where face seal stability is more frequently hampered. Because these fluids produce more restoring effects on the primary seal ring.

Figure 6.7 is a graph of the leakage ratio defined in equation (6.36) versus the tilt parameter ε. This ratio increases as n decreases. The rate of decrease is much more rapid for small values of n and large values of ε, i.e. for pseudoplastic fluids with large angle of tilt. This suggests that the leakage is larger for pseudoplastic fluids than for Newtonian and dilatant fluids. This may be the consequence of increase in separating force and decrease in restoring moment for pseudoplastics as indicated in figures 6.1 and 6.2.

On the basis of above findings it may be concluded that for a radial face seal, the dilatant fluids as the lubricant are more useful than the Newtonian and pseudoplastic fluids.

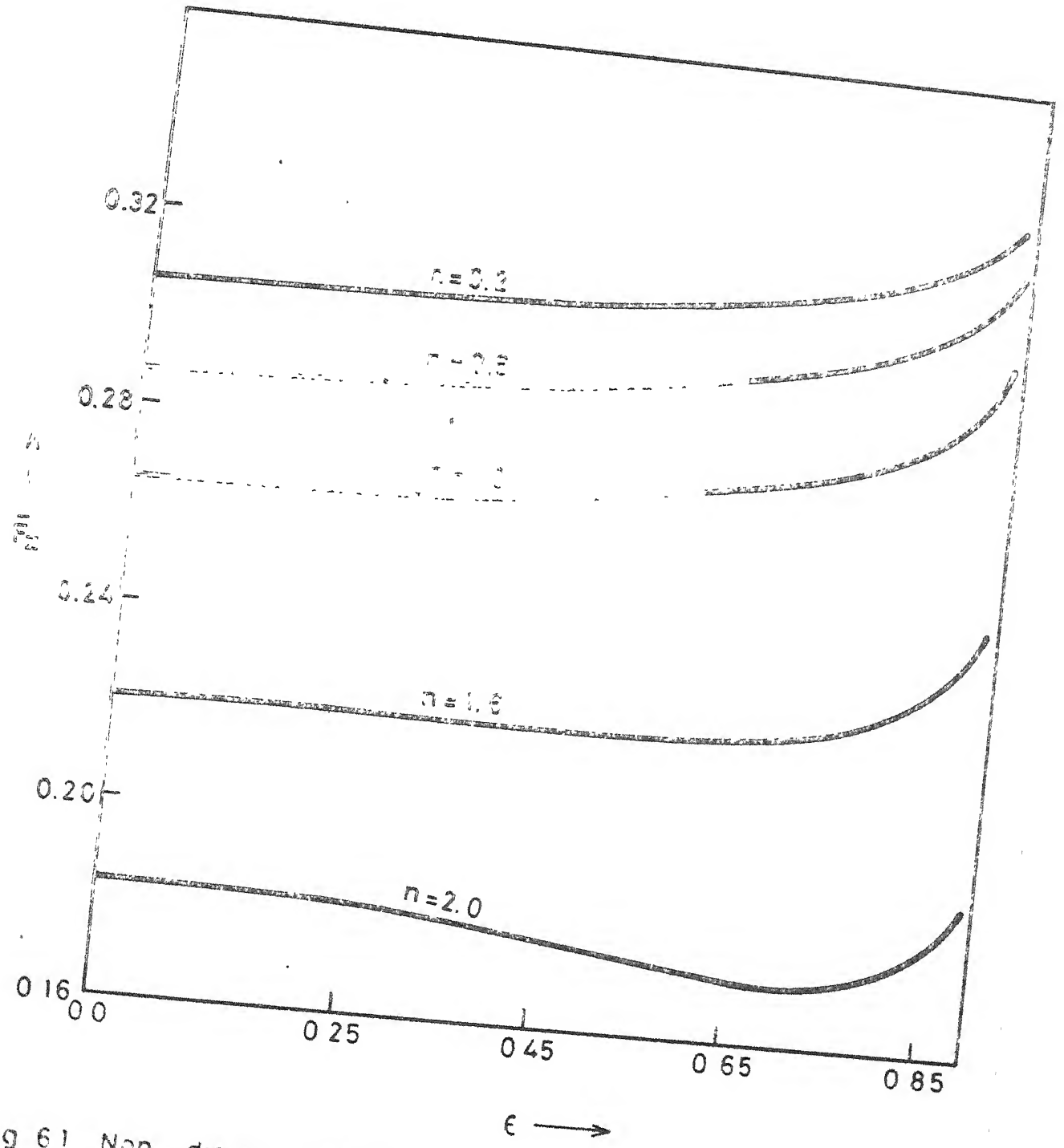

Fig 6 1 Non - dimensional axial force versus tilt parameter for various values of the flow behaviour index

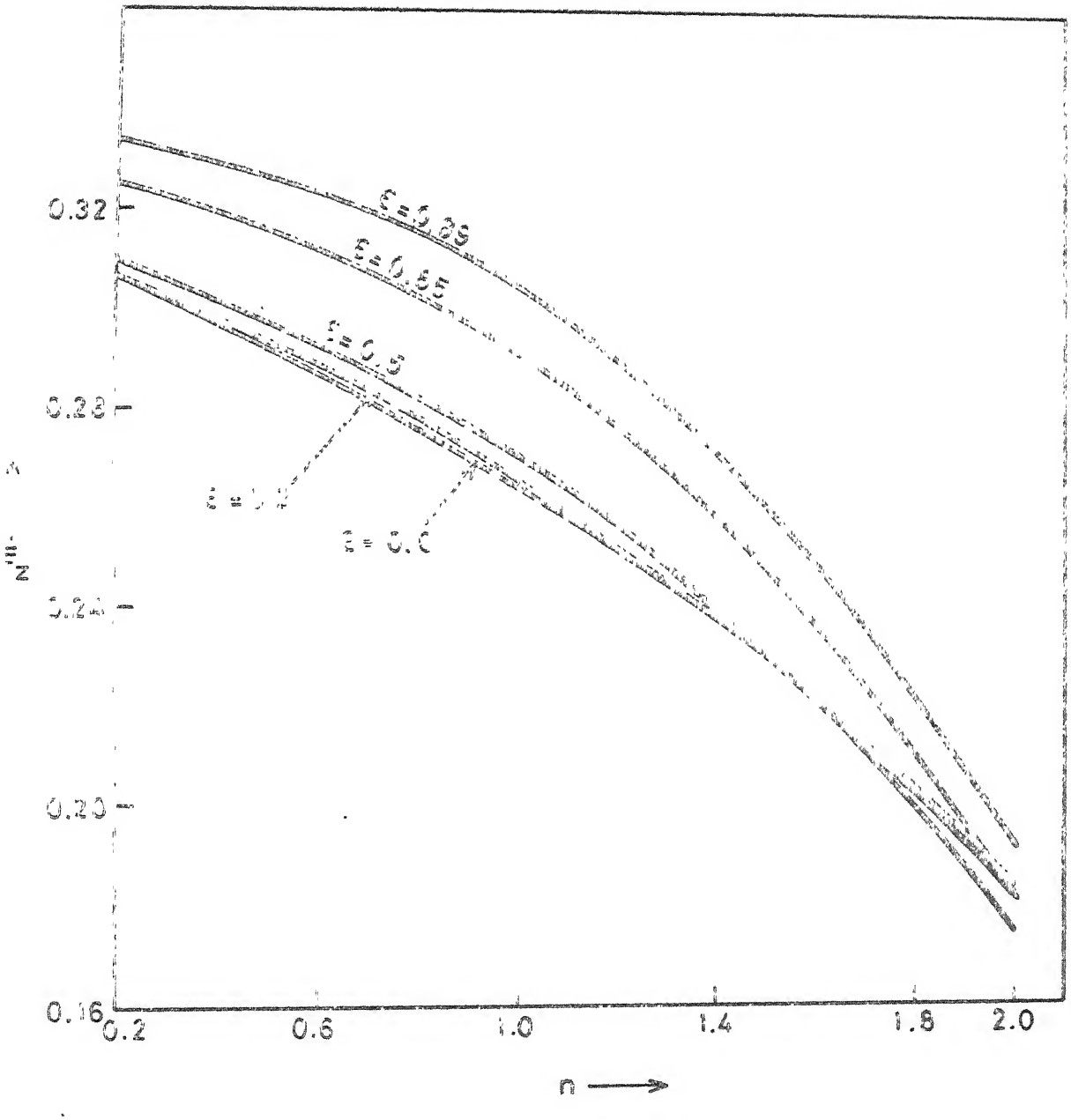

Fig 6 2 Non - dimensional axial force versus the flow behaviour index for various values of the tilt parameter.

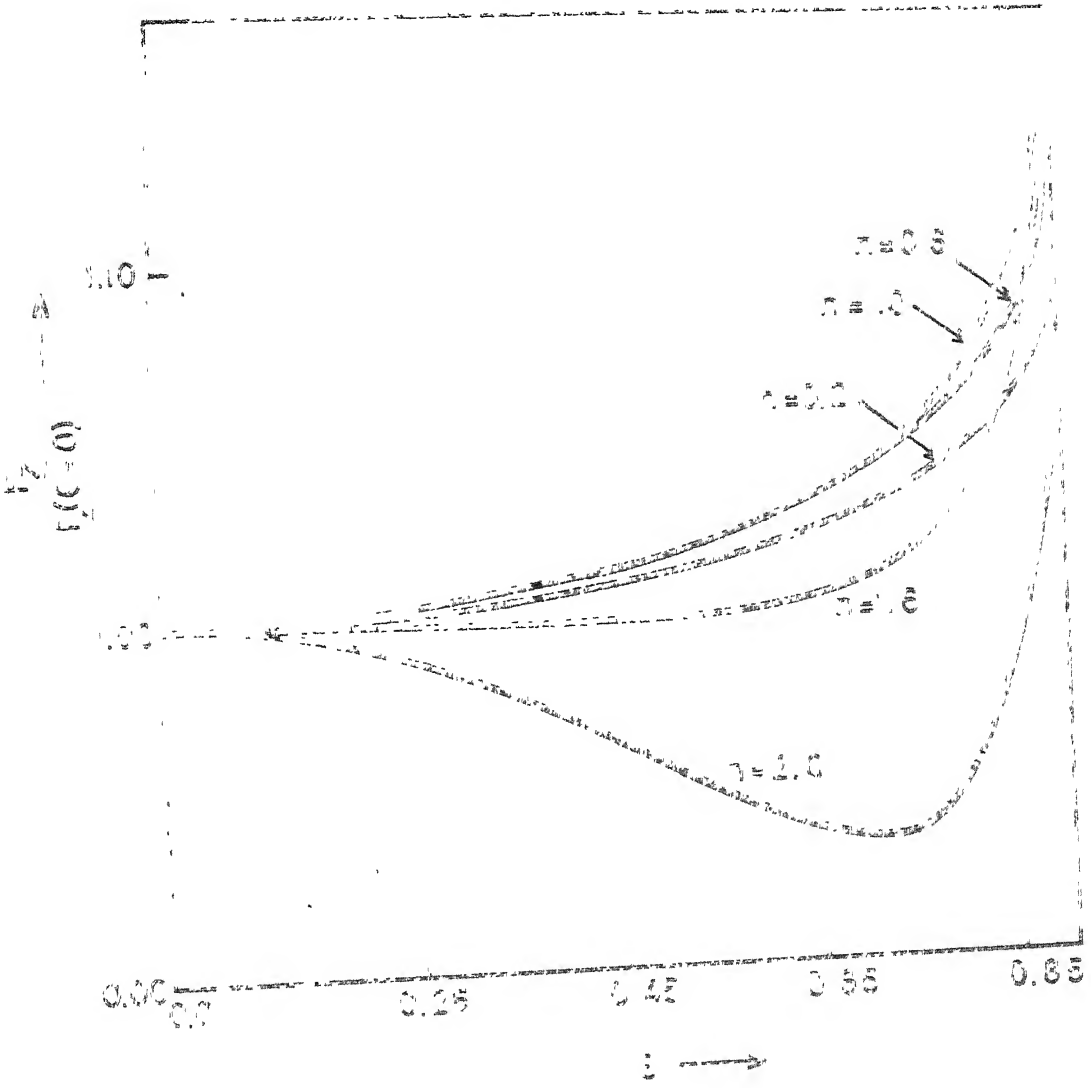

Fig. 6.3 Axial forces-ratio versus the tilt parameter ξ for various values of the flow behaviour index n.

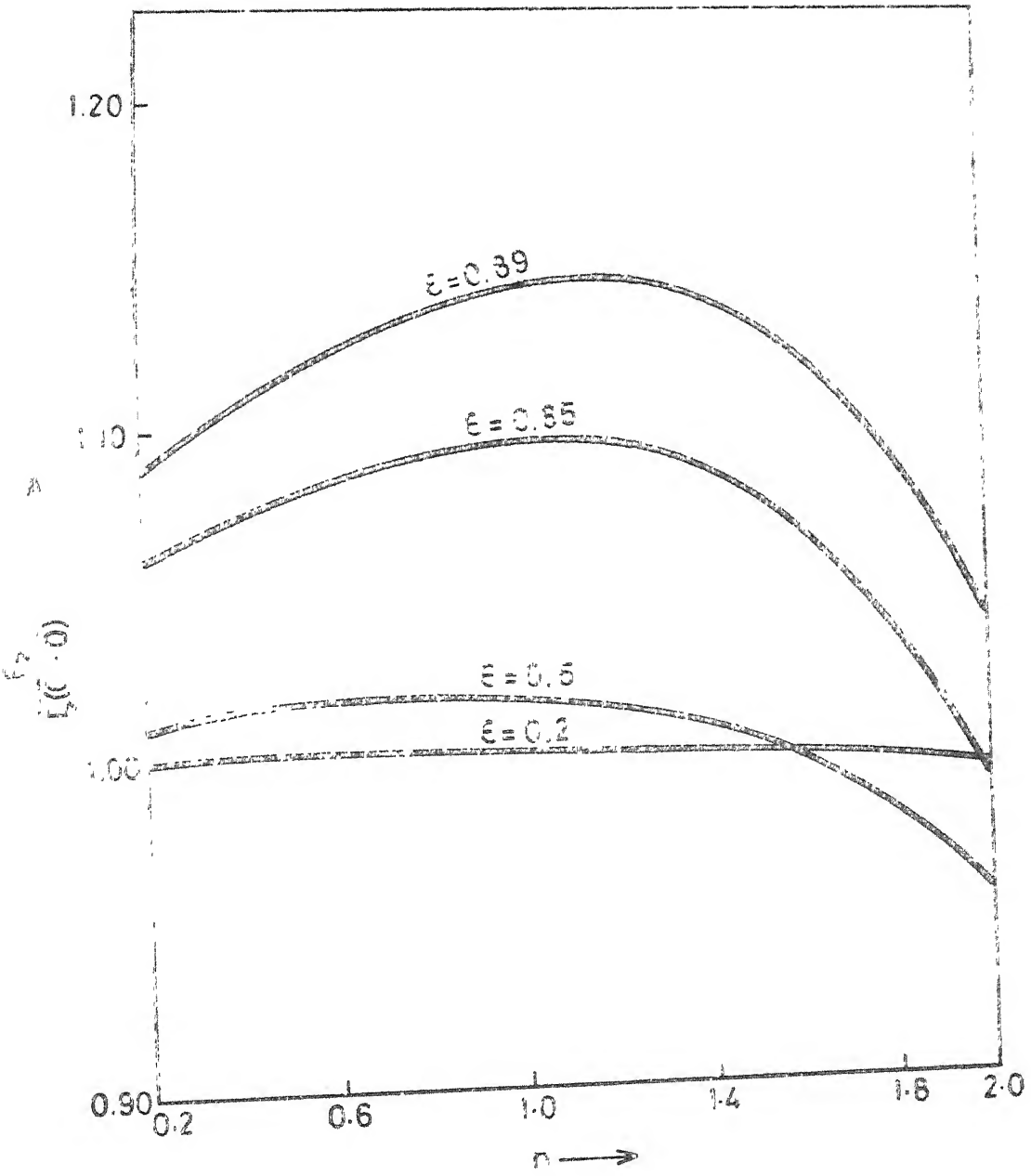

Fig 6.4 Axial forces - ratio versus the flow behaviour index for various values of the tilt parameter

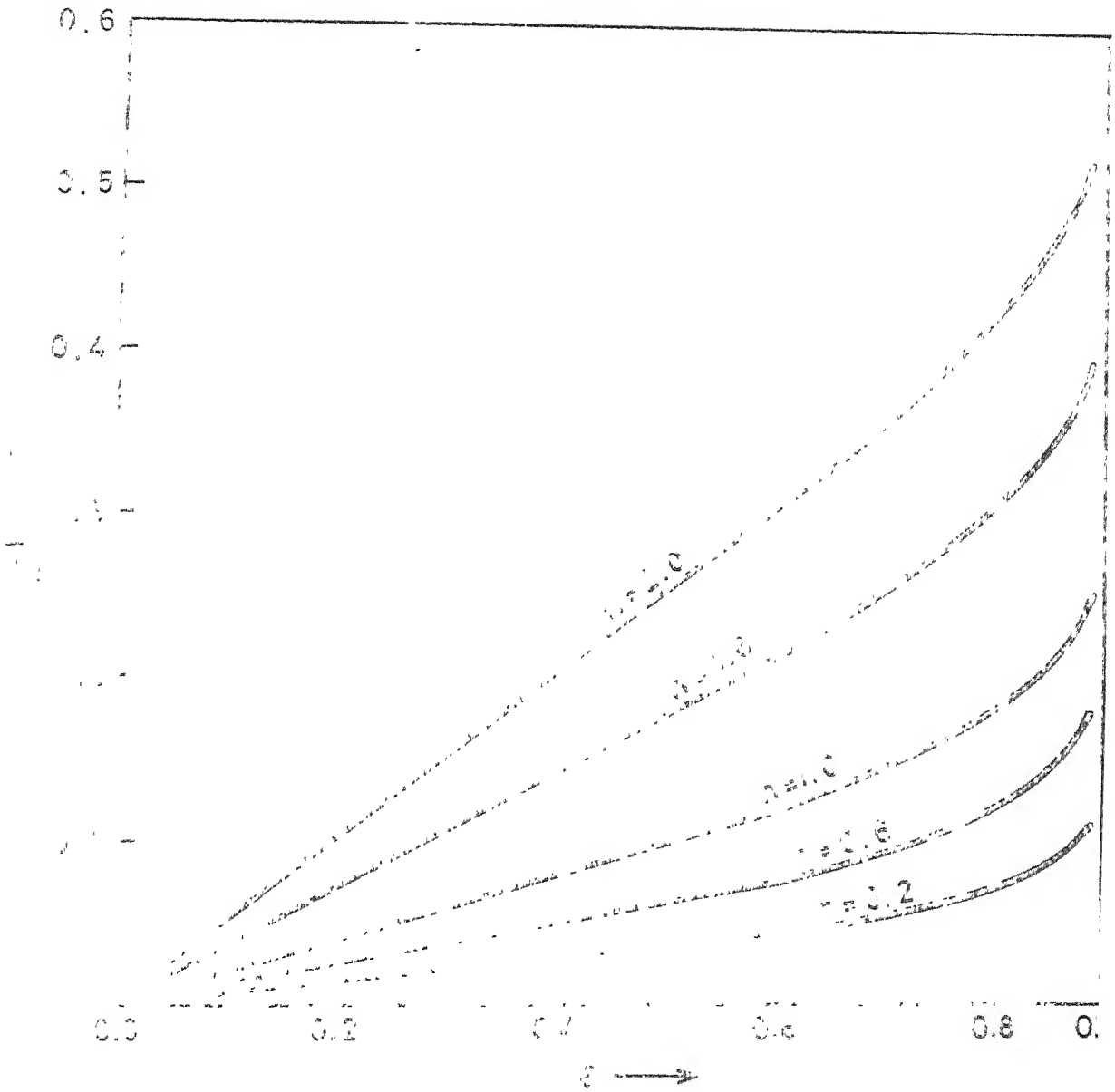

Fig. 6.3 Non-dimensional rolling moment versus the tilt parameter for various values of the flow behaviour index

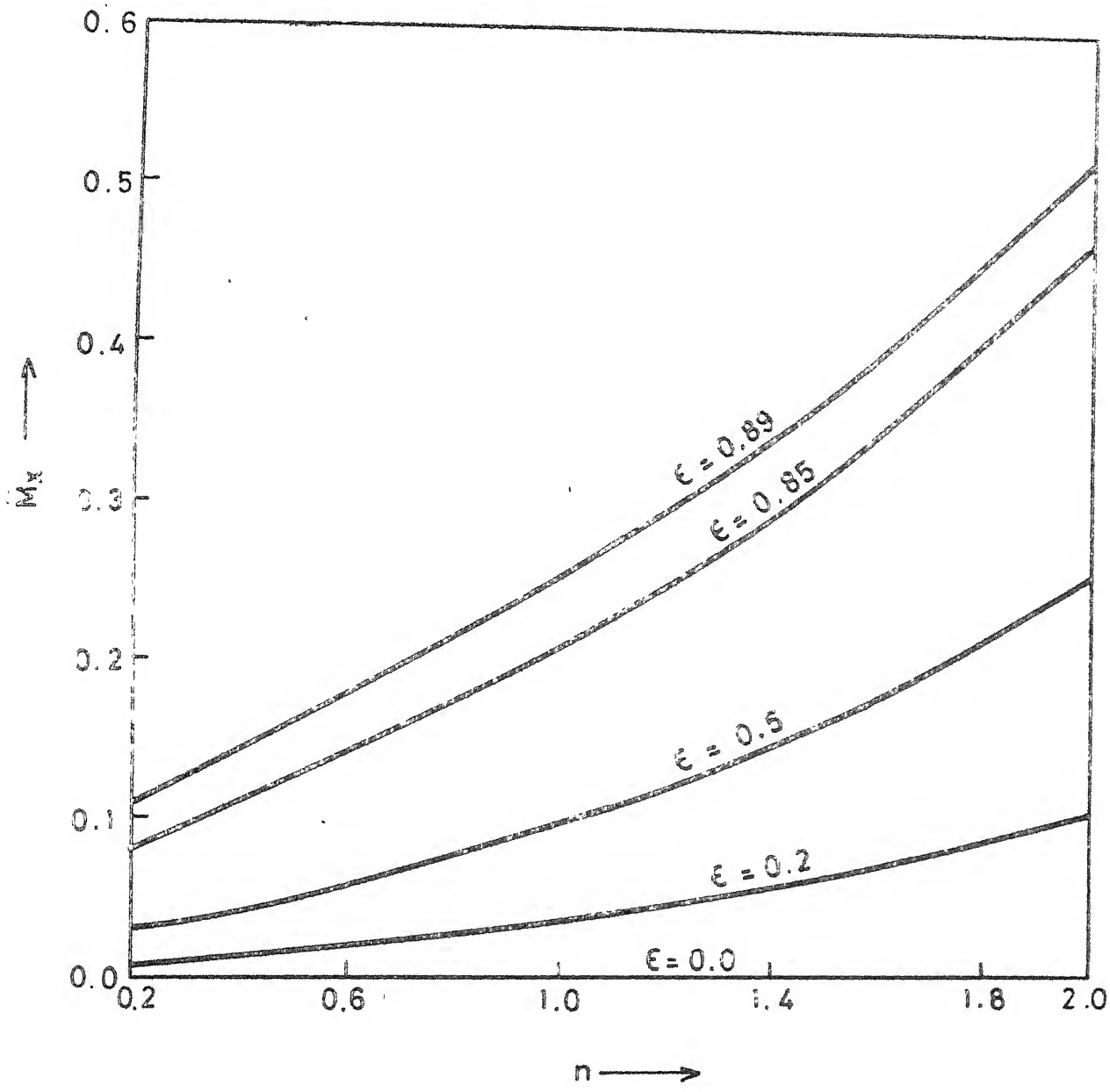

Fig. 6.6 Non-dimensional tilting moment versus the flow behaviour index for various values of the tilt parameter.

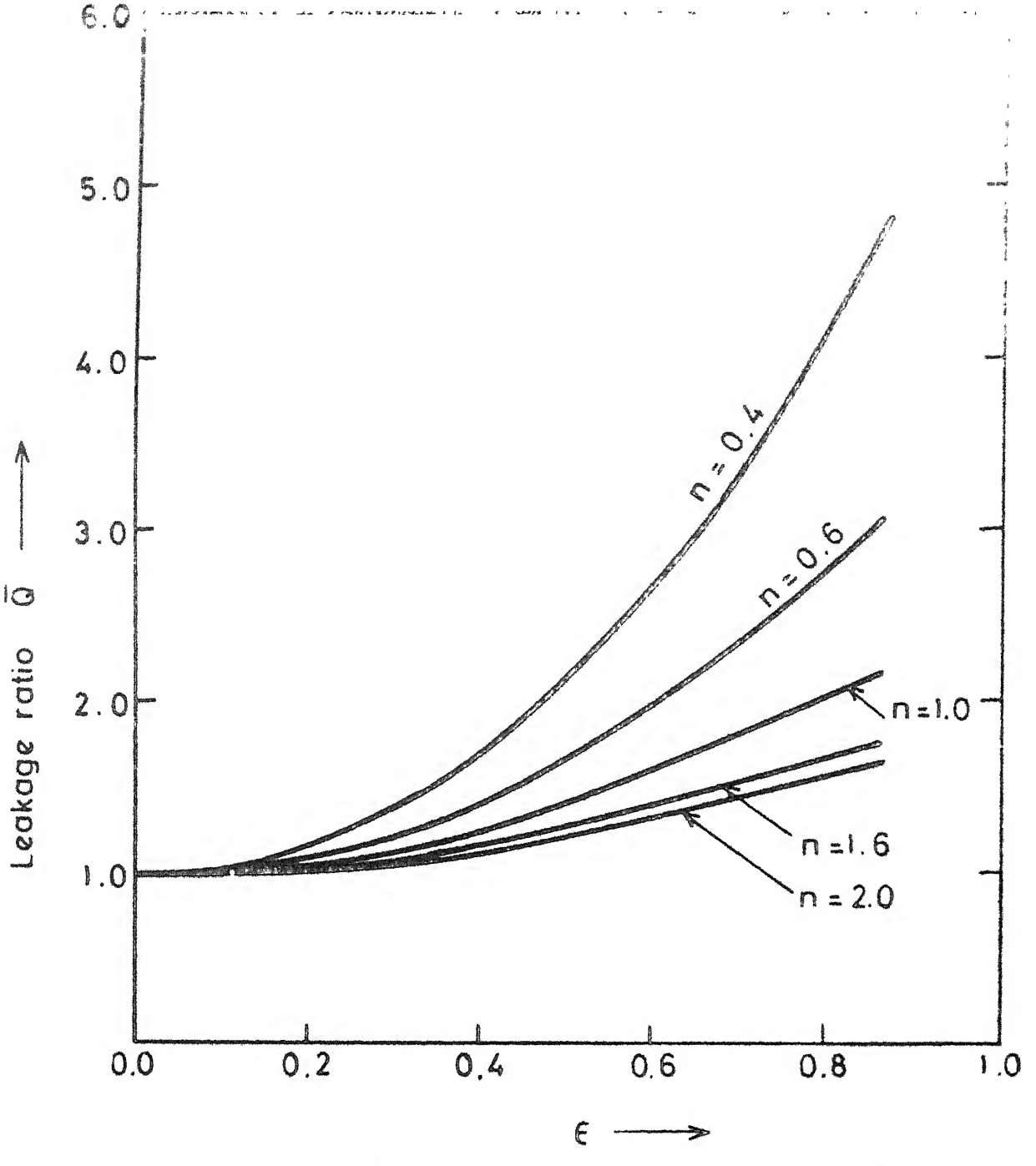

Fig. 6.7 Non-dimensional leakage ratio versus the tilt parameter for various values of the flow behaviour index.

CHAPTER VII

RADIAL AND FRICTIONAL FORCES IN A MISALIGNED RADIAL FACE SEAL WITH A NON-NEWTONIAN FLUID

7.1 INTRODUCTION

Ever since Denny [8] demonstrated the existence of a lubricating fluid film between the mating faces of a mechanical face seal, a considerable amount of fundamental research has been done in an attempt to understand the mechanism that enables face separation. A recent review is by Ludwig [54] in which various models and theories are listed. Much attention has been paid in the last two decades to the radial face seals. In particular axial forces and tilting moments were studied. The radial forces which may cause the radial displacement of the primary seal ring has not been analysed throughly.

These forces may be of important consequence in the onset of radial misalignment. Radial forces may well be the origin of radial eccentricity and hence directly influence the primary seal leakage. In addition to their influence on leakage, the radial forces may also affect the dynamic stability of the seal.

Recently Etsion [78] has analysed the radial forces in a misaligned radial face seal and shown that radial forces are most pronounced when the high pressure is on the

---

This chapter was presented in paper form at the Winter Annual Meeting of the American Society of Mechanical Engineers, Phoenix, Arizona, November , 1982.
(To be published in Jour.Fluid.Engng.,Trans.ASME).

outside periphery of the seal. In such cases the inward pumping generated by the radial forces, adds to the hydrostatic leakage and this may provide a possible seal failure reason.

Shapiro and Colsher [47] and Ludwig and Allen [55] considered the dynamic behaviour of a radial face seal and studied the frictional force on the secondary seal ring. This friction provides the damping of the axial and angular vibrations of the primary seal ring and is dependent on the radial pressure exerted by the primary seal ring and seal housing on the flexible element of the secondary seal.

Most of the work devoted to the understanding of the seal mechanism, which has so far appeared in the literature assumes that the lubricant behaves essentially as a Newtonian viscous fluid. Non-Newtonian behaviour is, however, almost invariably observed in various lubrication processes. The reason for this has been amply discussed in the previous chapter.

It is thus felt that the application of the power law model to the analyses of a misaligned radial face seal may well lead to a better visualization of the origin of the radial and the frictional forces which affect the seal performance considerably. The results

of the analysis might also be useful in an instance where a non-Newtonian situation is encountered. Curvature effects neglected by Etsion [78], might be of important consequence in this context and hence are considered is this chapter. Further, in this analysis no approximation of the type made by Etsion [78] has been resorted to, thus leading to more accurate results.

7.2 MATHEMATICAL ANALYSIS

The schematic of misaligned radial face seal is given in figure 3.1.

Mathematically, for a power law fluid,

$$\tau = m\left|\frac{\partial v}{\partial z}\right|^{n-1}\frac{\partial v}{\partial z} \tag{7.1}$$

The equation of motion is

$$\frac{dp}{dr} = \frac{\partial \tau}{\partial z} \tag{7.2}$$

and the equation of continuity is

$$\frac{1}{r}\frac{\partial}{\partial r}(rv) + \frac{\partial w}{\partial z} = 0 \tag{7.3}$$

Substituting the value of τ from equation (7.1) into equation (7.2), we get

$$\frac{dp}{dr} = \frac{\partial}{\partial z}\left\{m\left|\frac{\partial v}{\partial z}\right|^{n-1}\frac{\partial v}{\partial z}\right\} \tag{7.4}$$

We confine our attention to the region where $\frac{\partial v}{\partial z} \leq 0$. Thus equation (7.4) reduces to

$$\frac{dp}{dr} = -m\frac{\partial}{\partial z}\left(-\frac{\partial v}{\partial z}\right)^{n} \tag{7.5}$$

Integrating equation (7.5) with the boundary conditions

$$\frac{\partial v}{\partial z} = 0 \text{ at } z = h/2 \tag{7.6}$$

$$v = 0 \text{ at } z = h \text{ and } z = 0 \tag{7.7}$$

We obtain the velocity profile as :

$$v = \left(-\frac{1}{m}\frac{dp}{dr}\right)^{1/n} \left[\frac{\left(\frac{h}{2}\right)^{\frac{n+1}{n}} - \left(z-h/2\right)^{\frac{n+1}{n}}}{\frac{n+1}{n}} \right], \frac{h}{2} \leq z \leq h \tag{7.8}$$

and similarly

$$v = \left(-\frac{1}{m}\frac{dp}{dr}\right) \left[\frac{\left(h/2\right)^{\frac{n+1}{n}} - \left(h/2-z\right)^{\frac{1+n}{n}}}{\frac{n+1}{n}} \right], 0 \leq z \leq h/2 \tag{7.9}$$

where h is the film thickness.

Substituting for v from equation (7.9) in the equation of continuity (7.3) and integrating with respect to z with the conditions

$$w = 0 \text{ at } z = h \text{ and } z = 0 \tag{7.10}$$

we get the final equation controlling the motion of a power law lubricant in the gap between the faces of a radial face seal as below :

$$\frac{1}{r}\frac{d}{dr}\left\{ \frac{2n}{2n+1} r\left(\frac{h}{2}\right)^{\frac{2n+1}{n}} \left(-\frac{1}{m}\frac{dp}{dr}\right)^{\frac{1}{n}} \right\} = 0 \tag{7.11}$$

The boundary conditions for the pressure are :

$$p = p_1 \text{ at } r = r_1 \; ; \; p = p_2 \text{ at } r = r_2 \tag{7.12}$$

where r_1 is the inner radius and r_2 is the outer radius.

Integrating equation (4.11) twice and then using the boundary conditions in the equation (4.12) and assuming the consistency to be constant, we get :

$$p = C_1(\theta) \int_{r_1}^{r} \frac{dr}{r^n h^{2n+1}} + p_1 \qquad (7.13)$$

where

$$C_1(\theta) = \frac{(p_2 - p_1)}{\int_{r_1}^{r_2} \left(\frac{1}{r^n h^{2n+1}}\right) dr} \qquad (7.14)$$

The film thickness h is (see figure 4.1)

$$h = c + \gamma\, r \cos\theta \qquad (7.15)$$

where c is the axial clearance and γ is the angle of tilt. Thus p has the following form :

$$p = \left[\frac{(p_2 - p_1)}{\int_{r_1}^{r_2} \frac{dr}{r^n (c + \gamma\, r \cos\theta)^{2n+1}}}\right] \times \left[\int_{r_1}^{r} \frac{dr}{r^n (c+\gamma\, r \cos\theta)^{2n+1}}\right] + p_1 \qquad (7.16)$$

(i) Radial Force :

The radial force in a seal is defined as

$$F_r = -2 \int_0^{\pi} \int_{r_1}^{r_2} \tau \cos\theta\, r\, d\theta\, dr \qquad (7.17)$$

Thus the radial force F_r on the surface z = h is obtained by substituting the value of τ at z = h, in equation (7.17).

Thus

$$F_r = (p_2-p_1)\int_0^{\pi}\left[\left\{\frac{1}{\int_{r_1}^{r_2}\frac{dr}{r^n(c+\gamma\ r\cos\theta)^{2n+1}}}\right\}\right.$$

$$\left.\times\left\{\int_{r_1}^{r_2}\frac{dr}{r^{n-1}(c+\gamma\ r\cos\theta)^{2n}}\right\}\right]\cos\theta\ d\theta \qquad (7.18)$$

(ii) Frictional Force :

The radial frictional force is defined by

$$F_R = -2\int_0^{\pi}\int_{r_1}^{r_2} c\ r\ d\theta\ dr \qquad (7.19)$$

and at z = h the radial frictional force assumes the form :

$$F_R = (p_2-p_1)cr_2\int_0^{\pi}\left[\left\{\frac{1}{\int_{r_1}^{r_2}\frac{dr}{r^n(c+\gamma\ r\cos\theta)^{2n+1}}}\right\}\right.$$

$$\left.\times\left\{\int_{r_1}^{r_2}\frac{dr}{r^{n-1}(c+\gamma\ r\cos\theta)^{2n}}\right\}\right]d\theta \qquad (7.20)$$

7.3 NON-DIMENSIONAL SCHEME

We resort to the following dimensionless scheme :

$$\bar{h} = 1 + \varepsilon\ \bar{r}\cos\theta\ ;\ \bar{r} = \frac{r}{r_2}\ ;\ \varepsilon = \frac{\gamma\ r_2}{c}\ ;\ \bar{r}_1 = \frac{r_1}{r_2}$$

$$\bar{F}_r = \frac{F_r}{(p_2-p_1)cr_2}\ ;\ \bar{F}_R = \frac{F_R}{(p_2-p_1)cr_2} \qquad (7.21)$$

Thus the non-dimensional radial force becomes :

$$\bar{F}_r = \int_0^{\pi} I \cos\theta \, d\theta \tag{7.22}$$

where

$$I = \left[\frac{1}{\int_{\bar{r}_1}^{1} \frac{d\bar{r}}{\bar{r}^n (1+\varepsilon\, \bar{r} \cos\theta)^{2n+1}}} \right] x \left[\int_{\bar{r}_1}^{1} \frac{d\bar{r}}{\bar{r}^{n-1} (1+\varepsilon\, \bar{r} \cos\theta)^{2n}} \right] \tag{7.23}$$

And the non-dimensional frictional forces is

$$\bar{F}_R = \int_0^{\pi} \left[\frac{1}{\int_{\bar{r}_1}^{1} \frac{d\bar{r}}{\bar{r}^n (1+\varepsilon\, \bar{r} \cos\theta)^{2n+1}}} \; x \int_{\bar{r}_1}^{1} \frac{dr}{\bar{r}^{n-1} (1+\varepsilon\, \bar{r} \cos\theta)^{2n}} \right] d\theta \tag{7.24}$$

For Newtonian, fluids, i.e. when n = 1

$$\bar{F}_r(n=1) = -\frac{1}{\varepsilon} \int_0^{\pi} \frac{q_1(\theta)}{q_2(\theta)} \, d\theta \,, \quad \varepsilon \neq 0 \tag{7.25}$$

where

$$q_1(\theta) = \left[\frac{1}{1+\varepsilon \cos\theta} - \frac{1}{1+\varepsilon\, \bar{r}_1 \cos\theta} \right] \tag{7.26}$$

and

$$q_2(\theta) = \left[\log\left(\frac{1+\varepsilon\, \bar{r}_1 \cos\theta}{\bar{r}_1 + \varepsilon\, \bar{r}_1 \cos\theta} \right) + \left(\frac{1}{1+\varepsilon \cos\theta} - \frac{1}{1+\varepsilon\, \bar{r}_1 \cos\theta} \right) \right.$$

$$\left. + \frac{1}{2} \left(\frac{1}{(1+\varepsilon \cos\theta)^2} - \frac{1}{(1+\varepsilon\, \bar{r}_1 \cos\theta)^2} \right) \right] \tag{7.27}$$

And

$$\bar{F}_R(n=1) = \int_0^{\pi} \frac{q_1(\theta)}{q_2(\theta)} \, d\theta \tag{7.28}$$

For $n = 1$, $\varepsilon = 0$,

$$\bar{F}_r(n = 1,\ \varepsilon = 0) = 0 \tag{7.29}$$

$$\bar{F}_R(n = 1,\ \varepsilon = 0) = -\pi \times \frac{(1-\bar{r}_1)}{\log(\bar{r}_1)} \tag{7.30}$$

7.4 RESULTS AND DISCUSSION

The most important parameter for discussing the behaviour of various seal characteristics, in the present context, is the flow behaviour index n. The fact that the power law model can actually be used for realistic fluids is obvious from table 6.1.It is seen that the value of n, generally lies between 0.5 to 2.5. In the discussion that follows each of the seal characteristics is analysed from this view point.

Fig. 7.1 is the graph for non-dimensional radial force versus the tilt parameter ε. It is seen that an increasing value of the tilt parameter increases this force. This force is almost a linear function of ε for all values of radii ratio r_1/r_2 and flow behaviour index n. The force $\bar{F}_r$ acts along the line connecting the maximum and the minimum film points of the primary seal ring. The direction of this force is determined by the sign of (p_2-p_1). When the high pressure is inside the periphery of the seal, $\bar{F}_r$ is directed towards the point of maximum film thickness, and vice versa. It is

also seen that lower the value of n, higher the radial force.

Fig.7.2 is a plot of friction force $\bar{F}_R$ vs. tilt parameter. It is seen that higher the value of tilt, lower the value of frictional force on the primary seal ring. Thus tilting may be utilized in the reduction of the frictional forces. However, the tilting does not produce a significant difference in the frictional force. The behaviour of the frictional force, with respect to n, is similar to that of the radial force.

The qualitative behaviour of Fig. 7.3 is similar to that of Fig. 7.2 with difference that Fig. 7.3 gives the value of $\bar{F}_r$ as a function of n, thus includes a wide range of fluids for different tilt parameters and radii ratio r_1 / r_2. The curves for $n < 1$, depict an increase in the radial force (Fig.7.1) , frictional force (Fig. 7.2). It can thus be concluded that for pseudoplastic fluids the radial force as well as the frictional force increases, when compared with the corresponding Newtonian results ($n = 1$) .

Table 7.1, given a comparision between the radial forces $\bar{M}_o$ (obtained by Etsion [78], neglecting curvature effects) and $\bar{M}_1$ (present analysis, curvature effects included) for various values of eccentricity ratio

TABLE 7.1. Comparison between radial forces, $\bar{M}_o$ (Curvature effects neglected, Etsion [1]) and $\bar{M}$ (Curvature effects included, present results), for various values of eccentricity ratio and inner/outer radii ratio, for Newtonian fluids.

Force	$\bar{r}_1 = 0.8$		$\bar{r}_1 = 0.86$		$\bar{r}_1 = 0.9$		$r_1 = 0.96$		$r_1 = 0.98$		$\bar{r}_1 = 0.99$	
ε	$\bar{M}_o$	$\bar{M}_1$	$\bar{M}_o$	$\bar{M}_1$	$\bar{M}_o$	$\bar{M}_1$	$\bar{M}_o$	$\bar{M}_1$	$\bar{M}_o$	$\bar{M}_1$	$\bar{M}_o$	$\bar{M}_1$
0.1	0.12724	0.12515	0.13586	0.13484	0.14177	0.14124	0.15086	0.15078	0.15295	0.15293	0.15551	0.15552
0.2	0.25455	0.25036	0.27176	0.26970	0.28355	0.28250	0.30172	0.30155	0.30791	0.30787	0.31103	0.31101
0.3	0.38198	0.37569	0.40772	0.40464	0.42537	0.42380	0.45259	0.45234	0.46186	0.46180	0.46654	0.46652
0.4	0.50962	0.50125	0.54379	0.53969	0.56725	0.56516	0.60347	0.60613	0.61582	0.61574	0.62205	0.62203
0.5	0.62761	0.62715	0.68005	0.67492	0.70923	0.70661	0.75437	0.75395	0.76979	0.76968	0.77757	0.77754
0.6	0.76614	0.75360	0.81661	0.81046	0.85138	0.84824	0.90529	0.90479	0.92376	0.92363	0.93309	0.93305
0.7	0.89559	0.88100	0.95369	0.94652	0.99382	0.99015	1.05628	1.05569	1.07774	1.07759	1.08861	1.08857
0.8	1.02669	1.01014	1.09176	1.08360	1.13683	1.13266	1.20737	1.20670	1.23176	1.23159	1.24414	1.24409
0.9	1.16137	1.14314	1.23216	1.22312	1.28132	1.27666	1.35880	1.35805	1.38587	1.38567	1.39969	1.39963
0.99	1.29119	1.27278	1.36546	1.35626	1.41666	1.41187	1.49702	1.49622	1.52529	1.52509	1.53992	1.53987
1.0	1.30683	1.28235	1.38151	1.37035	1.43282	1.43200	1.51323	1.51320	1.54133	1.54130	1.55580	1.55575

and inner to outer radii ratio, $\bar{r}_1$, for Newtonian fluids. It is seen that the curvature effects are not significant for values of $\bar{r}_1$ exceeding 0.9. However, for lower values, the inclusion of curvature may decrease the radial force by over 2 percent in the Newtonian case. A similar result may be expected for non-Newtonian fluid.

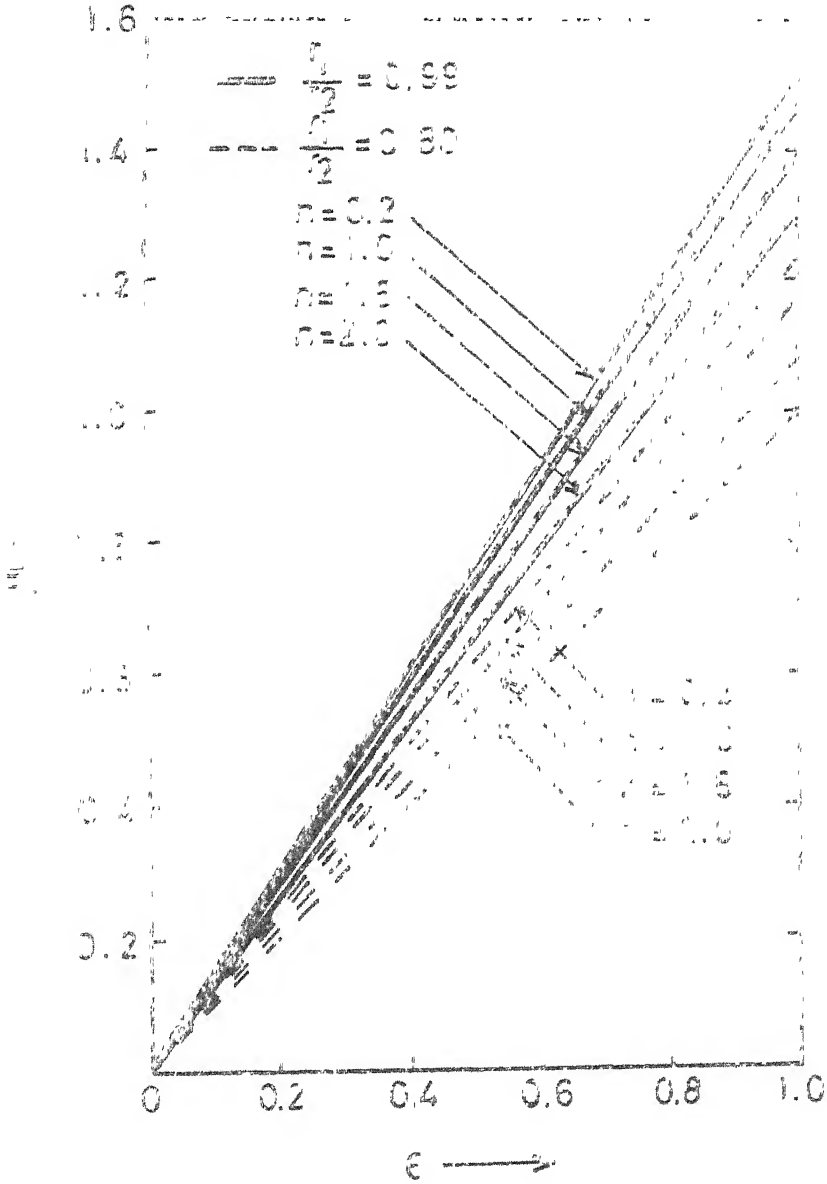

Fig 7 : Non-dimensional radial force as a function of tilt parameter for various values of flow behaviour index

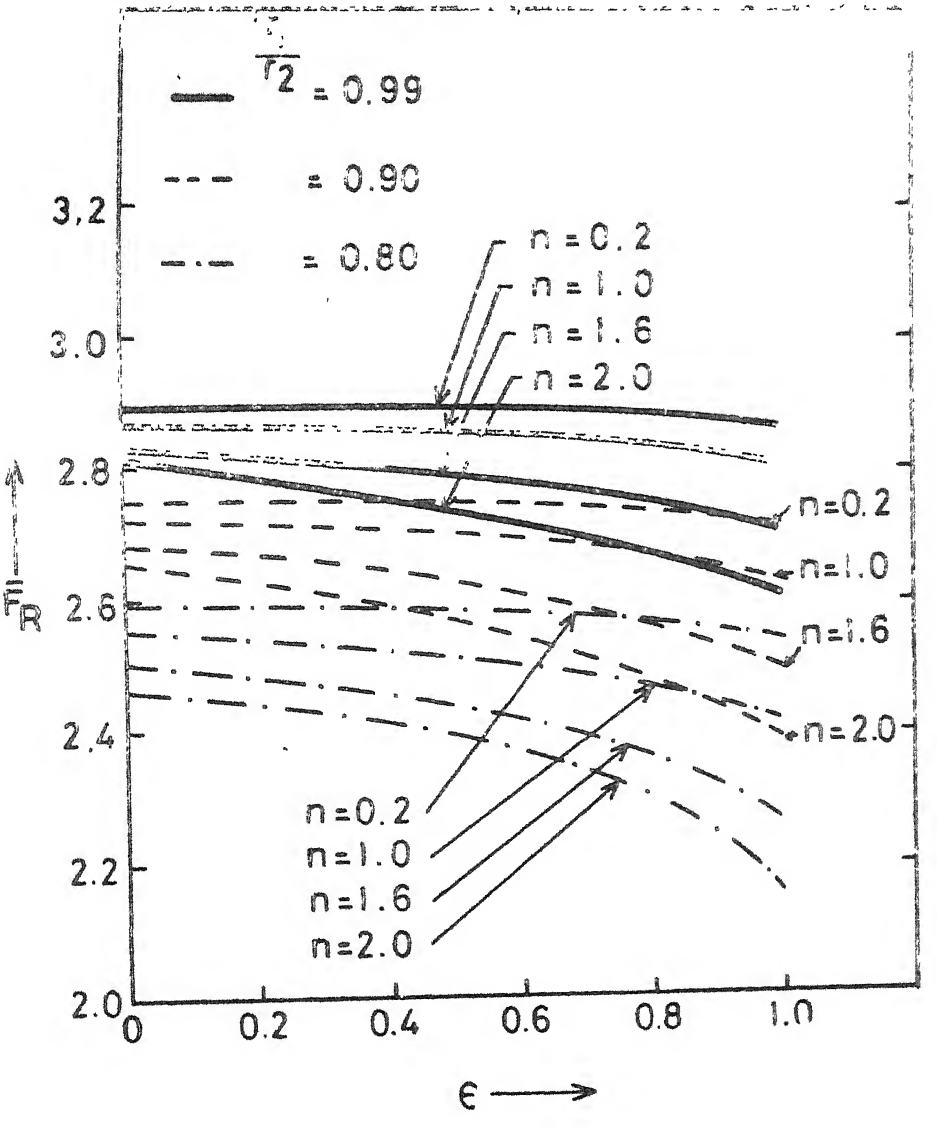

Fig. 7.2 Non-dimensional frictional force as a function of tilt parameter for various values of flow behaviour index

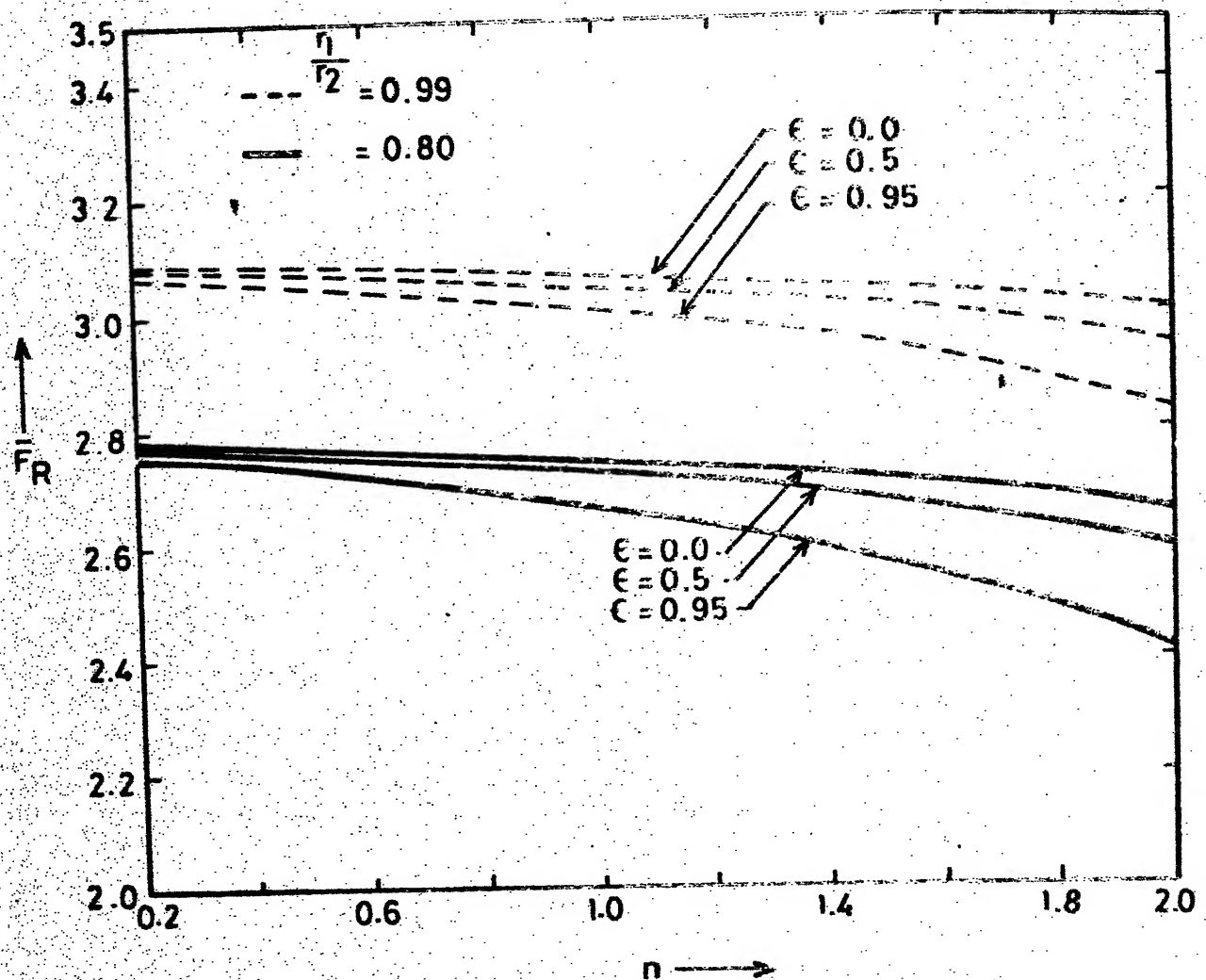

Fig. 7.3 Non-dimensional frictional force as a function of flow behaviour index for various values of tilt parameter.

CHAPTER VIII*

ELASTOHYDROSTATIC LUBRICATION OF CIRCULAR PLATE THRUST BEARING WITH POWER LAW LUBRICANTS

8.1 INTRODUCTION

The increasing number of practical bearing employing layered elastic solids as mating surfaces has led to a substantial interest in the elastohydrodynamic and elastohydrostatic lubrication of such bearings. To avoid wear and seizure and to make the supply of the lubricant easier, thin layers of softer materials, such as the stiffer plastics, are sometimes coated on the bearing surfaces. In such cases the bearing characteristics and film geometry are modified substantially in comparision to the corresponding rigid bearing.

Dowson and Taylor [90] analysed the behaviour of elastohydrostatic circular thrust plates. An increase in load carrying capacity and change in film geometry which was predicted theoretically was varified experimentally in the same paper. Although the theoretical analysis was based

---

*This chapter has been published in the form of following research paper ''Elastohydrostatic Lubrication of Circular Plate Thrust Bearing With Power Law Lubricants'', Jour.Lub. Tech.,Trans. ASME, Vol.104,1982,p.243.

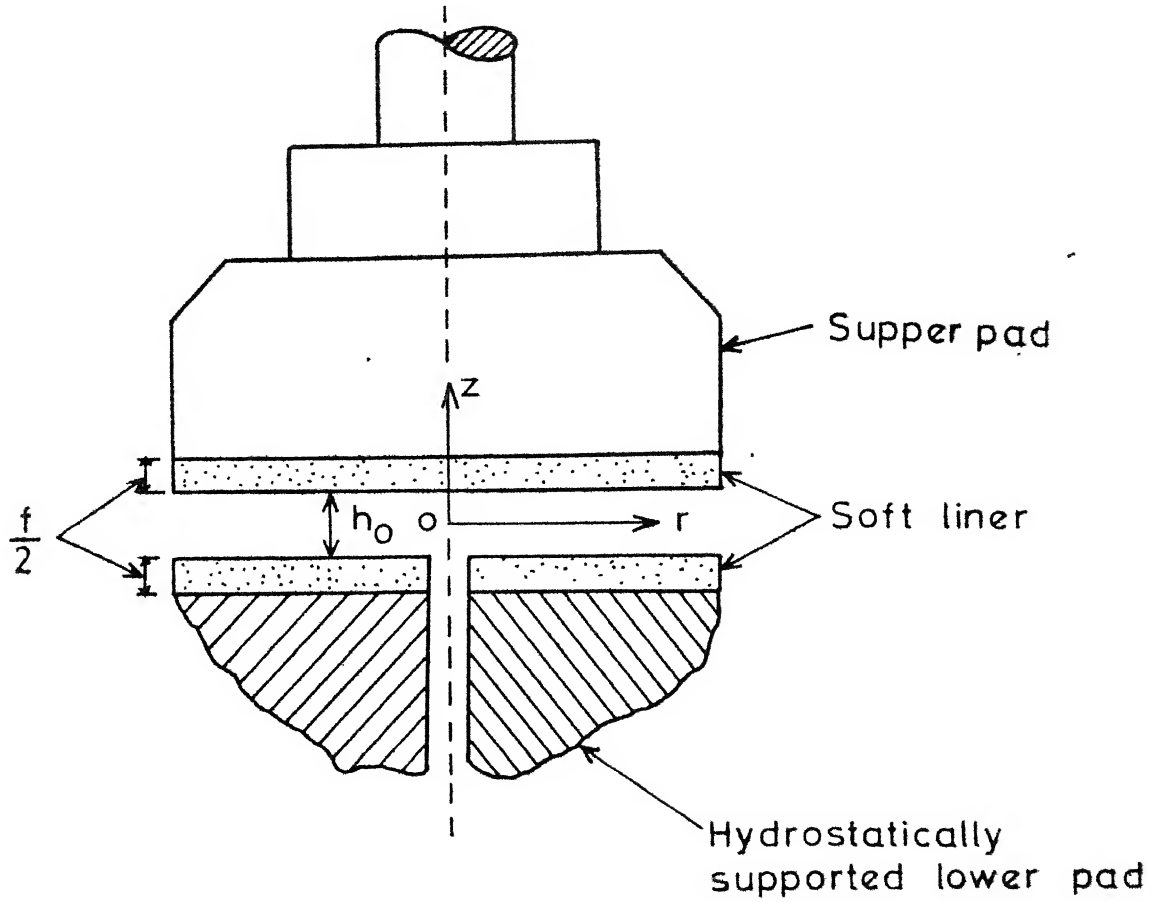

Fig 8.1 A schematic diagram of elastohydrostatic thrust bearing.

upon some approximations, some useful deductions were made for such bearings.

The results of [90] are based on the fact that the lubricant used was Newtonian. This chapter extends this work to lubricants which may display non-Newtonian behaviour due to the presence of certain additives. The non-Newtonian model chosen here is that of a power law which has been considerably discussed in Chapter 6.

The circular plate thrust bearings considered in this chapter are of the type used in the fluid sealing and are known as radial face seals. The analysis and the results discussed in this chapter may therefore be extended to predict the behaviour of radial face seals.

8.2 MATHEMATICAL ANALYSIS

The elastohydrostatic lubrication of circular thrust plates is analysed using a non-Newtonian power law lubricant.

Consider the flow of a power law fluid between two externally pressurized circular plates separated by a constant distance h apart. The lubricant is supplied through a central hole of radius r_1 with constant pressure p_1. The upper and lower plates are lined with material much softer than the rigid backing and the thickness of each layer is $f/2$ where $f \ll r_2$, where r_2 is the outer radius of the plate. Figure 8.1 shows a schematic diagram of such a bearing.

As has been derived in Chapter 6, the final equation governing the flow of power law lubricant in the gap between the plates is as following

$$\frac{d}{dr}\left[r H'^{\left(\frac{2n+1}{n}\right)} \left(\frac{dp}{dr}\right)^{\frac{1}{n}} \right] = 0 \qquad (8.1)$$

Let h_o be the film thickness which is constant in the unstressed case. For stressed case, when the pressure modifies the film shape, the film thickness h can be written as

$$H' = h + sp \qquad (8.2)$$

where sp is the local compression of the elastic layer, given by [90]

$$s = \frac{f}{E'} \qquad (8.3)$$

where E is the modulus of elasticity of the soft material and E' is the elastic onstant and is given by

$$\frac{1}{E'} = \frac{1}{E}\left[1 - \frac{2\nu^2}{1-\nu} \right] \qquad (8.4)$$

(ν is Poisson's ratio)

If the variation of f with radius is neglected, equation (8.1) can be integrated for pressure distribution and other bearing characteristics.

The pressure boundary conditions are

$$p = p_1 \text{ at } r = r_1 \tag{8.5}$$

$$p = 0 \text{ at } r = r_2 \tag{8.6}$$

Solving equation (8.1) for pressure distribution with the pressure boundary conditions (8.5) and (8.6), we get for $n \neq 1$,

$$p = \frac{1}{s}\left[\left(\frac{\{(sp_1+h_o)^{(2n+2)} - h_o^{(2n+2)}\}}{\left(\frac{1}{r_1^{(n-1)}} - \frac{1}{r_2^{(n-1)}}\right)} \left(\frac{1}{r^{(n-1)}} - \frac{1}{r_2^{(n-1)}} \right) + h_o^{(2n+2)} \right)^{\frac{1}{(2n+2)}} - h_o \right] \tag{8.7}$$

for $n = 1$,

$$p = \frac{h_o}{s}\left[\left\{ \frac{\log\left(\frac{r}{r_1}\right) + \left(1+p_1\frac{s}{h_o}\right)^4 \log\left(\frac{r_2}{r}\right)}{\log\left(\frac{r_2}{r_1}\right)} \right\}^{1/4} - 1 \right] \tag{8.8}$$

8.2.1 Load Capacity :

The load carrying capacity of the bearing is

$$W = \pi r_1^2 p_1 + 2\pi \int_{r_1}^{r_2} pr \, dr \tag{8.9}$$

for $n \neq 1, 3$,

$$W = \pi r_1^2 p_1 + \frac{2\pi}{s}\left[\int_{r_1}^{r_2}\left\{\frac{(h+sp_1)^{(2n+2)}-h^{(2n+2)}}{\left(\frac{1}{r_1^{(n-1)}}-\frac{1}{r_2^{(n-1)}}\right)}\left(\frac{1}{r^{(n-1)}}-\frac{1}{r_2^{(n-1)}}\right)\right.\right.$$

$$\left.\left.+\, h^{(2n+2)}\right\}\frac{1}{(2n+2)}\, r\, dr\right] - \frac{\pi h}{s}(r_2^2-r_1^2) \qquad (8.10)$$

for $n = 1$,

$$W = \pi r_1^2 p_1 - \frac{\pi h}{s}(r_1^2-r_1^2)$$

$$+ \frac{2\pi h}{s}\left[\int_{r_1}^{r_2}\left\{\frac{\log(\frac{r}{r_1})+(1+\frac{sp_1}{h})^4\log(\frac{r_2}{r})}{\log(\frac{r_2}{r_1})}\right\}^{1/4} r\, dr\right] \qquad (8.11)$$

Taking the limit $s \to 0$, the equations (8.7)-(8.8) and (8.10)-(8.11) yield the pressure distribution and the load carrying capacity for rigid bearings as follows

for $n \neq 1$,

$$p = \frac{p_1}{\left(\frac{1}{r_1^{(n-1)}}-\frac{1}{r_2^{(n-1)}}\right)}\left(\frac{1}{r^{n-1}}-\frac{1}{r_2^{n-1}}\right) \qquad (8.12)$$

for $n = 1$,

$$p = p_1 \frac{\log(\frac{r_2}{r})}{\log(\frac{r_2}{r_1})} \qquad (8.13)$$

for $n \neq 1,3$;

$$W = \pi r_1^2 p_1 + \frac{2\pi p_1}{\left(\frac{1}{r_1^{(n-1)}} - \frac{1}{r_2^{(n-1)}}\right)}\left[\frac{1}{(3-n)}\left(\frac{1}{r_2^{(n-3)}} - \frac{1}{r_1^{(n-3)}}\right)\right.$$

$$\left. - \frac{1}{2}\left(\frac{1}{r_2^{(n-3)}} - \frac{r_1^2}{r_2^{(n-1)}}\right)\right] \qquad (8.14)$$

for n = 1,

$$W = \frac{\pi p_1}{2} \frac{(r_2^2 - r_1^2)}{\log\left(\frac{r_2}{r_1}\right)} \qquad (8.15)$$

for n = 3,

$$W = \pi r_1^2 p_1 + \frac{\pi p_1 r_2^2}{\left(\frac{r_1^2}{r_2^2} - 1\right)}\left[\left(\frac{r_1^2}{r_2^2} - 1\right) - 2\log\left(\frac{r_1}{r_2}\right)\right] \qquad (8.16)$$

8.3 NON-DIMENSIONAL SCHEME

We adopt the following non-dimensional scheme

$$\bar{h}' = \frac{h'}{h} \; ; \quad \bar{r} = \frac{r}{r_2} \; ; \quad \bar{r}_1 = \frac{r_1}{r_2} \; ; \quad \bar{s} = \frac{s p_1}{h} \; ;$$

$$\bar{p} = \frac{p}{p_1} \; ; \quad \bar{W} = \frac{W}{\pi r_2^2 p_1} \qquad (8.17)$$

The dimensionless for various bearing characteristics for elastic layered bearings are given by

$$\bar{h}' = 1 + \bar{s}\,\bar{p} \qquad (8.18)$$

for $n \neq 1$,

$$\bar{p} = \frac{1}{\bar{s}}\left[\left\{ \left(\frac{(\bar{s}+1)^{(2n+2)} - 1}{(1-\bar{r}_1^{(n-1)})} \right)\left(\frac{\bar{r}_1^{(n-1)}}{\bar{r}^{(n-1)}} - \bar{r}_1^{(n-1)} \right) + 1 \right\}^{\left(\frac{1}{2n+2}\right)} - 1 \right] \tag{8.19}$$

for $n = 1$,

$$\bar{p} = \frac{1}{\bar{s}}\left[\left\{ \frac{(1+\bar{s})^4 \log(\bar{r}) - \log\left(\frac{\bar{r}}{\bar{r}_1}\right)}{\log(\bar{r}_1)} \right\}^{1/4} - 1 \right] \tag{8.20}$$

for $n \neq 1$,

$$\bar{W} = \bar{r}_1^{-2} - \frac{(1-\bar{r}_1^{-2})}{\bar{s}} + \frac{2}{\bar{s}} \int_{\bar{r}_1}^{1} \left[\frac{(\bar{s}+1)^{(2n+2)} - 1}{(1-\bar{r}_1^{(1-n)})} (1-\bar{r}^{(1-n)}) + 1 \right]^{\frac{1}{(2n+2)}} \bar{r}\, d\bar{r} \tag{8.21}$$

for $n = 1$,

$$\bar{W} = \bar{r}_1^{-2} - \frac{(1-\bar{r}_1^{-2})}{\bar{s}} + \frac{2}{\bar{s}} \int_{\bar{r}_1}^{1} \left[\frac{(\bar{s}+1)^4 \log(\bar{r}_1) - \log\left(\frac{\bar{r}}{\bar{r}_1}\right)}{\log(\bar{r}_1)} \right]^{1/4} \bar{r}\, d\bar{r} \tag{8.22}$$

For a rigid bearing, equation (8.18) to (8.22) take the forms

$$\bar{h}^r = 1 \tag{8.23}$$

for $n \neq 1$,

$$\bar{p} = \left(\frac{\frac{\bar{r}_1^{(n-1)}}{\bar{r}^{(n-1)}} - \bar{r}_1^{(n-1)}}{1-\bar{r}^{(n-1)}} \right) \tag{8.24}$$

for n = 1,

$$\bar{p} = \frac{\log(\bar{r})}{\log(\bar{r}_1)} \tag{8.25}$$

for $n \neq 1,3$;

$$\bar{w} = \bar{r}_1^2 + \frac{2\bar{r}_1^2}{(1-\bar{r}_1^{(n-1)})}\left[\left(\frac{1}{3-n}\right)(\bar{r}_1^{(n-3)}-1) - \frac{1}{2}(\bar{r}_1^{(n-3)}-\bar{r}_1^{(n-1)})\right] \tag{8.26}$$

for n = 1,

$$\bar{w} = \frac{(1-\bar{r}_1^2)}{-2\log(\bar{r}_1)} \tag{8.27}$$

for n = 3,

$$\bar{w} = \bar{r}_1^2 + \frac{\bar{r}_1^2}{(1-\bar{r}_1^2)}\left[(\bar{r}_1^2-1)-2\log(\bar{r}_1)\right] \tag{8.28}$$

To study the variations in load, a load coefficient C_L is defined as follows

$$C_L = \frac{W(\text{elastohydrostatic})-W(\text{rigid})}{W(\text{rigid})} \times 100 \tag{8.29}$$

It is seen that C_L is a function of the elastic parameter $\bar{s}$ and the flow behaviour index n for a given value of $\bar{r}_1$.

8.4 RESULTS AND DISCUSSION

The integrations involved in equations (8.2 1) and (8.22) have been evaluated numerically using the Romberg Method. The value of parameter $\bar{r}_1$ has been taken as 0.05. For most of the fluids the value of n lies between 0.5 to 2.5.

The most important parameter for discussing the effects of power law fluid as a lubricant on the performance of elastohydrostatic lubrication of circular thrust bearings is the flow behaviour index n.

Figure 8.2 shows the variation of non-dimensional load capacity $\bar{W}$ as a function of elastic parameter $\bar{s}$ for various values of n. The rigid bearing case is depicted by the value at $\bar{s} = 0$. It is seen that the load capacity increases, for all n, for a bearing with elastic layer as compared to rigid bearing. It is also seen that lower the value of n, higher is the load carrying capacity of bearing.

Figure 8.3 is the graph between nondimensional load capacity $\bar{W}(\bar{W} = \frac{W}{\pi p_1 r_2^2})$ and the flow behaviour index n for various values of $\bar{s}$. Again it is seen that the elastic property of the layer improves the load capacity of the bearing, for all values of n, whereas the effect of increasing

n reduces the rate of increase of the load capacity.

The load coefficient C_L, which determines the percentage rate of increase of load, is a function of elastic parameter $\bar{s}$ and flow behaviour index n. Figure 8.4 is the graph between C_L and $\bar{s}$ for various values of n and figure 8.5 shows the variation of C_L with respect to n for different values of $\bar{s}$. From this graph it is seen that C_L is higher for higher values of n and the coefficient increases with increase in $\bar{s}$. The result reveals that although the load capacity is lower for higher values of n, when elastic layer is attached to the surfaces, the load capacity is increased and this increase is enhanced by higher values of n.

Figure 8.6 is the graph for the nondimensional film profile $\bar{h}'$ as a function of $\bar{r}$. It is seen that the deviation of the film profile from the rigid bearing case ($\bar{s}$=0) is higher for lower values of n. This is because of the strong pressure generation for these values of n. The rigid bearing film profile is constant and is given by $\bar{h}' = 1$ (shown by dotted line).

The results of [90] and [92] are particular cases of t present study and can be obtained by taking n = 1 and $\bar{s} = 0$ respectively, the case of [93] is obtained for incompressible fluids.

Again, it is to be noted that the increase in load carrying capacity obtained by [90] is more than that obtained in present case (n = 1). This difference seens to be due to the approximation adopted by those authors. They have expanded the expression for the pressure gradient in the powers of $\bar{s}$($s=pf/E'h$). They further assume that $s \ll 1$, this enables them to resort to the first order approximation. Subsequently, approximate analytical solution for the pressure distribution and the load carrying capacity are obtained. They further mention that the difference between the first order and the third order approximations in the dimensionless load coefficient (C_L) may be 13 percent in the most severe conditions. However, in the present analysis, no such restriction , i.e. $s \ll 1$, is imposed. Hence the results of the present analysis are likely to be more accurate.

The analysis of present chapter reveals that the load capacity increases with the elastic parameter $\bar{s}$ and it decreases with an increase in the value of flow behaviour index (fig. 8.2). When extended to parallel face seals, this result enables us to say that the face separating axial force is increased by the flexibility of the faces. Thus it may be inferred that coating soft

material on seal-face improves the performance of those face seals which witness early failure because of inadequate axial force that provides separation of the faces.

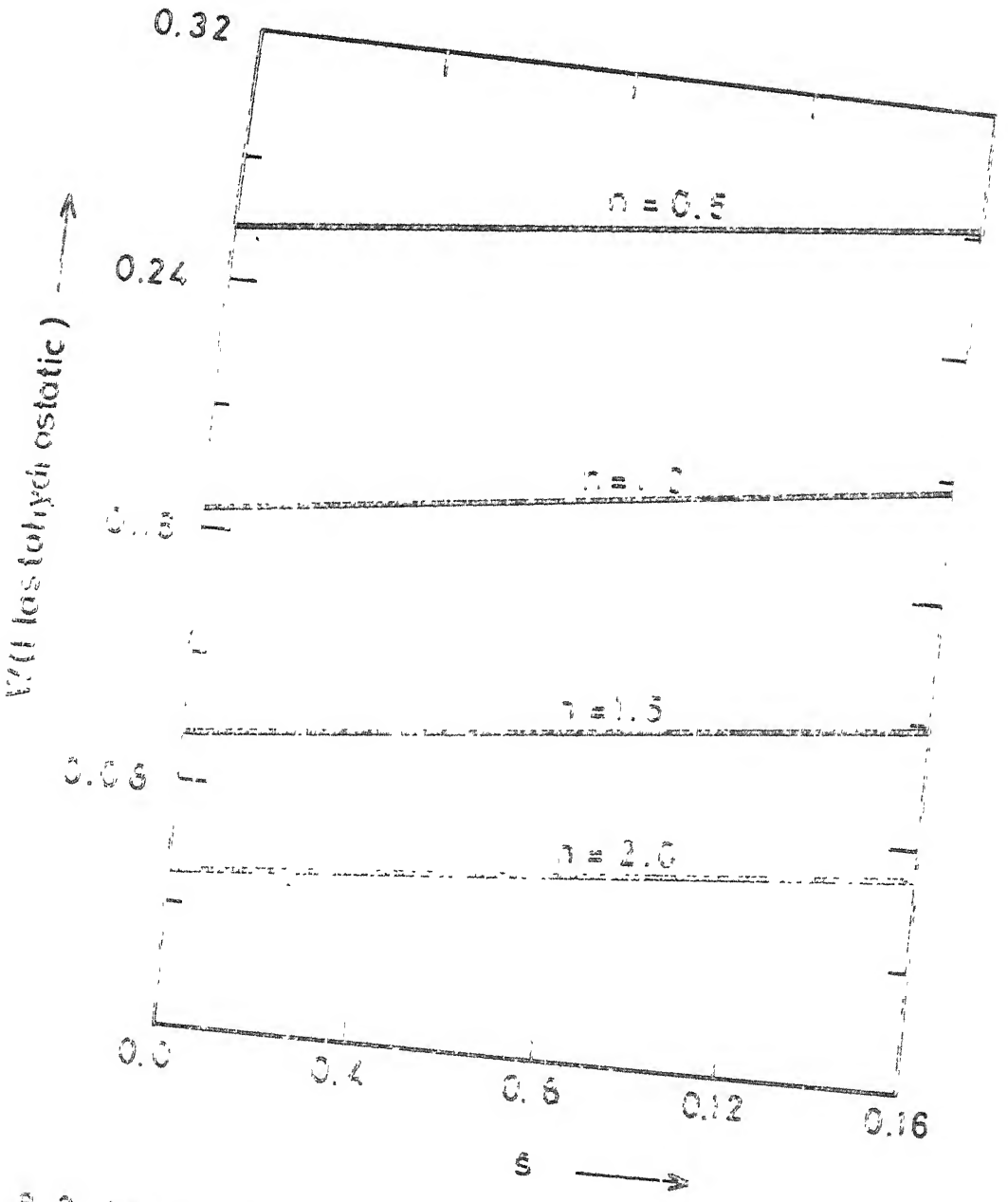

Fig 8.2 Variation of dimensionless load capacity with the elasticity parameter for various values of flow behaviour index.

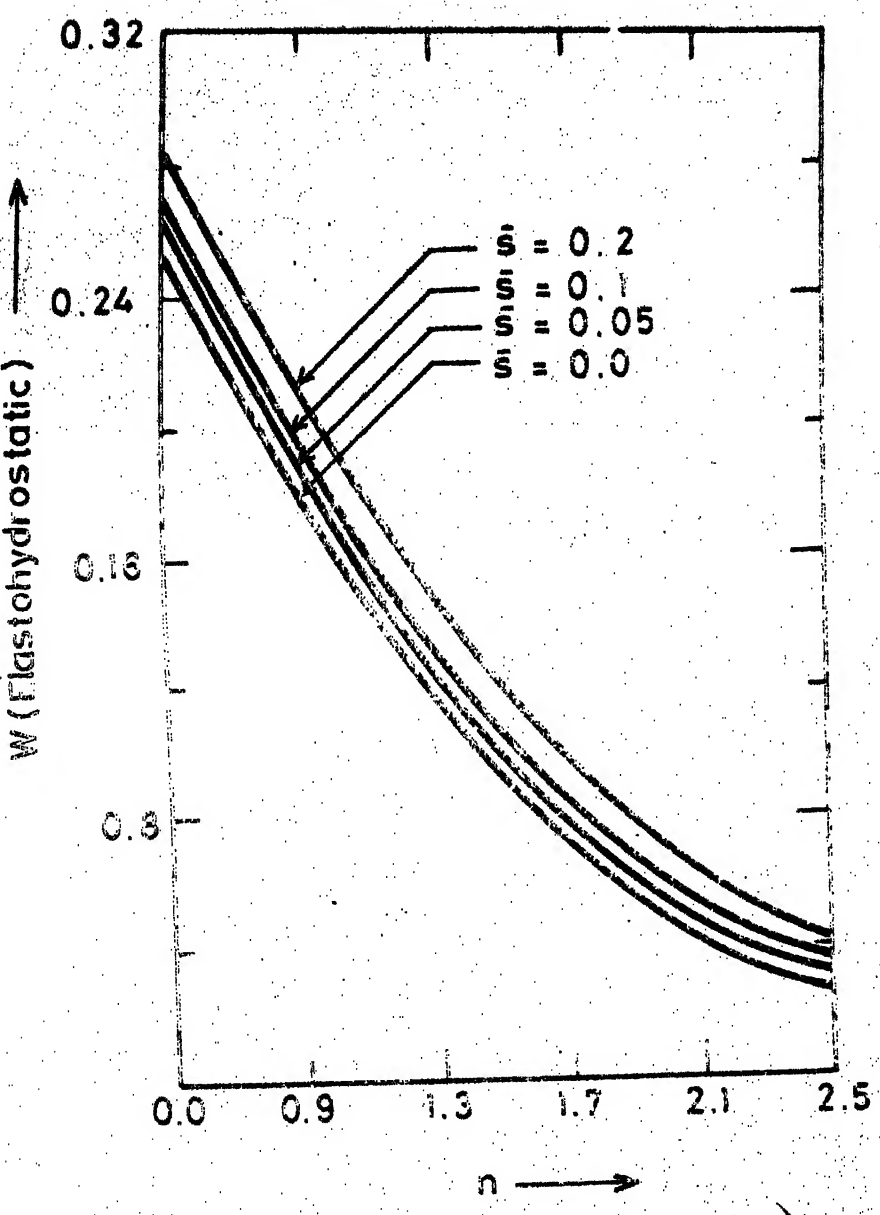

Fig. 8.3 Variation of dimensionless load capacity with flow behaviour index for various values of elasticity parameter.

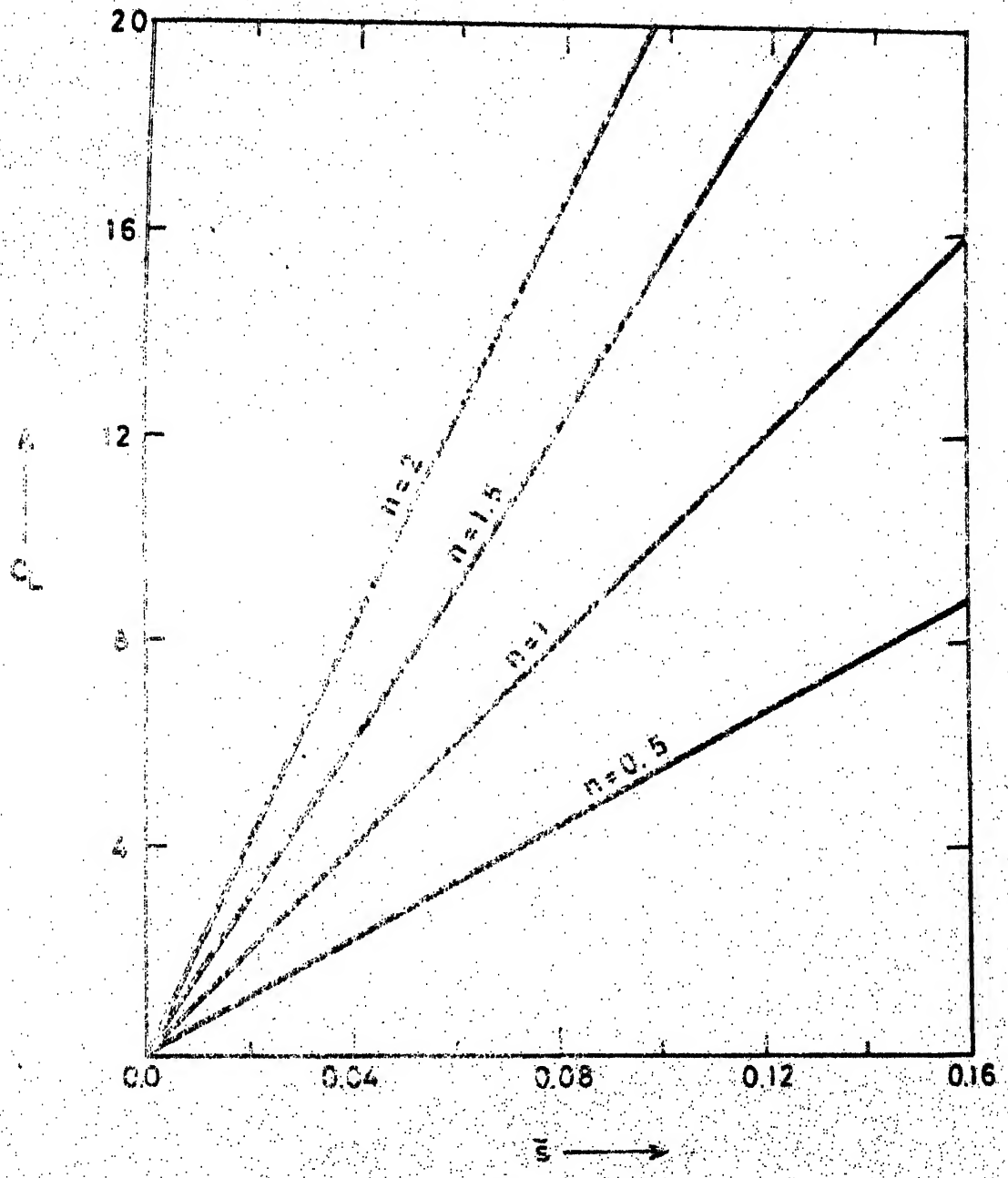

Fig 8.4 Variation of dimensionless load coefficient with elasticity parameter for various values of flow behaviour index

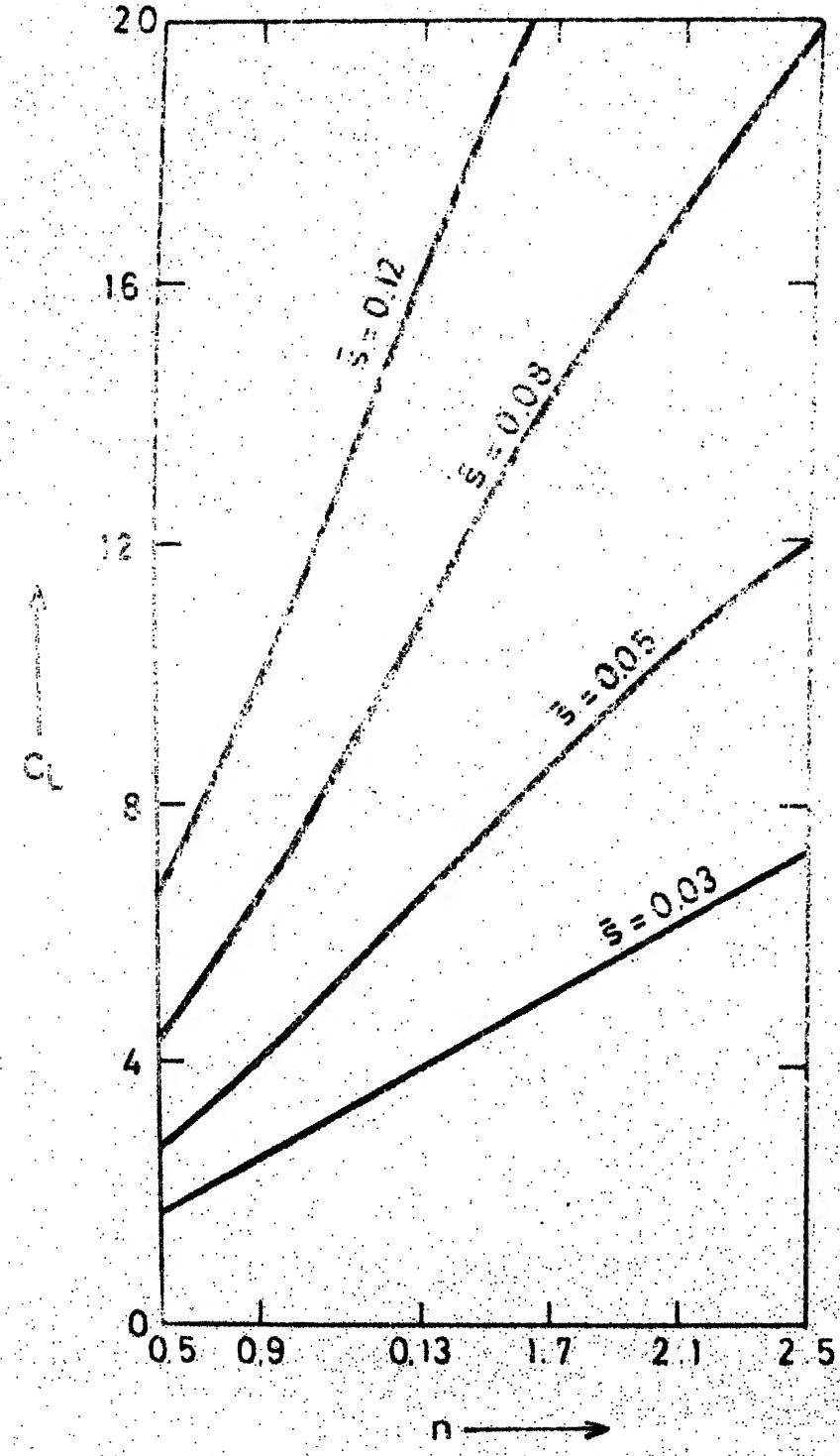

Fig 8 5 Variation of dimensionless load coefficient with flow behaviour index for various values of elastic parameter.

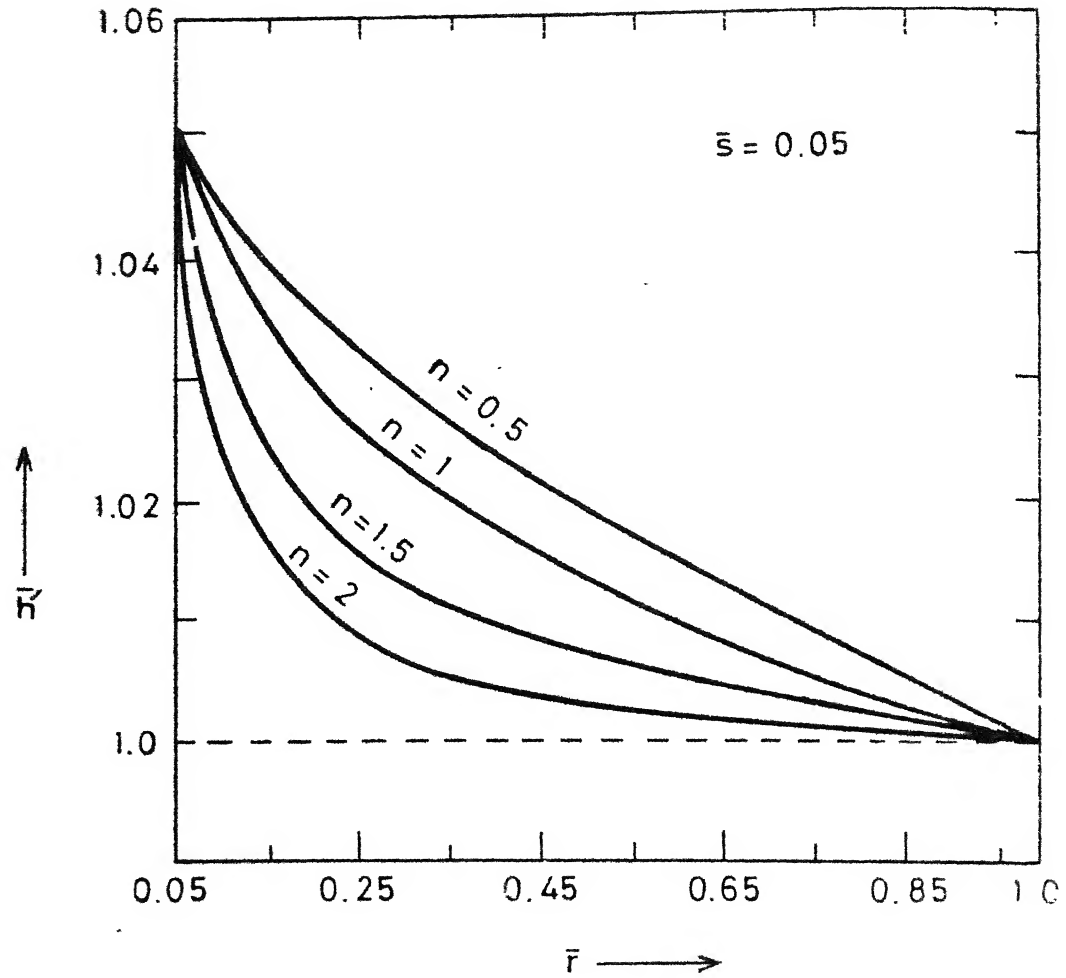

Fig. 8.6 Variation of film profile with dimensionless radius for various values of flow behaviour index.

REFERENCES

1. Fogg,A. (1946)
   Fluid Film Lubrication of Parallel Thrust Surfaces.
   Instn. of Mech.Engrs.,Vol.155,p.136.

2. Brkich, A. (1950)
   Mechanical Seals Theory and Criteria for Their Design.
   Prod. Engng.,Vol.21.

3. Salama, M.E. (1950)
   The Effect of Macro-Roughness on the Performance of Parallel Thrust Bearing.
   Proc.Instn. Mech. Engrs.,Vol.163.

4. Wood, T.H.(1954)
   Mechanical Shaft Seals in the Chemical Industry.
   Trans.Instn.Chem.Engng.,Vol.32,

5. Zienkiewics, O.C. (1957).
   Temperature Distribution Within Lubricating Film Between Parallel Bearing Surfaces and its Effect on the Pressure Developed.
   Proceedings of the Conference on Lubrication and Wear.Instn. Mech. Engng.

6. Jagger, E.T. (1957).
   Rotary Shaft Seals : The Sealing Mechanism of Synthetic Rubber Seals Running at Atmospheric Pressure.
   Proc.Instn. Mech. Engrs.,Vol.171.

7. Whitley, S. and William, L.G. (1959).
   The Gas Lubricated Spiral Groove Thrust Bearing.
   I.G.Report 28 (RD/CA), (H.M.Stationary Office).

8. Denny, D.F. (1960)
   Some Measurements of Fluid Pressures Between Plane Parallel Thrust Surfaces With special Reference to Radial Face Seals.
   Wear, Vol.4, p.64.

9. Nahavandi, A. and Osterle, F.(1960).
   The Effect of Vibration on the Load Carrying Capacity of Parallel Surface Thrust Bearing.
   ASME Paper No.60-Lub-3.

10. Tanner,R.I.(1960)
Non-Newtonian Flow and the Oil Seal Problem.
J.Mech.Engg.Sc.,Vol.2, p.25.

11. Tanner,R.I.(1961)
The Riener Centripetal Effect in Face deals.
Proc.Intl. Conf. on Fluid Sealing, BHRA, cranfield, U.K.,MK43, OAJ, Paper E1.

12. Davies, M.G. (1961)
The Generation of Lift by Surface Roughness in a Radial Face Seal.
Intl. Conf. on Fluid Sealing, BHRA, Paper C4.

13. Ishiwata, H. and Hirabayashi, H.(1961)
Friction and Sealing Characteristics of Mechanical Face Seals.
Intl. Conf. on Fluid Sealing, BHRA, Paper D5.

14. Huhn, D. (1961)
Theory of Fluid Sealing.
Intl. Conf. on Fluid Sealing BHRA, Paper D2.

15. Mayer, E. (1961)
Unbalanced Mechanical Seals for Liquids.
Intl. Conf. on Fluid Sealing, BHRA, Paper E2.

16. Mayer, E. (1961)
Leakage and Friction of Mechanical Seals With Special Consideration of Hydrodynamic Mechanical Seals.
Intl. Conf. on Fluid Sealing, BHRA, Paper E3.

17. Summers-Smith, D.(1961)
Laboratory Investigation of The Performance of a Radial Face Seal.
Intl. Conf. on Fluid Sealing,BHRA, Paper D1.

18. Whiteley, S. and William, L.G. (1962)
Principles of Gas Lubricated Shaft Seals.
Jour. of Mech.Engng.Sc. Vol.4, No.2,

19. Davies, M.G. (1963)
The Generation of Pressure Between Rough, Fluid Lubricated, Moving, Deformable Surfaces.
Lub.Engng.,Vol.24,No.11.

20. Lyman, F.A. and Saibel, E. (1963)
Leakage Through Rotary Shaft Seals.
Proc.Fourth Applied Mechanics Congress,
Paper C1.

21. Nau, B.S.(1967)
Hydrodynamic Lubrication in Face Seals.
Third Intl. Conf. on Fluid Sealing, BHRA,
Paper E5.

22. Kojabshian, C. and Richardson,H.H.(1967)
A Micropad Model for the Performance of
Carbon Seals.
Third Intl. Conf. on Fluid Sealing, BHRA,
Paper E4.

23. Cheng, H.S. and Snapp,R.B.(1967)
A study of Radial Film and Pressure Distribution
of High Pressure Face Seals.
Presented at the Third Intl. Conf. on Fluid
Sealing, Cambridge, BHRA, Paper No.E3.

24. Findlay, J.A. (1968)
Cavitation in Mechanical Face Seals.
J.Lub.Tech.,Trans. ASME, p.356.

25. Anno, J.N.,Walowit, J.A. and Allen, C.M.(1968)
Microasperity Lubrication.
J.Lub.Tech.,Trans. ASME, Vol.90,p.351.

26. Cheng,H.S.,Chow, C.Y. and Wilcock,D.F.(1968)
Behaviour of Hydrostatic and Hydrodynamic
Non Contacting Face Seals.
J.Lub.Tech.,Trans.ASME, Vol.90,No.2,p.510.

27. Pape, J.G.(1968)
Fundamental Research on a Radial Face
seal.
Trans. ASLE, Vol.11,No.3, p.302.

28. Sneck, H.J.(1969)
The Misaligned, Eccentric Face Seal.
J.Lub.Tech, Trans.ASME, Vol.91,No.4,p.695.

29. Sneck,H.J.(1969)
The Eccentric Face Seal With Tangentially Varying Film Thickness.
Presented at the Fourth International Conference on Fluid Sealing held in Conjunction with the 24th ASLE Annual Meeting in Philadelphia, FICFS Preprint No.15A.

30. Anno,J.N.,Walowit, J.A. and Allen, C.M.(1969)
Load Support and Leakage and Microasperity-Lubricated Face Seals.
Presented at the Fourth International Conference on Fluid Sealing held in Conjunction With the 24th ASLE Annual Meeting in Philadelphia, FICFS, Preprint No.21.

31. Findlay, J.A.(1969)
Measurements of Leakage in Mechanical Face Seals.
Presented at the Fourth Intl. Conference on Fluid Sealing held in Conjunction With 24th ASLE Annual Meeting in Philadelphia, FICFS Preprint No.19.

32. Adams, M.L. and Colsher, R.J.(1969)
An Analysis of Self, Energiged Hydrostatic Shaft Seals.
Jour. Lub.Tech.,Trans.ASME,Vol.91,No.4, pp.658.

33. Nau, B.S. (1969)
Film Cavitation observation in Face Seal.
Presented at the Fourth International Conference on Fluid Sealing held in Conjunction with the 24th ASLE Annual Meeting in Philadelphia, FICFS,Preprint No.20.

34. Lymer,A. (1969)
An Engineering Approach to Selection and Application of Mechanical Seals.
Presented at the Fourth International Conference on Fluid Sealing held in Conjunction with the 24th ASLE Annual Meeting, Philadelphia, FICFS Preprint No.25.

35. Orcutt,F.K.(1969)
An Investigation of the Operation and Failure of Mechanical Face Seals.
Presented at the Fourth International Conference on Fluid Sealing, held in Conjunction with the 24th ASLE Annual Meeting, Philadelphia, FICFS Preprint No.22.

36. Gibson, I.A.,Hooke,C.J. and O. Donoghue,J.P.(1970)
Elastohydrodynamic Lubrication of O-ring seals.
Proc.Instn.Mech.Engrs.,Vol.14,p.34.

37. Iny,E.H.(1971)
The Design of Hydrodynamic Lubricated Seals With Predictable Operating Characteristics.
5th Intl. Conf. on Fluid Sealing, Coventry, England, Paper H1.

38. Iny,E.H.(1971)
A Theory of Sealing With Radial Face Seals.
Wear,Vol.18,p.51.

39. Iny,E.H., Stangham-Batch,B.A. and Winney,P.E.(1971)
Face Lubrication In Mechanical Face Seals.
Inst.Mech.Engrs.,C 59/71, p.54.

40. Field,G.J. and Nau,B.S.,(1972)
An Experimental Study of Reciprocating Rubber Seals.
Proc.Inst. of Mech.Engrs. Symposium on Elastohydrodynamic Lubrication.

41. Lohou, J. and Godel,M.(1973)
Angular Misalignment and Squeeze Film Effects In Radial Face Seals.
6th Intl, Conf. on Fluid Sealing, Munich, Published by BHRA, Cranfield, England, Paper D2.

42. Stangham-Batch,B.A. and Iny,E.H.(1973)
A Hydrodynamic Theory of Radial Face Seals.
Jour. of Mech.Engng.Sc., Vol.15,No.1.

43. Snapp,R.B. and Sasdelli,K.R.(1973)
Performance Characteristics of a High Pressure Face Seal With Radially Converging Interface Shapes.
Sixth Intl. Conf. on Fluid Sealing, Munich, Paper E4.

44. Metcalfe,R.(1973)
Performance Analysis of Axisymmetric Flat Face Mechanical Seals.
Sixth Intl. Conf. on Fluid Sealing, Munich, Paper D1.

45. Mayer, E.(1973)
Mechanical Seals.
Iliffe Books Limited, London, American Elsevier, New York, II Edition, 250 pages.

46. Zuk, J.(1974)
Analytical Study of Pressure Balancing in Gas Film Seals.
Trans.ASLE, Vol.17,No.2, p.97.

47. Shapiro,W. and Colsher, R.(1974)
Steady State and Dynamic Analysis of Jet Engine Gas Lubricated Shaft Seals.
Trans. ASLE, Vol.17,No.3, p.190.

48. Haardt, R. (1974)
Flow Consideration Around Cavitation Area in Radial Face Seals.
Proc. I Leeds-Lyon - Lyon Symp. on Tribology, Paper VIII(i).

49. Ruskell, L.E.C. and Westcotl,M.J.(1974)
High Performance Reciprocating Seals for Aircraft Hydraulic System.
Tribology, Vol.5, p. 365.

50. Haardt, R. and Godet, M. (1975)
Axial Vibration of a Misaligned Face Seal Under a Constant Closure Force.
Trans. ASLE, Vol.18,No.1,p.55.

51. Griskin,E.N.(1975).
The Effect of Dynamics on Fluid Flow in a Face Seal.
Proc. 7th Intl. Conf. on Fluid Sealing, Paper B2.

52. Kupperman, D.S.(1975)
Dynamic Tracking of Non Contacting Face Seals.
Trans. ASLE, Vol.18,No.4,p.306.

53. Field, G.J. and Nau, B.S.(1975)
A Theoretical Study of the Elastohydrodynamic Lubrication of Reciprocating Rubber Seals.
J.Lub.Tech, Trans.ASME,Vol.18,p.48.

54. Ludwig, L.P.(1976)
Face Seal Lubrication I-Proposed and Published Models.
NASA, Technical Note NASA, TND-8101,

55. Ludwig, L.P. and Allen G.P.(1976)
Face Seal Lubrication II -Theory of Response to Angular Misalignment.
NASA, Technical Note NASA, TND-8102.

56. Metcalfe,R.(1976)
The use of Finite Element Deflection Analysis in Performance Predictions for End Face Seals.
Presented at the Third Symposium on Engg. Application of Solid Mechanics, University of Toronto.

57. Li Chin-Hsiu (1976)
Thermal Deformation in a Mechanical Face Seal.
Trans.ASLE, Vol.19,p.146.

58. Kilaparti, S.R. and Burton,R.A.(1976)
Pressure Distribution for Patch-Like Contact in Seals with Frictional Heating,Thermal Expansion and Wear.
J.Lub.Tech.,Trans. ASME, Vol. 98, No.4, p.569.

59. Ruskell,L.E.C.(1976)
Reynolds Equation and Elastohydrodynamic Lubrication in Metal Seals.
Proc.Royal Soc.London,A.349,p.383.

60. Lebeck,A.O.,Teale J.L. and Pierce,R.E.(1977)
Hydrodynamic Lubrication and Wear in Wavy Contacting Face Seals.
Presented at the 1977 ASLE-ASME Lubrication Conference, Kansa, City,ASME Paper No.77-Lub-18.

61. Lebeck, A.O.(1977)
A Study of Mixed Lubrication in Contacting Mechanical Face Seals. Presented at the Fourth Leeds-Lyon Symposium on Lubrication,Lyon.

62. Lebeck, A.O.(1977)
Mechanical Loading-A Primary Source of of Waviness in Face Seals. Trans. ASLE,Vol.20,No.3,p.195.

63. Lebeck, A.O., Teale, J.L. and Pierce,R.E.(1978)
Hydrodynamic Lubrication with Wear and Asperity Contact in Mechanical Face Seals. Annual Report ME-86(78) ONR-414-1, Prepared for the Office of Naval Research under Contact No.ONR-N-00014-76-C-0071.

64. Etsion, I. (1978)
The Accuracy of Narrow Seal Approximation in Analysing Radial Face Seals. Trans.ASLE,Vol.22,No.2,p.208.

65. Etsion,I.(1978)
Nonaxisymmetric Incompressible Hydrostatic Pressure Effects in Radial Face Seals. J.Lub.Tech.,Trans.ASME,Vol.100,No.3, p.379.

66. Hughes, W.F., Winowich, N.S., Birchak, M.J. and Kennedy,W.C. (1978)
Phase Change in Liquid Face Seals. J.Lub.Tech.,Trans.ASME,Vol.100,p.74.

67. Patir, N. and Cheng, H.S. (1978)
An Average Flow Model for Determining the Effects of Three Dimensional Roughness on Partial Hydrodynamic Lubrication. J.Lub.Tech.,Trans.ASME,Vol.100,p.12.

68. Metcalfe,R., Pothier,M.E. and Rod,B.H.(1978)
Diametral Tilt and Leakage of End Face Seals With Convergent Sealing Gap.
Proc.8th Intl.Conf. on Fluid Sealing, BHRA,

69. Kaneta, M., Fukahori, M. and Hirano, F. (1978)
Dynamic Characteristics of Face Seals.
Proc.8th Intl. Conf. on Fluid Sealing, Paper A2.

70. Lebeck, A.O. (1979)
A Mixed Friction Hydrostatic Mechanical Face Seal Model With Thermal Rotation and Wear.
Presented at the 34th ASLE Annual Meeting in St. Louis, ASLE Preprint No.79-AM-4C-3.

71. Lebeck, A.O. (1979)
A Mixed Friction Hydrostatic Face Seal Model With Phase Change.
J.Lub.Tech.,Trans.ASME, Paper No. 79-Lub-5,p.1.

72. Sharoni, A. and Etsion, I. (1979)
Performance of End Face Seals With Diametral Tilt and Coning — Hydrodynamic Effects.
Trans. ASLE, Vol.24,No.1,p. 61.

73. Etsion, I., (1979)
Performance of End Face Seals With Diametral Tilt and Conting — Hydrostatic Effects.
Trans.ASLE, Vol.23,No.3,p.279.

74. Etsion, I., (1979)
Hydrodynamic Effects in a Misaligned Radial Face Seal.
J.Lub. Tech., Trans. ASME, Vol.101, p. 283.

75. Etsion, I. and Burton, R.A. (1979)
Observation of Self Excited Wobbles in Face Seals.
J.Lub.Tech.,Trans. ASME, Vol.101, No.4, p.526.

76. Etsion, I. (1979)
Squeeze Film Effects in Radial Face Seals.
ASME Paper No.79-Lub-10.

77. Etsion,I.and Sharoni,A.(1979)
The Effects of Coning on Radial Forces in Misaligned Radial Face Seals.
ASME Paper No.79-Lub-17.

78. Etsion,I.(1979)
Radial Forces in a Misaligned Radial Face Seal.
J.Lub.Tech.,Trans.ASME,Vol.101,No.1, p.81.

79. Ruskell,L.E.C.(1979)
The Elastohydrodynamic Performance of Low-Friction, Zero-Leakage Metal Seals.
J.Mech.Engg.Sc.,Vol.21,No.4, p.275.

80. Lebeck,A.O.(1980)
A Test Apparatus for Measuring the Effects of Waviness in Misaligned Face Seals.
Presented at the ASLE Annual Meeting, Anahiem,

81. Young,L.A.(1980)
Experimental Evaluation of a Mixed Friction Hydrostatic Face Seal Model.
Masters Thesis, The University of New Mexico, Albuquerque, New Mexico.

82. Etsion, I. and Dan, Y. (1981).
An Analysis of Mechanical Face Seal Vibrations.
J.Lub.Tech.,Trans.ASME,Vol.103,p,428.

83. Walowit, J.A. and Pinkus, O.(1982)
Analysis of Face Seals With Shrouded Pockets.
J.Lub.Tech, Trans. ASME, Vol.104,No.2, p.262.

84. Suyanami,T. Masuda, T., Oishi, N. and Shimazu,T.(1982)
A Study of Thermal Behaviour of Large Seal Ring.
J.Lub.Tech.,Trans.ASME,Vol.104,p.449.

85. Krauter,A.I.(1982)
Measurement of Oil Film Thickness for Application to Elastomeric Stirling Engine Rod Seals.
J.Lub.Tech.,Trans.ASME,Vol.1o4,p.455.

86. Etsion,I.(1982)
Dynamic Analysis of Noncontacting Face Seals.
J.Lub.Tech.,Trans.ASME,Vol.1o4,p.460.

87. Mak,W.C. and Conway, H.D. (1977)
The Lubrication of a Long, Porous, Flexible Journal Bearing.
Jr.Lub.Tech, Trans. ASME,Vol.99,p.449.

88. Sinha,P. and Singh, C. (1982)
Lubrication of a Cylinder on a Plane With a Non-Newtonian Fluid considering Cavitation.
J.Lub.Tech.,Trans.ASME,Vol.1o4,p.168.

89. Thomas,B.D. and John, W.H.(1956)
Advances in Chemical Engineering.
Academic Press Inc.,Ist ed.,Vol.1,New York, p.1o3.

9o. Dowson, D., and Taylor, C.M.(1966)
Elastohydrostatic Lubrication of Circular Plate Thrust Bearing.
ASME Paper No.66-Lub-S-15.

91. Bird,R.B. , Stewart, W.E. and Lightfoot,E.N. (1960)
Transport Phenomena, Wiley.

92. Shukal,J.B. and Prakash,J.(1969)
The Rheostatic Thrust Bearing Using a Power Law Fluid as Lubricant.
Japanese Jour. of Applied Phys.,Vol.8, p.1557.

93. Pinkus,O., and Sternlicht,B. (1961)
Theory of Hydrodynamic Lubrication, McGraw Hill,New York.